MERCURY ISOTOPES AS BIOGEOCHEMICAL AND ECOLOGICAL TRACERS: ASSESSING MERCURY SOURCES AND EXPOSURE PATHWAYS IN FOOD WEBS

by

Sae Yun Kwon

A dissertation submitted in partial fulfillment
of the requirements for the degree of
Doctor of Philosophy
(Earth and Environmental Sciences)
in The University of Michigan
2015

Doctoral Committee:

Professor Joel D. Blum, Chair
Professor Niladri Basu, McGill University
Professor G. Allen Burton
Professor Gregory J. Dick
Professor J. Timothy Dvonch
Professor Knute J. Nadelhoffer

ACKNOWLEDGEMENT

I acknowledge these following people, as I would not have been able to complete this without their close guidance and positive support…

Joel Blum, my phD advisor

Nil Basu, Allen Burton, Greg Dick, Tim Dvonch, and Knute Nadelhoffer, my committee members

Co-authors

BEIGL, my lab members

Friends and staffs in the Earth and Environmental Sciences department

Families and friends back in Korea and Canada

My grandfather, who has always been an inspiration

TABLE OF CONTENTS

ACKNOWLEDGEMENT ii

LIST OF FIGURES vi

LIST OF TABLES viii

ABSTRACT ix

CHAPTER 1 Introduction 1

1.1. Mercury sources 1

1.2. Mercury biogeochemical cycling 2

1.3. Bioaccumulation and toxicity of MMHg 3

1.4. Mercury stable isotope ratios 4

1.5. Applications of Mercury isotopes: Dissertation structure 5

CHAPTER 2 Absence of fractionation of mercury isotopes during trophic transfer of methylmercury to freshwater fish in captivity 13

2.1. Introduction 13

2.2. Materials and methods 16

2.2.1. Experimental Design 16

2.2.1.1. Experiment 1: Yellow perch feeding experiments 16

2.2.1.2. Experiment 2: Lake trout feeding experiments 17

2.2.2. Mercury concentration analysis 18

2.2.3. Mercury isotope analysis 18

2.3. Results and Discussion 20

2.3.1. Hg Concentrations and Bioaccumulation Factors in Fish 20

2.3.2. Hg Isotopic Compositions in the Food 21

2.3.3. Hg Isotopic Variation during Bioaccumulation and Trophic Transfer 22
2.3.4. Application of Hg Isotopes in Aquatic Ecosystems 25
2.4. Supporting Information 31

CHAPTER 3 Application of mercury isotopes for tracing trophic transfer and internal distribution of mercury in marine fish feeding experiments 34
3.1. Introduction 34
3.2. Material and methods 36
3.2.1. Experimental design 36
3.2.2. Total mercury concentration analysis 37
3.2.3. Methylmercury analysis 38
3.2.4. Mercury isotope analysis 38
3.3. Results 40
3.3.1. Total mercury concentrations in Amberjack 40
3.3.2. Hg isotopic compositions in the diets 41
3.3.3. Hg isotopic compositions in Amberjack 41
3.3.4. Tuna treatment 42
3.3.5. Shrimp treatment 42
3.3.6. Photochemical degradation of Hg in the Gulf of Mexico 43
3.4. Discussion 43
3.4.1. Hg isotopic compositions of the diets and of Amberjack before feeding 43
3.4.2. Tuna treatment 44
3.4.3. Shrimp treatment 45
3.4.4. Application of Hg isotopes in natural marine systems 47

CHAPTER 4 Mercury isotope study of sources and exposure pathways of methylmercury in estuarine food webs in the Northeastern U.S. 57
4.1. Introduction 57
4.2. Materials and Methods 60
4.2.1. Site description 60
4.2.2. Sampling & analysis 61
4.2.3. Hg isotope analysis 62

4.3. Results & Discussion 63
4.3.1. Hg concentrations and isotopic compositions in the sediments 63
4.3.2. Hg concentrations and isotopic compositions in biota 65
4.3.3. Sources and biogeochemical pathways of MMHg 67
4.3.4. Ecological variability in MMHg sources 70
4.4. Supporting Information 80

CHAPTER 5 Isotopic study of mercury sources and transfer between a freshwater lake and adjacent forest food web 83
5.1. Introduction 84
5.2. Materials & Methods 86
5.2.1. Sample collection and processing 86
5.2.2. Stable C and N isotope analyses 88
5.2.3. Hg and MMHg concentration and Hg stable isotope analyses 88
5.3. Results & Discussion 90
5.3.1. MMHg biomagnification in the aquatic food web 90
5.3.2. Sources and biogeochemical processing of MMHg in the aquatic food web 91
5.3.3. MMHg biomagnification in the riparian and forest food webs 95
5.3.4. Hg transfer between aquatic and forest ecosystems 96
5.3.5. Sources and biogeochemical processing of MMHg in the riparian and forest food webs 97
5.4. Conclusion 99

CHAPTER 6 Conclusion 115
6.1. Summary of key findings 115
6.1.1. Mercury isotope fractionation 115
6.1.2. Mercury sources and biogeochemistry in aquatic ecosystems 116
6.2. Suggestions for future work 117

LIST OF FIGURES

Figure 2.1 Plot of mean δ^{202}Hg and Δ^{199}Hg values from Experiment 1.. 30

Figure 2.2 Plot of individual δ^{202}Hg and Δ^{199}Hg values from *Experiment 1* 30

Figure 2.3 Plot of δ^{202}Hg and Δ^{199}Hg values from *Experiment 2*. 31

Figure 2.S1 δ^{202}Hg (A) and Δ^{199}Hg (B) differences between the mean food pellet and the mean yellow perch tissues (fish minus food).. 31

Figure 3.1 Total Hg (THg) concentrations (ng/g, dry weight) of the organs of A) Amberjack fed a tuna diet and B) Amberjack fed a shrimp diet at different time periods. 54

Figure 3.2 Plot of δ^{202}Hg and Δ^{199}Hg values of Amberjack fed a tuna diet at A) day 0, B) day 10, C) day 30, and D) day 50 55

Figure 3.3 Plot of δ^{202}Hg and Δ^{199}Hg values of Amberjack fed a shrimp diet at A) day 10, B) day 30, C) day 50, D) day 80, and E) day 80 with shrimp-IHg and shrimp-MMHg. 56

Figure 3.4 Plot of percent MMHg (% MMHg) and Δ^{199}Hg of the Amberjack organs at day 0 .. 56

Figure 4.1 Plot of 1/THg concentration (ng/g) versus δ^{202}Hg and Δ^{199}Hg values of the Northeast coast estuary sediments. 78

Figure 4.2 Plot of % MMHg versus δ^{202}Hg (a) and Δ^{199}Hg values (b) of estuarine sediments and biota. 78

Figure 4.3 Plot of δ^{202}Hg and Δ^{199}Hg values of all sediments and estuarine biota..... 79

Figure 4.S1 Map of the Northeast coast, USA representing the sampling locations (Maine; ME, Massachusetts; MA, Rhode Island, RI; Connecticut, CT, New Jersey; NJ) 80

Figure 5.1 Sampling locations at the University of Michigan Biological Station, Michigan.... 107

Figure 5.2 Plot of % MMHg versus δ^{202}Hg (a) and Δ^{199}Hg values (b) of aquatic organisms ... 108

Figure 5.3 Plot of Δ^{201}Hg and Δ^{199}Hg values of aquatic and forest organisms. 108

Figure 5.4 Plot of δ^{202}Hg and Δ^{199}Hg values of precipitation, sediment and aquatic organism 109

Figure 5.5 Plot of δ^{202}Hg and $\boldsymbol{\Delta}^{199}$Hg values of basal resources from adjacent forest and aquatic ecosystems, and precipitation. 109

Figure 5.6 Plot of % MMHg versus δ^{202}Hg (a) and Δ^{199}Hg values (b) of forest organisms..... 110

Figure 5.7 Plot of ^{202}Hg and $\boldsymbol{\Delta}^{199}$Hg values estimated for IHg and MMHg from aquatic and forest ecosystems..... 110

Figure 5.8 Plot of forest gradient (meters) versus δ^{202}Hg (a) and $\boldsymbol{\Delta}^{199}$Hg values of beetles, beetle larvae, and spiders. 111

Figure 5.9 Plot of δ^{202}Hg and $\boldsymbol{\Delta}^{199}$Hg values of precipitation, soil, and forest organisms..... 111

LIST OF TABLES

Table 2.S1 THg concentrations (µg/g), and Hg isotopic compositions (‰) of the food pellet (P), muscle (M) and liver tissues (L) of YP-P0, YP-P1, and YP-P4 after 2-month feeding..... 32

Table 2.S2 THg concentrations (µg/g), Hg isotopic compositions (‰) of the food pellet (P), LT-P, bloater-1 (B1), bloater-2 (B2), LT-B(2M) and LT-B(6M). 33

Table 3.1 List of average organ mass (g, wet weight), total body mass (g, wet weight), and total fork length (mm) of AJ(S) and AJ(T) at different time periods. 53

Table 3.2 List of BAFs of AJ(S) and AJ(T) at different time periods. 53

Table 4.S1 THg concentrations (ng/g), % MMHg, stable carbon and nitrogen values and Hg isotope ratios of all sediment and estuarine biotas. 81

Table 5.1 Water quality parameters for Douglas Lake. The data shown were obtained from the Douglas Lake Buoy during the aquatic sampling period of May-June, 2013. 112

Table 5.2 THg concentrations (ng/g), % MMHg, stable carbon and nitrogen values and Hg isotope ratios of all basal resources and biota. 113

ABSTRACT

Monomethylmercury (MMHg) is a toxic and bioaccumulative compound that poses serious health threats to wildlife and humans consuming fish. There are significant uncertainties concerning the MMHg sources and exposure pathways to aquatic food webs and mercury stable isotope studies are beginning to shed new light on these processes. In Chapter 2 and 3, we conducted a series of controlled feeding experiments to understand the behavior of mercury isotopes during bioaccumulation and trophic transfer in freshwater and marine food webs. We found that there is an absence of mercury isotope fractionation during bioaccumulation, trophic transfer, and transport of MMHg between food sources and different tissues within fish. We used this information to develop the application of mercury isotopes as a monitoring tool for identifying MMHg sources in natural environments. In Chapter 4 and 5, we applied mercury isotopes to investigate the MMHg sources and exposure pathways in coastal marine food webs and in lacustrine-terrestrial transition food webs. Our work has elucidated spatial and ecological variability in MMHg sources as well as movements between terrestrial and aquatic ecosystems. This dissertation demonstrates that mercury stable isotopes can enhance our knowledge of the complexities of MMHg sources and biogeochemistry in natural ecosystems.

CHAPTER 1

Introduction

1.1. Mercury sources

Mercury (Hg) is a naturally occurring trace metal, which can be found as geologic ore deposits at various locations throughout the world (*1*). Hg has been mined and purified since antiquity for use in precious metal extraction, medicine, and decorative product making (*2*). Even to date, Hg is found in many commercial products including batteries, fluorescent light bulbs, electrical switches, and thermometers due to its many useful industrial properties.

A long history of Hg mining, anthropogenic use, as well as its release from various industrial activities has resulted in a significant amount of Hg emission to the atmosphere. In fact, a number of estimates have shown that anthropogenic activities have contributed to 2- to 5-fold increase in atmospheric Hg deposition relative to pre-industrial levels (*3*). Anthropogenic emission sources are largely categorized as primary and secondary. Primary anthropogenic sources occur when Hg of geologic origin is mobilized via mining of Hg-bearing ore or burning of fossil fuel. Secondary anthropogenic sources occur during intentional use of Hg such as industrial processes, product manufacturing and use, and gold mining operations. A recent estimate has shown that anthropogenic Hg emission sources are ranked in the order: gold mining (42%), fossil fuel combustion (25%), ferrous and non-ferrous metal (Al, Cu, Pb, Zn) production (12%), cement production (9%), waste incineration (6%), and oil refining (1%) (*4*). These anthropogenic sources together constitute 30% of the total Hg emission into the atmosphere (*4*).

Hg can also be emitted into the atmosphere through various natural processes such as volcanic activity and hydrothermal vents, and constitute 10% of the total atmospheric Hg emission (*2, 5*). Estimating the amount of natural Hg emission is subject to significant debate as Hg deposited from both natural and anthropogenic sources can be re-emitted into the atmosphere through processes such as forest fires and evasion from geochemical reservoirs including water

bodies and soils (*6*, *7*). Re-emission of anthropogenic Hg from geochemical reservoirs is considered to be the largest Hg emission source, accounting for 60% of the total atmospheric Hg emission (*3*). It is estimated that these three emission sources (anthropogenic; 30%, natural; 10%, re-emission; 60%) together amount to a total of 5500-8900 tons of Hg annually in the global atmosphere (*3*).

1.2. Mercury biogeochemical cycling

Hg is subject to complex biogeochemical cycling pathways as it can change speciation by undergoing redox reactions, photochemical reactions, and biological processes. In the atmosphere, Hg exists as three chemical species; elemental Hg (Hg^0), oxidized gaseous Hg (Hg^{2+}), and particulate Hg (Hg_p). These chemical species vary dramatically in reactivity and atmospheric mobility. The extent to which Hg is deposited to the lithosphere can also vary depending on the chemical species, type and proximity of point sources, atmospheric chemistry, and meteorology affecting Hg transport and deposition (*6, 8*). In general, Hg^0 is the dominant form of atmospheric Hg and is relatively stable and inert. Because Hg^0 has a long residence time (~1 year), it is well mixed in the atmosphere and can be transported globally (*9, 10*). In contrast, Hg^{2+}, and Hg_p are highly reactive and water-soluble, and thus they bind rapidly with particles or water droplets in the atmosphere. While these species are less common, their reactive properties make them vulnerable to rapid scavenging and deposition to local environments (*6, 9, 10*).

Hg that is deposited to the earth's surface can be subjected to various biogeochemical processes, which can determine the ecosystem fate of Hg. The processes governing Hg transformation and fate have been studied extensively in aquatic ecosystems, compared to terrestrial ecosystems, due to the important health implications related to human consumption of fish (*see section 1.3*). Specifically, Hg exists in three general chemical forms in aqueous solution; dissolved Hg^0, oxidized Hg^{2+} bound to ligands, and dissolved monomethylmercury (MMHg). Multiple biogeochemical processes (i.e. microbial, photochemical reactions) can induce the reduction of Hg^{2+} to Hg^0, and can cause Hg^0 removal to the atmosphere (*2, 10, 11*). Hg^{2+} that remains in aqueous solution can also be removed through processes involving particle sorption followed by sedimentation (*11*). In certain regions, the accumulation of Hg in sediments can provide long-term records of atmospheric Hg sources and deposition (*12-14*). A fraction of the Hg that remains in aquatic ecosystems can also be transformed into an organic form of Hg,

known as monomethylmercury (MMHg). Biotic methylation via sulfate- and iron-reducing bacteria is thought to be the dominant MMHg production pathway in many aquatic ecosystems (*15*). It has been found that two genes responsible for methyl-group transfer (hgcA) and electron donor for corrinoid cofactor reduction (hgcB) are the key components to biotic Hg methylation (*16*). Biotic methylation typically occurs in oxic/anoxic interfaces of various aquatic compartments (*15*). In freshwater and coastal systems, surface sediments, algal mats, and wetlands are thought to be the primary sites for biotic methylation (*17-19*). In the open ocean, Hg can be methylated at intermediate depths or within oxygen minimum zones (200-1000 meters) in the water column (*20, 21*).

1.3. Bioaccumulation and toxicity of MMHg

While MMHg represents a small fraction of total Hg in many freshwater and marine reservoirs, it is MMHg that readily bioaccumulates in organisms. Multiple biological properties have been proposed to explain the efficient bioaccumulation and biomagnification of MMHg in aquatic food webs. Dissolved MMHg in aqueous solution can be readily incorporated into microorganism cells and cause >10,000-fold higher MMHg concentrations in microorganisms relative to MMHg concentrations in water (*22, 23*). In higher animals, it has been found that MMHg can be transported to different organs via the blood stream and become assimilated by crossing intestinal membranes (*24, 25*). Once MMHg reaches internal organs, it binds strongly with sulfur ligands and accumulates in biological tissues (*26*). Because MMHg is rapidly assimilated and slowly eliminated, it becomes preferentially transferred to subsequent trophic positions, resulting in elevated MMHg levels in high trophic level organisms (*27*).

Exposure to MMHg can result in multiple detrimental health impacts to humans and wildlife. The toxicity of MMHg was first recognized in the 1950s at Minamata Bay, Japan (*28*). It was found that a local chemical company, which used Hg as a catalyst, released MMHg directly into Minamata Bay. The consumption of fisheries products impacted by the anthropogenic MMHg discharge caused significant health impacts to the local community. Even in areas unaffected by point-source contamination, the consumption of marine fisheries products is considered to be the dominant MMHg exposure pathway to humans (*29*). Multiple guidelines have been developed to prevent humans from being exposed to high levels of MMHg. These guidelines include fish consumption advisories, and reference doses (RfD; 0.1 ug/kg bw/day)

established by agencies such as the U.S. Environmental Protection Agency (*30*). Exceeding the RfD can lead to obvious physiological symptoms, and serious diseases. In humans, chronic MMHg exposure can damage the central nervous system, and cause neurological impairment, muscle spasms, and paralysis (*31-33*). Moderate to acute MMHg exposure can result in cardiovascular diseases and autoimmune disorders (*34*). In wildlife such as birds and bats, high MMHg levels have been shown to be linked to reproductive failure, physiological alteration, and neurological deficit (*35, 36, 37*).

1.4. Mercury stable isotope ratios

Mercury has seven stable isotopes with varying natural abundances: ^{196}Hg=0.155%, ^{198}Hg=10.04%, ^{199}Hg=16.94%, ^{200}Hg=23.14%, ^{201}Hg=13.17%, ^{202}Hg=29.73%, ^{204}Hg=6.83% (*38*). Mercury isotopes can undergo mixing and fractionation via various environmentally relevant processes, and impart distinct Hg isotopic compositions on natural environmental samples. Recently, the utilization of multi-collector inductively coupled plasma mass spectrometry, and the development of new laboratory methods have enabled precise measurement of Hg isotope ratios (*39*). The ability to precisely measure Hg isotope ratios in diverse environmental samples has added valuable insight to the sources and transformation pathways of Hg in many natural ecosystems.

Mercury isotopes can undergo two types of fractionation pathways: mass-dependent fractionation (MDF), and mass-independent fractionation (MIF). MDF is reported as δ^{202}Hg in units of permil (‰) referenced to the standard reference material NIST 3133:

$$\delta^{202}Hg = \{[(^{202}Hg/^{198}Hg)_{sample}/ (^{202}Hg/^{198}Hg)_{NIST3133}]-1\}*1000 \quad (1)$$

The mechanism of MDF is similar to the traditional light isotope systems (i.e., carbon and nitrogen stable isotopes) such that the degree of fractionation is dependent on the nuclear mass of the isotopes. MDF of Hg isotopes have been shown to occur during processes such as photochemical reduction and degradation of inorganic Hg (IHg) and MMHg (*40, 41*), microbial methylation and demethylation (*42-44*), thiol-ligand exchange (*45*), and volatilization of Hg^0 (*46*).

MIF is calculated using the difference between a measured δ^{xxx}Hg value and a value predicted based on MDF.

$$\Delta^{199}Hg = \delta^{199}Hg - (\delta^{202}Hg * 0.252) \quad (2)$$

$$\Delta^{200}Hg = \delta^{200}Hg - (\delta^{202}Hg * 0.5024) \quad (3)$$

$$\Delta^{201}Hg = \delta^{201}Hg - (\delta^{202}Hg * 0.752) \quad (4)$$

$$\Delta^{204}Hg = \delta^{204}Hg - (\delta^{202}Hg * 1.4930) \quad (5)$$

Three common mechanisms have been proposed to cause MIF: the nuclear volume effect (< 0.3 ‰), the magnetic isotope effect (> 1‰), and nuclear self-shielding. The nuclear volume effect occurs mainly during equilibrium reactions and the fractionation is thought to be dependent on the nuclear charge radii of isotopes (*47*). In contrast, the magnetic isotope effect occurs only during kinetic reactions. High levels of MIF via the magnetic isotope effect have been observed predominantly during photochemical reduction and degradation of IHg and MMHg (*40*). The magnetic isotope effect has been documented primarily in the odd-mass-number isotopes (^{199}Hg, ^{201}Hg). This is because the odd-mass-number isotopes have nuclear magnetic moments, unpaired nuclear spin, and radical pairs (*48, 49*), which can cause either the reactant or the product to be preferentially enriched in the odd-mass-number isotopes during reactions. Several recent studies have also suggested that the magnetic isotope effect as well as the nuclear self-shielding may also occur in even-mass-number isotopes (*50, 51*). The mechanism that causes MIF in the even-mass-number isotopes is still unclear.

1.5. Applications of mercury isotopes: Dissertation structure

While multiple aspects of Hg biogeochemical cycling have been investigated, previous studies have relied on indirect measurements (e.g., Hg concentration measurements) to trace important Hg sources, and ecosystem processes. The ability to precisely measure Hg isotope ratios in diverse environmental samples has enabled us to accurately link Hg sources to receptors, and to understand complex biogeochemical processes in natural environments. Particularly in aquatic ecosystems, significant uncertainties remain concerning the MMHg sources and exposure pathways in aquatic food webs. The research described in this dissertation demonstrates that the utilization of Hg isotopes is beginning to shed light on important sources and processes governing MMHg in diverse aquatic ecosystems.

The heart of this dissertation is Chapters 2 to 5, each of which was written as an independent research article. Chapters 2 to 4 are published in the peer reviewed literature and Chapter 5 has been submitted for publication. The citations and copyright for each of these chapters are given below:

- Chapter 2: Reprinted with permission from Kwon, S. Y.; Blum, J. D.; Carvan, M. J.; Basu, N.; Head, J. A.; Madenjian, C. P.; Solomon, R. D. Absence of fractionation of mercury isotopes during trophic transfer of methylmercury to freshwater fish in captivity. *Environ Sci Technol,* **2012,** 46, 7527-7534. Copyright 2012 American Chemical Society.

- Chapter 3: Reprinted with permission from Kwon, S. Y.; Blum, J. D.; Chirby, M. A.; Chesney, E. J. Application of mercury isotopes for tracing trophic transfer and internal distribution of mercury in marine fish feeding experiments. *Environ Toxicol Chem,* **2013,** 23, 2322-2330. Copyright 2013 Wiley.

- Chapter 4: Reprinted with permission from Kwon, S. Y.; Blum, J. D.; Chen, C. Y.; Meattey, D. E.; Mason, R. P. Mercury isotope study of sources and exposure pathways of methylmercury in estuarine food webs in the Northeastern U.S. *Environ Sci Technol,* **2014,** 48, 10089-10097. Copyright 2014 American Chemical Society.

- Chapter 5: Kwon, S. Y.; Blum, J. D.; Nadelhoffer, K. J.; Dvonch, J. T.; Tsui, M. T. K. Isotopic study of mercury sources and transfer between a freshwater lake and adjacent forest food web. *Sci Tot Environ,* **2015**—in review.

In Chapters 2 and 3, we explore the changes of Hg isotope ratios during bioaccumulation and trophic transfer in freshwater (*Perca flavescens*, *Salvelinus namaycush*), and marine fish (*Seriola dumerili*). We conducted a series of controlled fish feeding experiments, and characterized the Hg isotopic compositions of the diet and fish tissues both before and after the feeding experiments. We documented the absence of Hg isotope fractionation during bioaccumulation, trophic transfer, and transport of MMHg to different tissues. When fish were fed with diets composed of both IHg and MMHg, the isotope values of fish tissues displayed isotopic compositions reflecting MMHg due to the preferential trophic transfer and bioaccumulation of MMHg. The fact that the isotopic composition representing an environmental source of MMHg is retained in fish tissue indicates that we can now confidently use Hg isotope ratios in fish as a monitoring tool for tracing MMHg sources and biogeochemical processes in natural environments.

In Chapter 4, we applied this monitoring tool to investigate the sources and exposure pathways of MMHg in estuarine food webs located across the northeastern, USA. We first characterized the Hg isotopic compositions of sediments and various estuarine organisms representing different feeding guilds (green crab, blue mussel, killifish, and eider). We then estimated the isotopic composition representing MMHg by plotting % MMHg against Hg isotope values of the sediment and the estuarine organisms. We found significant positive relationships

between % MMHg and Hg isotopes values at all sites, indicating that MMHg accumulated from the local environment is indeed retained in fish tissues during bioaccumulation and trophic transfer. We found that MMHg associated with sediments and has undergone small amounts of photochemical degradation acts as the dominant source to many estuarine organisms. This study confirms that the measurement of Hg isotope ratios in organisms can be a valuable monitoring tool for deciphering MMHg sources and biogeochemical processes in aquatic ecosystems.

In Chapter 5 we explored the sources and biogeochemical processes of MMHg in Douglas Lake and adjacent forest food webs located at the University of Michigan Biological Station (Pellston, Michigan, USA), and assessed the importance of Hg transfers across ecosystem boundaries. We characterized the Hg isotopic compositions of basal resources (sediment, soil, leaf litter), and estimated the isotopic compositions representing IHg and MMHg by measuring aquatic and forest organisms with varying % MMHg values (macroinvertebrates, birds, bats, and fish). We found that MMHg produced *in situ* and that has undergone photochemical degradation is the dominant source to both the aquatic and forest food webs. In addition to MMHg, the measurement of Hg isotope ratios in organisms with low % MMHg allowed us to differentiate between the IHg associated with the basal resources and the IHg that has bioaccumulated in the food web. By comparing the isotopic compositions estimated for IHg, we found that the aquatic and forest food webs share a similar IHg source originated from terrestrial soil and that IHg deposited via watershed runoff provides an important Hg transfer pathway between the forest and aquatic ecosystems.

References

(1) Kesler, S. E. Mineral Resources, Economics and the Environment. *Macmillan, New York*. **1994**

(2) Fitzgerald, W. F.; Lamborg, C. H. Geochemistry of Mercury in the Environment. In *Treatise on Geochemistry 9*, Holland, H. D., and Turekian, K.K., Ed. *Elsevier Oxford*, **2003**, *9*, 107-148.

(3) United Nations Environment Programme. Global mercury assessment: Sources, emissions, releases and environmental transport. **2013**, 1-44.

(4) Pacyna, E.G.; Pacyna, J.M.; Sundseth, K.; Munthe, J.; Kindbom, K.; Wilson, S.; Steenhuisen, F.; Maxson, P. Global emission of mercury to the atmosphere from anthropogenic sources in 2005 and projections to 2020. *Atmos Environ.* **2010**, *44*, 2487-2499.

(5) Koski, R. A.; Benninger, L. M.; Zierenberg, R. A.; Jonasson, I. R. Composition and growth history of hydrothermal deposits in Escanaba Trough, southern Gorda Ridge. In Geologic, Hydrothermal, and Biologic Studies at Escanaba Trough, Gorda Ridge, Offshore Northern California, Morton, J.L.; Zierenberg, R.A.; Reiss, C.A., Ed. *US Geological Survey Bulletin* **1994**, 293–324.

(6) Lindberg, S.; Bullock, R.; Ebinghaus, R.; Engstrom, D.; Feng, X.; Fitzgerald, W.; Pirrone, N.; Prestbo, E.; Seigneur, C. A synthesis of progress and uncertainties in attributing the sources of mercury in deposition. *Ambio* **2007,** *36*, 19-32.

(7) Schluter K. Review: evaporation of mercury from soils. An integration and synthesis of current knowledge. *Environ. Geol.* **2000**, *39*(3–4), 249–271.

(8) White, E. M.; Keeler, G. J.; Landis, M. S. Spatial variability of mercury wet deposition in eastern Ohio: Summertime meteorological case study analysis of local source influences. *Environ. Sci. Technol.* **2009,** *43*, 4946-4953.

(9) Lin, C. J.; Pehkonen, S. O. The chemistry of atmospheric mercury: A review. *Atmos. Environ.* **1999,** *33*, 2067-2079.

(10) Schroeder, W. H.; Munthe, J. Atmospheric mercury - An overview. *Atmos. Environ.***1998,** *32* (5), 809-822.

(11) O'Driscoll, N. J.; Rencz, A.; Lean, D. R. The biogeochemistry and fate of mercury in the environment. *Metal ions in biological systems*, **2005,** *43*, 221-238.

(12) Bindler, R.; Renberg, I.; Appleby, P. G.; Anderson, N. J.; Rose, N. L. Mercury accumulation rates and spatial patterns in lake sediments from West Greenland: A coast to ice margin transect. *Environ. Sci. Technol.* **2001,** *35* (9), 1736-1741.

(13) Lamborg, C. H.; Fitzgerald, W. F.; Damman, A. W. H.; Benoit, J. M.; Balcom, P. H.; Engstrom, D. R. Modern and historic atmospheric mercury fluxes in both hemispheres: Global and regional mercury cycling implications. *Global Biogeochem. Cycles.* **2002,** *16* (4), 1-11.

(14) Schuster, P. F.; Krabbenhoft, D. P.; Naftz, D. L.; Cecil, L. D.; Olson, M. L.; Dewild, J. F.; Susong, D. D.; Green, J. R.; Abbott, M. L.; Atmospheric mercury deposition during the last 270 years: A glacial ice core record of natural and anthropogenic sources. *Environ. Sci. Technol.* **2002,** *36* (11), 2303-2310.

(15) Benoit, J. M.; Gilmour, C. C.; Heyes, A.; Mason, R. P.; Miller, C. L. Geochemical and biological controls over methylmercury production and degradation in aquatic ecosystems. In Biogeochemistry of Environmentally Important Trace Elements, Cai, Y.; Braids, O. C., Ed. *American Chemical Society: Washington DC***, 2003,** *835,* 262-297.

(16) Parks, J. M.; Johs, A.; Podar, M.; Bridou, R.; Hurt, R. A.; Smith, S. D.; Tomanicek, S. J.; Qian, Y.; Brown, S. D.; Brandt, C. C.; Palumno, A. V.; Smith, J. C.; Wall, J. D.; Elias, D. A.; Liang, L. The genetic basis for bacterial mercury methylation. *Science.* **2013,** 1230667.

(17) Eckley, C. S.; Hintelmann, H. Determination of mercury methylation potentials in the water column of lakes across Canada. *Science of the Total Environment.* **2006,** *368* (1), 111-125.

(18) Gilmour, C. C.; Henry, E. A. Mercury methylation in aquatic systems affected by acid deposition. *Environmental Pollution.* **1991,** *71,* 131-169.

(19) Ullrich, S. M.; Tanton, T. W.; Abdrashitova, S. A. Mercury in the aquatic environment: A review of factors affecting methylation. *Critical Reviews in Environmental Science and Technology.* **2001,** *31* (3), 241-293.

(20) Blum, J.D.; Popp, B.N.; Drazen, J.C.; Choy, C.A.; Johnson, M.W. Methylmercury production below the mixed layer in the North Pacific Ocean. *Nat Geosci*. **2013**, *6,* 879-884.

(21) Sunderland, E.M.; Krabbenhoft, D.P.; Moreau, J.W.; Strode, S.A.; Landing, W.M. Mercury sources, distributions and bioavailability in the North Pacific Ocean: Insights from data and models. *Global Biogeochem Cycl.* **2009,** *23,* 1-14.

(22) Mason, R.P.; Reinfelder, J.R.; Morel, F.M.M. Uptake, toxicity, and trophic transfer of mercury in a coastal diatom. *Environmental Science & Technology.* **1996**, *30,* 1835–1845.

(23) Pickhardt, P.C.; Fisher, N.S. Accumulation of inorganic and methylmercury by freshwater phytoplankton in two contrasting water bodies. *Environmental Science & Technology*. **2007,** *41,* 125–131.

(24) Boudou, A.; Ribeyre, F. Experimental study of trophic contamination of *Salmo gairdneri* by two mercury compounds- $HgCl_2$ and CH_3HgCl- Analysis at the organism and organ levels. *Water. Air. Soil. Pollut.* **1985**, *26*, 137-148.

(25) Wang, W. X.; Wong, R. S. K. Bioaccumulation kinetics and exposure pathways of inorganic mercury and methylmercury in a marine fish, the sweetlips *Plectorhinchus gibbosus*. *Mar. Ecol. Progr. Ser.* **2003,** *261*, 257-268.

(26) Rabenstein, D.L. The chemistry of methylmercury toxicology. *J Chem Education.* **1978,** 292-296.

(27) Watras, C.J.; Bloom, N.S. Mercury and methylmercury in individual zooplankton – implications for bioaccumulation. *Limnology and Oceanography,* **1992,** *37*, 1313–1318. Chen et al. Page 12 *Ecohealth*. Author

(28) Harada, M. Minamata disease: Methylmercury poisoning in Japan caused by environmental pollution. *Crit. Rev. Toxicol.* **1995,** *25*, 1-24.

(29) Sunderland, E. M. Mercury exposure from domestic and imported estuarine and marine fish in the U.S. seafood market. *Environ Health Persp.* **2007,** *115*, 235-242.

(30) U.S. Environmental Protection Agency, *2008 Biennial National Listing of Fish Advisories* EPA-823-F-09-007: Washington, D.C., **2009**.

(31) Clarkson, T. W.; Magos, L. The toxicology of mercury and its chemical compounds. *Crit. Rev. Toxicol.* **2006,** *36*, 609-662.

(32) Krabbenhoft, D. P.; Rickert, D. A. Mercury Contamination of Aquatic Ecosystems. *United States Geological Survey Fact Sheet* **1995,** 216-95.

(33) U.S. Environmental Protection Agency, EPA's Roadmap for Mercury: Executive Summary EPA-HQ-2005-0013: Washington, D.C., **2006.**

(34) Mergler, D.; Anderson, H. A.; Chan, L. H. M.; Mahaffey, K. R.; Murray, M.; Sakamoto, M.; Stern, A. H. Methylmercury exposure and health effects in humans: A worldwide concern. *Ambio.* **2007,** *36*, 3-11.

(35) Brasso, R.L.; Cristol, D.A. Effects of mercury exposure on the reproductive success of tree swallows (Tachycineta bicolor). *Ecotox.* **2008**, *17*, 133-141.

(36) Evers, D.C.; Savoy, L.J.; DeSorbo, C.R.; Yates, D.E.; Hanson, W.; Taylor, K.M. Adverse effects from environmental mercury loads on breeding common loons. *Ecotox.* **2008,** *17*, 69-81.

(37) Scheuhammer, A. M.; Meyer, M. W.; Sandheinrich, M. B.; Murray, M. W. Effects of environmental methylmercury on the health of wild birds, mammals, and fish. *Ambio: A Journal of the Human Environment* **2007,** *36* (1), 12-19.

(38) Blum, J. D.; Bergquist, B. A. Reporting the variations in the natural isotopic composition of mercury. *Anal. Bioanal. Chem.* **2007,** *388* (2), 353-359.

(39) Bergquist, B. A.; Blum, J. D. The odds and evens of mercury isotopes: Applications of mass-dependent and mass-independent isotope fractionation. *Elements* **2009**, 5, 353-357.

(40) Bergquist, B. A.; Blum, J. D. Mass-dependent and mass-independent fractionation of Hg isotopes by photo-reduction in aquatic systems. *Science* **2007,** *318*, 417-420.

(41) Zheng, W.; Hintelmann, H. Mercury isotope fractionation during photoreduction in natural water is controlled by its Hg/DOC ratio. *Geochim et Cosmochim Acta.* **2009,** *73*, 6704-6715.

(42) Perrot, V.; Bridou, R.; Pedrero, Z.; Guyoneaud, R.; Monperrus, M.; Amouroux, D. Identical Hg isotope mass dependent fractionation signature during methylation by sulfate-reducing bacteria in sulfate and sulfate-free environment. *Environ Sci Technol.* **2015,** DOI: 10.1021/es5033376

(43) Rodriguez-Gonzalez, P.; Epov, V. N.; Bridou, R.; Tessier, E.; Guyoneaud, R.; Monperrus, M.; Amouroux, D. Species-specfic stable isotope fractionation of mercury during Hg(II) methylation by an anaerobic bacteria (*Desulfobulbus propionicus*) under dark conditions. *Environ. Sci. Technol.* **2009**.

(44) Kritee, K.; Barkay, T.; Blum, J. D. Mass dependent stable isotope fractionation of mercury during *mer* mediated microbial degradation of monomethylmercury. *Geochim. Cosmochim. Acta* **2009,** *73*, 1285-1296.

(45) Wiederhold, J.C.; Cramer, C.J.; Daniel, K.; Infante, I.; Bourdon, B.; Kretzschmar, R. Equilibrium mercury isotope fractionation between dissolved Hg(II) species and thiol-bound Hg. *Environ Sci Technol.* **2010,** *44*, 4191-4197.

(46) Zheng, W.; Foucher, D.; Hintelmann, H.; Mercury isotope fractionation during volatilization of Hg(0) from solution into the gas phase. *J. Anal. Atomic Spectro.* **2007,** *22*, 1097-1104.

(47) Schauble, E. A. Role of nuclear volume in driving equilibrium stable isotope fractionation of mercury, thallium, and other very heavy elements. *Geochim. Cosmochim. Acta* **2007,** *71*, 2170-2189.

(48) Buchachenko, A. L. Magnetic isotope effect: Nuclear spin control of chemical reactions. *J. Phys. Chem.* **2001,** *105* (44), 9995-10011.

(49) Turro, N. J. Influence of nuclear spin on chemical reactions: Magnetic isotope and magnetic field effects. *Proceedings of the National Academy of Sciences* **1983,** *80*, 609-621.

(50) Gratz, L. E.; Keeler, G. J.; Blum, J. D.; Sherman, L. S.; Isotopic composition and fractionation of mercury in Great Lakes precipitation and ambient air. *Environ. Sci. Technol.* **2010,** *44*, 7764-7770.

(51) Sherman, L. S.; Blum, J. D.; Keeler, G. J.; Demers, J. D.; Dvonch, J. T.; Investigation of local mercury deposition from a coal-fired power plant using mercury isotopes. *Environ. Sci. Technol.* **2012,** *46* (1), 382-390.

CHAPTER 2

Absence of fractionation of mercury isotopes during trophic transfer of methylmercury to freshwater fish in captivity

Abstract

We performed two controlled experiments to determine the amount of mass-dependent and mass-independent fractionation (MDF and MIF) of methylmercury (MeHg) during trophic transfer into fish. In Experiment 1, juvenile yellow perch (*Perca flavescens*) were raised in captivity on commercial food pellets and then their diet was either maintained on un-amended food pellets (0.1 µg/g MeHg), or was switched to food pellets with 1.0 µg/g or 4.0 µg/g of added MeHg, for a period of 2 months. The difference in δ^{202}Hg (MDF) and Δ^{199}Hg (MIF) between fish tissues and food pellets with added MeHg were within the analytical uncertainty (δ^{202}Hg; 0.07 ‰, Δ^{199}Hg; 0.06 ‰) indicating no isotope fractionation. In Experiment 2, lake trout (*Salvelinus namaycush*) were raised in captivity on food pellets, and then shifted to a diet of bloater (*Coregonus hoyi*) for 6 months. The δ^{202}Hg and Δ^{199}Hg of the lake trout equaled the isotopic composition of the bloater after 6 months, reflecting re-equilibration of the Hg isotopic composition of the fish to new food sources and a lack of isotope fractionation during trophic transfer. We suggest that the stable Hg isotope ratios in fish can be used to trace environmental sources of Hg in aquatic ecosystems.

2.1. Introduction

Mercury (Hg) is a globally distributed toxic metal that bioaccumulates in aquatic organisms. Aquatic ecosystems provide favorable methylation conditions and this can lead to elevated levels of methylmercury (MeHg) in fish through biomagnification (*1*). This ultimately poses serious health threats to humans and wildlife that depend on fish for their diet (*2*). There has been a growing scientific effort to develop various means of identifying the environmental sources and

exposure pathways of Hg in aquatic ecosystems. For instance, previous studies have indirectly identified Hg sources in aquatic food webs by coupling Hg concentrations in fish with potential sources (*3*). Other studies have examined various ecological factors that promote bioaccumulation of Hg (*4*). Ecological tracers such as stable carbon and nitrogen isotopes have been used in conjunction with Hg concentration measurements to allow comparisons of Hg concentrations in aquatic organisms with their feeding ecology (*5*). The potential application of small fish as biosentinels of Hg contamination has been somewhat limited by the lack of ability to capture the complex processes involved in the bioaccumulation of Hg. Techniques that can illuminate Hg sources and exposure pathways and offer a more direct link between Hg sources and potential receptors are clearly needed.

Application of the variation in natural abundance of stable Hg isotopes has expanded rapidly in recent years (*6*), with studies that now include atmospheric Hg cycling (*7*), point source identification (*8*), human exposure (*9*), and determination of Hg sources to aquatic ecosystems (*10-13*). The distinct Hg isotope ratios produced by fractionation and mixing through environmental processes provide insight into Hg sources and transformation pathways. Kinetic Hg isotope fractionation is a process where the different stable isotopes of Hg react at different rates in chemical reactions resulting in measurable differences in the Hg isotopic composition between reactants and products. This difference in the isotope ratios can become a proxy for tracing the sources of Hg. Depending on the reaction pathways, Hg isotope fractionation can occur as mass-dependent fractionation (MDF), similarly to common light-isotope fractionation, or by mass-independent fractionation (MIF), via the nuclear volume and magnetic isotope effects (*14*, *15*). Differences in MDF are reported as δ^{202}Hg, which is the difference in the ^{202}Hg/^{198}Hg ratio of a sample compared to the NIST-3133 standard in units of permil (‰). Differences in MIF are reported as Δ^{199}Hg and Δ^{201}Hg, which are the differences in the ^{199}Hg/^{198}Hg and ^{201}Hg/^{198}Hg ratios in ‰ from those predicted from the δ^{202}Hg value based on MDF (*6*).

Recently, Hg isotopes have been applied to aquatic ecosystems to establish links between sources and receptors of Hg. Gehrke et al.(*11*) demonstrated that δ^{202}Hg values in fish correlated strongly with δ^{202}Hg values in intertidal sediments collected at a series of sites in the San Francisco Estuary (USA), with a nearly constant isotopic difference of 0.6 ‰. Unfortunately, the utility of using the MDF signature in fish as a tracer of the isotopic composition of a particular

anthropogenic source of Hg is limited by a lack of understanding of Hg isotope fractionation between reservoirs within sediments and during trophic transfer to fish.

High positive Δ^{199}Hg values have been observed in fish (*10, 12, 13, 16-19*) and this has led to two contrasting explanations for the origin of MIF in fish. Bergquist and Blum (*16*) documented large magnitude MIF (>0.5‰ change in Δ^{199}Hg) during photochemical reduction of inorganic Hg (Hg_I) and photodemethylation of MeHg in aqueous medium, but not in dark abiotic control experiments. They suggested that MIF occurs in the odd-mass number isotopes (^{199}Hg and ^{201}Hg) via photochemical reactions and used the Δ^{199}Hg values in fish collected from multiple lakes to estimate the extent of photodegradation of MeHg that took place prior to uptake by organisms at the base of the food web. Several subsequent studies have adopted this approach to estimate the extent of ecosystem-scale MeHg photodegradation and have assumed that Δ^{199}Hg values are not modified by trophic transfer to fish (*10, 12, 16, 20*). In contrast, Jackson et al. (*19*) and Das et al. (*17*) found a significant positive relationship between Δ^{199}Hg and the trophic level (based on δ^{15}N) along various freshwater food chains. Based on these observations, Das et al. (*17*) suggested that MIF of Hg isotopes occurs, at least in part, *in vivo* by internal metabolic processes within fish. The interpretation of Δ^{199}Hg signatures in aquatic ecosystems is thus dependent on whether or not MIF of Hg isotopes occurs *in vivo*, and controlled experimental studies are needed to determine whether Δ^{199}Hg values are changed by fractionation during trophic transfer to fish.

In the study reported here, we performed two sets of experiments to compare Hg isotopic compositions and concentrations in tissues of two freshwater fish species at different levels of MeHg exposure to test whether Hg isotopes are fractionated during trophic transfer to fish. In *Experiment 1*, we raised juvenile yellow perch (*Perca flavescens*) for three months on regular food pellets and then switched some of them for 2 months to a diet of food pellets amended with MeHg. The food pellets were spiked with varying concentrations of MeHg to allow determination of the isotope fractionation of MeHg. We chose to use juvenile yellow perch for *Experiment 1* because it is an ideal biosentinel organism for studying Hg bioaccumulation in freshwater food webs due to its ubiquitous distribution in freshwater bodies (*21*). Their omnivorous feeding behavior is also advantageous for raising them in a controlled environment. In a second experiment designed to mimic natural trophic transfer processes of Hg *(Experiment 2),* we raised lake trout (*Salvelinus namaycush*), a top predator in many freshwater food webs, on

food pellets for 47 months until they reached an adult phase. We then switched their food for 6 months to bloater (*Coregonus hoyi*), which is their natural prey. The degree of fractionation was determined by comparing the Hg isotope values of the food fed to the fish with the Hg isotope values of the fish tissues.

2.2. Materials and methods

2.2.1. Experimental Design

2.2.1.1. Experiment 1: Yellow perch feeding experiments

Three-month-old yellow perch were raised at the Great lakes WATER Institute at the University of Wisconsin-Milwaukee during the summer of 2010. Twenty-four individuals were randomly selected to determine the average initial body length (47.6 ± 5.4 mm) and body weight (2.01 ± 0.62 g). In August, 2010, the fish were transferred into tanks that were maintained by a flow-through system at 8-10°C and in which water was filtered to remove suspended residues. They were divided into three different treatments (20 individuals in each tank and 4 replicate tanks for each level, totaling 240 fish) and fed with commercial food pellets (Zeigler Finfish Starter Diet, 2 mm) composed mainly of marine by-catch products, poultry by-products, hydrolyzed feather meal, fish oil, wheat, soy flour, and brewers dried yeast. The food pellets were manipulated to three different MeHg concentrations. To vary MeHg concentration in the food pellets, two batches of food pellets were soaked in synthetic MeHg solutions for two days at 1.0 µg/g and 5.0 µg/g (nominal concentrations) and then evaporated to dryness. Synthetic MeHg solution was prepared by diluting solid methylmercury (II) chloride (Sigma-Aldrich) in 100% ethanol. We achieved three different total-Hg (THg) concentration levels (actual concentrations): 0.076 µg/g dry wt. (background without added MeHg), 1.0 µg/g and 4.0 µg/g (pellets with added MeHg) and these are referred to as 0.1, 1.0 and 4.0 µg/g treatments hereafter. All food pellets were kept at minus 80°C prior to use.

Across all treatments, fish were fed twice a day with approximately 6% of their body weight in food pellets, for a total period of two months. Yellow perch that were fed with 0.1, 1.0 and 4.0 µg/g food pellets are referred to as YP-P0, YP-P1 and YP-P4 respectively. All fish achieved similar body length and weight after the experiment (average length= 76.8 ± 8.6 mm, average weight= 8.97 ± 2.69 g, n= 240), regardless of the MeHg levels in the food pellets. The fish were dissected to different organs, frozen and shipped to the University of Michigan, where

subsamples of fish muscle and liver tissues were taken for THg concentration and stable Hg isotope analysis. We took either one or two fish from each of the 12 tanks for muscle tissues (n= 18) and pooled four to seven liver samples to achieve 2 liver analyses for each treatment (n= 6). The food pellets were analyzed in triplicate for each treatment level (n= 9).

2.2.1.2. Experiment 2: Lake trout feeding experiments

Lake trout were raised in the U.S. Fish and Wildlife Service Sullivan Creek National Fish Hatchery (Brimley, MI). Fish were fed with commercial fish food (Nelson Silver Cup extruded sinking feed), composed mainly of fish meal, soybean meal, blood meal, wheat flour, fish oil, hydrolyzed feather meal, and poultry by-products, for 47 months until they reached an average body mass of 570 g. A single individual was sacrificed and dissected for muscle tissue at this time (referred to as LT-P). Both the food pellets and the LT-P muscle tissues were sub-sampled to achieve 3 separate samples for analysis (LT-P, n= 3; pellets, n= 3). A total of 133 lake trout were sent to the U.S. Geological Survey Great Lakes Science Center (Ann Arbor, MI) in February 2010, distributed to 8 different tanks and switched to a diet of bloater. Tanks were maintained by a flow-through system at 8-10°C and water was filtered to remove suspended residues. The bloater fed to the lake trout were obtained from Lake Michigan in September 2009 and May 2010 and referred to as bloater-1 and bloater-2, respectively. The bloaters were caught at two different time periods because there was not enough of bloater-1 to complete the feeding experiment. The bloater diet was prepared by homogenizing whole fish in a stainless steel grinder and storing at minus 30°C prior to use. Bloater-1 and bloater-2 represent a composite of 3 and 6 bloaters respectively. Each bloater composite sample was analyzed twice for THg concentrations and isotopic composition (bloater-1, n= 2; bloater-2, n= 2).

We chose three tanks to analyze for THg concentrations and isotopic composition of the lake trout after 2 months (n= 3) and 6 months (n =3) of feeding with bloater. Lake trout were fed with bloater-1 for 2 months until they reached an average body mass of 694, 890 and 817 g in each tank (referred to as LT-B(2M)). From each tank, a total of 4 lake trout were sacrificed and homogenized as a composite sample. After an additional 3-months of feeding with bloater-1, the lake trout were switched to a diet of bloater-2 and fed for an additional 1-month period until they reached an average body mass of 1242, 1518 and 1566 g in each tank. The remaining 10 fish were sacrificed and homogenized as a composite sample representing 10 individuals from each

tank (referred to as LT-B(6M)). Additional information on feeding procedures can be found in Madenjian et al.(*22*). Individual fish were not analyzed after switching the food source, and the homogenized composite samples removed some of the possible effects of heterogeneity between individuals.

2.2.2. Mercury concentration analysis

All tissue and food pellet samples were analyzed for THg concentrations at the University of Michigan. The tissue samples were freeze-dried prior to analysis and concentrations are reported based on dry weight. Briefly, the samples were combusted at 800°C and THg was quantified using a Nippon Instruments MA-2000 AAS Hg analyzer. Calibration was obtained by a standard solution of NIST SRM 3133 and was checked between every three samples; the values were always within 5% of certified values. Two standard reference materials, ERM CE 464 (average measured THg = 4.71 µg/g, n=8) and NRCC DORM-2 (4.16 µg/g, n=7), were combusted along with samples, and always agreed within 10% of certified values.

MeHg concentrations were analyzed for the 0.1 µg/g food pellets from *Experiment 1*, as well as for the bloater-1 and bloater-2 and lake trout from *Experiment 2*, at the U. S. Geological Survey Mercury Research Lab in Middleton, Wisconsin, following the method described in Hammerschmidt and Fitzgerald (*23*). Briefly, samples were digested in Teflon digestion tubes with dilute nitric acid (5M HNO_3) at 60ºC for 8 hours. 4.5M KOH and sodium tetraethylboarate (NaTEB) were added to form methylethylmercury (MeEtHg). Argon (Ar) gas was used to strip the MeEtHg from the liquid phase, and transferred into Tenex traps. MeEtHg was then desorbed back into the sample stream and different Hg species were separated using a gas chromatography column. MeHg and Hg^{2+} were converted to Hg^0 and analyzed using a CVAFS detector. The detection limit was monitored on a daily basis and was 2 ng/g.

2.2.3. Mercury isotope analysis

Sample combustion and transfer - A two-stage combustion system was employed to thermally release and isolate Hg from fish tissue and fish food samples (*11*). Briefly, a pre-fired ceramic boat was loaded with sample powder, covered with sodium carbonate and aluminum oxide and placed in a dual-stage quartz tube furnace. The combustion compartment was heated in a step-wise fashion to 750°C over a 6 hour period. Mercury-free oxygen was fed to carry released Hg^0

from samples through the down-stream 1000°C decomposition compartment, and all Hg^0 was subsequently oxidized in a "trap solution" of 1% $KMnO_4$ in 10% H_2SO_4. To fully separate Hg from other combustion products, the sample trap solutions were partially neutralized by the addition of hydroxylamine, and then Hg^{2+} was reduced to Hg^0 by addition of $SnCl_2$. Hg^0 was purged into another 1% $KMnO_4$ trap solution using Ar gas, resulting in a matrix-free solution adequate for mass spectrometry analysis.

Recovery of Hg through combustion and transfer – Since the $\delta^{202}Hg$ value of Hg in samples can be affected by incomplete recovery of Hg through the combustion and transfer processes, we monitored the THg concentrations in trap solutions after both combustion and transfer steps. THg recoveries were calculated using standard reference materials, ERM CE 464 (n= 9) and NRCC DORM-2 (n= 2) and ranged between 96 and 103% and between 93 to 99%, respectively. Procedural blanks contained negligible amounts of THg (average = 0.017 ng/g, *n*=5) when compared to sample concentration for isotopic measurements (i.e. 1-5 ng/g).

MC-ICP-MS analysis - Stable Hg isotope ratios were measured using a Nu Instruments multi-collector inductively coupled plasma mass spectrometer (MC-ICP-MS). Neutralized trap solutions (after the final purge and trap step) were diluted with the same matrix to achieve THg concentrations between 1 and 5 ng/g. Hg^{2+} in solution was reduced by $SnCl_2$, and evolved Hg^0 was separated from the solution using a frosted glass tip phase separator and introduced to the MC-ICP-MS. On-peak zero corrections were applied, and instrumental mass bias was corrected using an internal Tl standard (NIST SRM 997) and sample-standard (NIST SRM 3133) bracketing at uniform THg concentrations and matrix composition[6]. The bracketing standard was diluted using the same matrix and matched to the THg concentration of the samples within 5 %. MDF is reported as $\delta^{202}Hg$ in permil (‰) referenced to NIST SRM 3133 and calculated as:

$$\delta^{202}Hg = \{[(^{202}Hg/^{198}Hg)_{sample}/ (^{202}Hg/^{198}Hg)_{NIST3133}]-1\}*1000. \quad (1)$$

MIF represents the difference between the measured $\delta^{xxx}Hg$ value and the value predicted based on MDF and the $\delta^{202}Hg$ value[16]. MIF is thus reported as $\Delta^{199}Hg$ and $\Delta^{201}Hg$ in permil (‰). MIF is calculated as below based on an approximation valid for δ <10‰:

$$\Delta^{199}Hg = \delta^{199}Hg - (\delta^{202}Hg * 0.252) \quad (2)$$

$$\Delta^{201}Hg = \delta^{201}Hg - (\delta^{202}Hg * 0.752) \quad (3)$$

We use $\Delta^{199}Hg$ as the default value to report MIF.

Analytical uncertainty of isotopic analysis - Analytical uncertainty at 2 s.d. was estimated as the larger of replicate measurements of the in-house standard (UM-Almáden) or of replicate analyses of procedural standards. UM-Almáden (n=81) had mean values (±2 s.d.) of $\delta^{202}Hg$= -0.57±0.06 ‰, $\Delta^{201}Hg$= -0.03±0.04 ‰, and $\Delta^{199}Hg$= -0.02±0.05 ‰. Standard reference material ERM CE 464 (freeze dried fish powder) was combusted, processed and analyzed in the same manner as samples (n=9) and its mean values were $\delta^{202}Hg$= 0.69±0.07 ‰, $\Delta^{201}Hg$= 1.97±0.03 ‰, and $\Delta^{199}Hg$= 2.39±0.06 ‰.

2.3. Results and Discussion

2.3.1. Hg Concentrations and Bioaccumulation Factors in Fish

The THg concentrations in the muscle and liver tissues of the yellow perch (*Experiment 1*) increased with increasing MeHg concentration in the three different food pellet treatments after two months of feeding. This is consistent with other studies that have documented a positive relationship between the Hg concentrations in commercial food pellets and Hg concentrations in the muscle and liver tissues of other fish species (*24*). The MeHg concentration analysis showed that the 0.1 µg/g food pellets were composed of 78% MeHg. The level of Hg_I in the 0.1 µg/g food pellets was used to calculate the % MeHg in the 1.0 µg/g and 4.0 µg/g pellets, which were 94% and 99% respectively. The average THg concentrations in the muscle tissues were 0.210±0.01 (n= 6, 1 s.d), 2.54±0.33 (n= 6), and 13.3±0.90 µg/g (n= 6) and in the liver tissues were 0.022±0.003 (n=2), 0.34±0.03 (n= 2), and 3.77±0.43 µg/g (n= 2) in YP-P0, YP-P1 and YP-P4, respectively (Supporting information Table S1).

The THg concentrations in the lake trout (*Experiment 2*) increased when their diet was switched to bloater, which had much higher THg concentrations than the food pellets. The average THg concentrations of the food pellets were 0.0267±0.001 µg/g (n= 3, 1 s.d) and the bloater-1 and bloater-2 were 0.312±0.001 (n= 2) and 0.463±0.006 µg/g (n= 2) respectively. The

LT-P, LT-B(2M) and LT-B(6M) had THg of 0.111±0.004 (n= 3), 0.138±0.02 (n= 3) and 0.316±0.02 μg/g (n= 3), respectively (Supporting information Table S2). The % MeHg in the LT-B(2M) and LT-B(6M) were 83% and 89% and the % MeHg in the bloater-1 and bloater-2 were 85% and 87%.

We calculated the bioaccumulation factors (BAFs) to determine the extent of Hg bioaccumulation at different levels of Hg exposure. In this study, the BAFs in *Experiment 1* were calculated as the THg concentration in fish muscle divided by the average THg concentration in food pellets. Muscle tissues concentrations are often used for this purpose, as muscle is the major site of MeHg accumulation (*25*). The BAFs were 2.8±0.2 (1 s.d), 2.7±0.3, and 3.1±0.2, for the 0.1, 1.0, and 4.0 μg/g treatments, respectively. The THg concentration of these small fish, which added over 400% body mass in the 2-month feeding period, appear to have risen to new Hg concentrations in equilibrium with their new diets and thus yielded constant BAF values across a >50-fold range in concentrations.

The BAF of LT-P in *Experiment 2* was calculated as the THg concentration in muscle divided by the THg concentration in food pellets, and the LT-B(2M) and LT-B(6M) were calculated based on the THg concentration in whole fish divided by the THg concentration in the whole fish bloater diet. Due to the two batches of bloater that were used as food during the course of the experiment, we took the weighted average of the THg concentration of the bloater-1 (88%) and bloater-2 (12%) to calculate the BAF for the LT-B(6M) (bloater 1 and 2= 0.330 μg/g). The BAFs calculated for *Experiment 2* are 4.1±0.2 (1 s.d), 0.44±0.1 and 0.96±0.1 for the food pellets (before the change to a bloater diet) and bloater diet after 2 and 6 months, respectively. Previous studies have reported BAFs of 3 to 5 between food and whole-body fish tissue concentrations of THg (*3, 26*). The lower BAF values after 2 and 6 months on the bloater diet indicate that for these adult fish (which added only 39% and 100% body mass) THg concentrations had presumably not yet risen to values in equilibrium with their new diet.

2.3.2. Hg Isotopic Compositions in the Food

The food pellets with added synthetic MeHg used in *Experiment 1* had much lower δ^{202}Hg and Δ^{199}Hg values than the food pellets without added MeHg (Fig 1; Fig 2; Supporting information Table S1). The isotopic composition of the un-amended food pellets reflects background Hg from marine by-catch products, poultry by-products and other materials from

which they are composed. The isotopic composition of the food pellets with added MeHg reflects the synthetically prepared MeHg, which is derived from industrial sources of Hg and therefore has a Δ^{199}Hg value near zero (*27*). The synthetic MeHg showed similar δ^{202}Hg as cinnabar (HgS) (*28-30*) and metallic Hg (e.g., Almaden standard) (*16*) from various sources. The Hg isotopic composition of the 0.1 µg/g and 4.0 µg/g food pellets are considered the "natural" pellet Hg and synthetic MeHg respectively, and as expected the isotopic composition of 1.0 µg/g food pellets fall on a mixing line between these end members (Fig 1).

In *Experiment 2*, the food pellets and the new diet (i.e., bloater) were also markedly different in Hg isotopic composition, but in this case they were higher in δ^{202}Hg and Δ^{199}Hg compared to *Experiment 1* (Fig 3; Supporting information Table S2). The bloater had a high proportion of MeHg and also naturally higher values of δ^{202}Hg and Δ^{199}Hg (without the use of synthetic MeHg). This allowed a comparison of possible isotopic fractionation during trophic transfer of naturally occurring MeHg, compared to the synthetic MeHg in *Experiment 1*. Significantly positive Δ^{199}Hg values in the food pellets from both experiments suggest that Hg in the food may have originated from marine by-catch products, because of the similarity in measured isotopic compositions in various marine fish (*11, 13*). The even higher Δ^{199}Hg values in the bloater used in *Experiment 2* were consistent with their origin as lake fish (*9, 10, 12, 16*) (Supporting information Table S2). Moreover, the Δ^{199}Hg/Δ^{201}Hg ratio observed in the 0.1 µg/g food pellets (1.21±0.03, 1 s.d.), and the bloater (1.27±0.02, 1 s.d.) are consistent with the ratios previously reported for fish (~1.20) (*11-13, 16, 20*).

2.3.3. Hg Isotopic Variation during Bioaccumulation and Trophic Transfer

After two months of feeding on the new food sources, and after an average body mass increase of over 400%, both δ^{202}Hg and Δ^{199}Hg in the muscle and liver tissues of yellow perch (*Experiment 1*) generally matched the respective food pellets used within each treatment (Fig. 1; Fig 2). The Hg isotopic compositions of the muscle tissues were indistinguishable from the liver tissues in each treatment despite considerable differences in the Hg concentrations. This indicates that Hg isotope fractionation does not occur under these conditions during the internal distribution of Hg between these tissues. To examine whether there were significant isotopic shifts in either δ^{202}Hg or Δ^{199}Hg during bioaccumulation and trophic transfer, we calculated the differences in measured δ^{202}Hg and Δ^{199}Hg between fish and their food (fish minus food) and

found no difference in δ^{202}Hg or Δ^{199}Hg for either of the MeHg amended pellet treatments (Supporting information Fig S1A, B). This indicates that the Hg isotopic composition is directly transferred to the fish without isotope fractionation. In contrast, small isotopic differences in both δ^{202}Hg and Δ^{199}Hg (≤0.2‰) were observed between the un-amended 0.1 µg/g food pellets and the muscle and liver tissues of YP-P0 (Supporting information Fig S1A, B). It is important to clarify that the small differences in the isotopic composition of Hg between the fish and 0.1 µg/g food pellets are not the result of isotope fractionation that occurred during chemical reactions. Instead, we attribute this to the preferential uptake of MeHg in the muscle and liver tissues of YP-P0 compared to Hg_I, leading to a small Hg isotopic shift upon bioaccumulation (discussed below in further detail).

In the lake trout study (*Experiment 2*), in which the food pellets and the bloater had contrasting Hg isotopic compositions, we observed considerable, but incomplete, turnover of the Hg isotopic compositions in the LT-B(2M) 2 months after switching the diet to the bloater (and following an average weight increase of only 39%) (Fig 3). Lake trout from two of the three tanks sampled at 2 months (LT-B(2M)) fall on a mixing line, as expected, between the Hg isotopic values of the food pellets and the bloater. We do not have a clear explanation for why a third LT-B(2M) sample does not fall on this line, but we speculate that it is due to heterogeneity of the bloater food source. For lake trout fed bloater for 6 months (LT-B(6M)) (with an average weight increase of 100%) complete isotopic equilibration to the value of the bloater-2 food source appears to have occurred. This also corresponded with the increase in the THg concentrations in LT-B(6M) compared to LT-B(2M), indicating further accumulation and incorporation of Hg into the lake trout tissues.

To summarize the experimental results, we find no evidence for MDF or MIF during trophic transfer of Hg. In *Experiment 1*, when the proportion of MeHg to THg and the concentrations in the food pellets was high (1.0 µg/g and 4.0 µg/g treatments), there was no detectable difference in δ^{202}Hg or Δ^{199}Hg between the food pellets and yellow perch muscle or liver tissue. Similarly, in *Experiment 2*, Hg was transferred from the bloater food source to the lake trout, and the δ^{202}Hg and Δ^{199}Hg of the LT-B(6M) shifted to the value of the bloater after 6 months. In the experiment where yellow perch (*Experiment 1*) were fed with food pellets with low MeHg concentration and a significant proportion of Hg_I (22%), the fish were observed to have δ^{202}Hg and Δ^{199}Hg values that were slightly offset from the food pellets. We suggest that the fraction of

Hg_I in the un-amended food pellets had a contrasting Hg isotopic composition compared to the MeHg, which seems reasonable given the widely contrasting materials (see above) that are used to make the food pellets and the observation that Hg_I and MeHg can have contrasting isotopic composition in individual tissues (*31*). More efficient accumulation of MeHg, compared to Hg_I, in the fish could then account for the small discrepancy between the Hg isotopic composition of the un-amended pellets and the fish raised on them.

Das et al.(*17*) previously reported a significant increase in Δ^{199}Hg with trophic level (inferred from δ^{15}N) and argued that *in vivo* processes in fish could cause MIF. It has, however, been suggested on theoretical grounds that internal metabolic processes are unlikely to cause the observed MIF of Hg isotopes (*32*). The suggestion of *in vivo* MIF is not supported by our experiments, which demonstrate that MeHg, whether synthetically prepared or natural, is transferred without fractionation. The absence of isotope fractionation of MeHg observed in both juvenile (yellow perch) and adult (4-year old lake trout) fish and following different time periods after dietary changes (2 months vs 6 months) suggests that differences in age, growth rate, and Hg turnover explored in our experiments do not lead to significant isotope fractionation of MeHg. It is unclear, without additional studies, whether other metabolic processes or physiological states of fish could influence the isotope fractionation of MeHg in the wild. Nevertheless, our controlled experiments suggest that differing isotopic compositions between MeHg and Hg_I in aquatic organisms are most likely responsible for the differences in δ^{202}Hg and Δ^{199}Hg that have been observed during bioaccumulation and trophic transfer in some studies. Much higher bioaccumulation of MeHg compared to Hg_I has been well documented in a number of studies that have exposed fish to both Hg species through their diet (*33-35*).

In contrast to Das et al.(*17*), some studies have failed to observe any relationship between Hg isotope values and trophic levels in fish (*10, 13*). Instead, in those studies, the variations of MIF in fish were explained by the extent of photochemical demethylation of MeHg in the natural environment prior to uptake into the aquatic food web. If we assume that both Hg_I and MeHg are present in water and are equally exposed to light in the water column, we would expect Hg_I to impart a lesser degree of MIF compared to MeHg. The experimental study by Bergquist and Blum (*16*) documented larger MIF of MeHg compared to Hg_I despite a similar rate of photoreduction. With bioaccumulation of two Hg species, Hg_I with lower δ^{202}Hg and Δ^{199}Hg values and MeHg with higher δ^{202}Hg and Δ^{199}Hg values, by low trophic level organisms such as

phytoplankton (*36*) and subsequent trophic transfer of predominantly MeHg, the pattern of increasing δ^{202}Hg and Δ^{199}Hg values with trophic position in aquatic food webs could be generated. As a side note we point out that the lack of Hg isotope fractionation during trophic transfer into fish does not imply that fractionation does not occur in other types of organisms. In fact, a recent study by Laffont et al.(*9*) noted an average enrichment of δ^{202}Hg by 2‰ in human hair compared to food sources (but no change in Δ^{199}Hg) and suggested that *in vivo* processes in humans may cause MDF during transfer into hair.

2.3.4. Application of Hg Isotopes in Aquatic Ecosystems

The lack of isotope fractionation of Hg (both MDF and MIF) during trophic transfer into fish that we observe in this study suggests that the application of Hg isotope measurements can provide direct linkages between Hg sources and Hg in fish tissues. In the study by Gehrke et al.(*11*), it was recognized that the use of young fish as biosentinels to detect spatial patterns of Hg sources was limited by a lack of understanding of Hg isotope fractionation between sediment and algae and during trophic transfer to fish. It was suggested that the observed constant offset of 0.6 ‰ in δ^{202}Hg between the sediment and fish was the result of the combined effect of chemical transformations in sediment and trophic transfer. Based on our findings, we now suggest that the offset of 0.6 ‰ is not due to trophic transfer into fish and is instead the result of other processes. Our demonstration of a lack of Hg isotope fractionation upon trophic transfer focuses our attention towards understanding fractionation during processes that occur within sediments.

The rate at which the Hg isotopic composition re-equilibrated to the value of new food sources in our experiments yields insight into the timescale of Hg exposure recorded by the Hg isotopic composition of fish. The age-0 juvenile yellow perch in *Experiment 1* and the mature age-4 lake trout in *Experiment 2* reflected their new food sources after 2 and 6 months, respectively. After only 2 months however, the lake trout retained an isotopic signal of a mixture of their old and new food sources. In the case of input of new Hg sources to the environment, we expect that it would take longer than 2 months for older fish, depending on size and growth rate, to fully reflect the Hg isotopic composition of new Hg sources.

A number of studies have reported spatial patterns of Δ^{199}Hg values both within and across aquatic systems (*10-13*). Ganter et al.(*10*) observed varying Δ^{199}Hg values in Arctic char depending on the latitude of the Canadian lakes in which the fish were sampled. Moreover, their

results exhibited species-specific variation in Δ^{199}Hg values such that zooplankton occupying the water column had higher Δ^{199}Hg values compared to benthic invertebrates. The interpretation of Δ^{199}Hg values was previously hindered by uncertainties concerning the effect of potential biological fractionation versus fractionation by photochemical degradation of MeHg. Our experimental study clearly suggests that biological MIF is unimportant, and we can now more confidently estimate the proportion of MeHg lost through photodegradation (*10-13*). Given the potentially diverse dietary sources, feeding behaviors and mobility of fish in natural ecosystems, there are clear limitations to using stable Hg isotopes in fish as tracers of Hg sources. We anticipate, however, that as we learn more about Hg isotope fractionation during specific processes in the environment, the application of δ^{202}Hg and Δ^{199}Hg in aquatic ecosystems will develop into a strong tracer of Hg sources in aquatic ecosystems.

Acknowledgement

The authors would like to thank M Pickens for raising yellow perch, the U. S. Fish and Wildlife Service staff at the Sullivan Creek National Fish Hatchery for raising the lake trout, M Johnson for expert operation of the MC-ICP-MS, and D Krabbenhoft for generously providing MeHg analyses of fish food pellets. The USGS has not endorsed this publication and the views expressed should not be considered the views of the USGS. Funding was provided by grants from NSF (EAR-0952108) and US DOE Office of Science (BER) to JD Blum, NOAA pilot funds to JA Head, and a Great Lakes Fishery commission grant to CP Madenjian. This article is Contribution 1699 of the U. S. Geological Survey Great Lakes Science Center.

References

(1) Gilmour, C. C.; Henry, E. A.; Mitchell, E. A. Sulfate stimulation of mercury methylation in freshwater sediments. *Environ. Sci. Technol.* **1992,** *26,* 2281-2287.

(2) Mergler, D.; Anderson, H. A.; Chan, L. H. M.; Mahaffey, K. R.; Murray, M.; Sakamoto, M.; Stern, A. H. Methylmercury exposure and health effects in humans: A worldwide concern. *Ambio.* **2007,** *36,* 3-11.

(3) Mason, R. P.; Sullivan, K. A. Mercury in Lake Michigan. *Environ. Sci. Technol.* **1997,** *31,* 942-947.

(4) Chen, C. Y.; Stemberger, R. S.; Kamman, N. C.; Mayes, B. M.; Folt, C. L. Patterns of Hg bioaccumulation and transfer in aquatic food webs across multi-lake studies in the northeast US. *Ecotoxicol.* **2005,** *14,* 135-147.

(5) Kwon, S. Y.; McIntyre, P. B.; Flecker, A. S.; Campbell, L. M. Mercury biomagnifications in the food web of a neotropical stream. *Sci. Total. Environ.* **2012,** *417-418,* 92-97.

(6) Blum, J. D. Handbook of environmental isotope geochemistry. Applications to stable mercury isotope biogeochemistry. Ed. Mark Baskaran. Berlin Germany: *Springer,* **2011.**

(7) Sherman, L.S.; Blum, J. D.; Keeler, G. J.; Demers, J. D.; Dvonch, T. Investigation of local mercury deposition from a coal-fired power plant using mercury isotope. *Environ. Sci. Technol.* **2012,** *46,* 382-390.

(8) Foucher, D.; Ogrinc, N.; Hintelmann, H. Tracing mercury contamination from the Idrija mining region (Slovenia) to the Gulf of Trieste using Hg isotope ratio. *Environ. Sci. Technol.* **2009,** *43,* 33-39.

(9) Laffont, L.; Sonke, J. E.; Maurice, L.; Hintelmann, H.; Pouilly, M.; Bacarreza, Y. S. Perez, T.; Behra, P. Anomalous mercury isotopic compositions of fish and human hair in the Bolivian Amazon. *Environ. Sci. Technol.* **2009,** *43,* 8985-8990.

(10) Gantner, N.; Hintelmann, H.; Zheng, W.; Muir, D. C. Variations in stable isotope fractionation of Hg in food webs of Arctic lakes. *Environ. Sci. Technol.* **2009,** *43,* 9148-9154.

(11) Gehrke, G. E.; Blum, J. D.; Slotton, D. G.; Greenfield, B. K. Mercury isotope link mercury in San Francisco Bay forage fish to surface sediments. *Environ. Sci. Technol.* **2011,** *45,* 1264-1270.

(12) Perrot, V.; Epov, V. N.; Pastukhov, M. V.; Grebenshchikova, V. I.; Zouiten, C.; Sonke, J. E.; Husted S.; Donard, O. F. X.; Amouroux D. Tracing sources and bioaccumulation of mercury in fish of Lake Baikal- Angara River using Hg isotopic composition. *Environ. Sci. Technol.* **2010,** *44,* 8030-8037.

(13) Senn, D. B.; Chesney, E. J.; Blum, J. D.; Bank, M. S.; Maage, A.; Shine, J. P. Stable isotope (N, C, Hg) study of methylmercury sources and trophic transfer in the Northern Gulf of Mexico. *Environ. Sci. Technol.* **2010,** *44,* 1630-1637.

(14) Buchachenko, A. L.; Ivanov, V. L.; Roznyatovskii, V. A.; Vorob'ev, A. K.; Ustynyuk, Y. A. Inversion of the sign of the magnetic isotope effect of mercury in photolysis of substituted dibenzylmercury. *Dokl. Phys. Chem.* **2008,** *420,* 85-87.

(15) Schauble, E. A. Role of nuclear volume in driving equilibrium stable isotope fractionation of mercury, thallium, and other very heavy elements. *Geochim. Cosmochim. Acta.* **2007,** *71,* 2170-2189.

(16) Bergquist, B. A.; Blum, J. D. Mass-dependent and -independent fractionation of Hg isotopes by photoreduction in aquatic systems. *Science* **2007,** *318,* 417-420.

(17) Das, R.; Salters, V. J. M.; Odom, A. L. A case for in vivo mass-independent fractionation of mercury isotopes in fish. *Geochem. Geophys. Geosyst.* **2009,** *10,* Q11012.

(18) Epov, V. N.; Rodriguez-Gonzalez, P.; Sonke, J. E.; Tessier, E.; Amouroux, D.; Bourgoin, L. M.; Donard, O. F. X. Simultaneous determination of species-specific isotopic composition of Hg by gas chromatography coupled to multicollector ICPMS. *Anal. Chem.* **2008,** *80,* 3530-3538.

(19) Jackson, T. A.; Whittle, D. M.; Evans, M. S.; Muir, D. C. G. Evidence for mass-independent and mass-dependent fractionation of the stable isotopes of mercury by natural processes in aquatic ecosystems. *Appl. Geochem.* **2008,** *23,* 547-571.

(20) Point, D.; Sonke, J. E.; Day, R. D.; Roseneau, D. G.; Hobson, K. A.; Vander Pol, S. S.; Moors, A. J.; Pugh, R. S.; Donard, O. F. X.; Becker, P. R. Methylmercury photodegradation influenced by sea-ice cover in Arctic marine ecosystems. *Nat. Geosci.* **2011,** *4,* 188-194.

(21) Greenfield, B. K.; Hrabik, T. R.; Harvey, C. J.; Carpenter, S. R. Predicting mercury levels in yellow perch: use of water chemistry, trophic ecology, and spatial traits. *Can. J. Aquat. Sci.* **2001,** *58,* 1419-1429.

(22) Madenjian, C. P.; David, S. R.; Pothoven, S. A. Effects of activity and energy budget balancing algorithm on laboratory performance of a lake trout bioenergetics model. *Trans. Am. Fish. Soc.* **2012,** in press.

(23) Hammerschmidt, C. R.; Fitzgerald, W. F. Methylmercury in freshwater fish linked to atmospheric mercury deposition. *Environ. Sci. Tehcnol.* **2006,** *40,* 7764-7770.

(24) Berntssen, M. H. G.; Hylland, K.; Julshamn, K.; Lundebye, A. K.; Waagbo, R. Maximum limits of organic and inorganic mercury in fish feed. *Aquacult. Nutr.* **2004,** *10,* 83-97.

(25) Bloom, N. S. On the methylmercury content of fish tissue. *Can. J. Fish. Aquat. Sci.* **1992,** *49,* 1010-1017.

(26) Watras, C. J.; Bloom, N. S. Mercury and methylmercury in individual zooplankton: Implications for bioaccumulation. *Limol. Oceanogr.* **1992,** *37,* 1313-1318.

(27) Bergquist, B. A.; Blum, J. D. The odds and evens of mercury isotope: Applications of mass-dependent and mass-independent isotope fractionation. *Elements* **2009,** *5,* 353-357.

(28) Hintelmann, H.; Lu, S. Y. High precision isotope ratio measurements of mercury isotopes in cinnabar ores using multi-collector inductively coupled plasma mass spectrometry. *Analyst* **2003,** *128,* 635-639.

(29) Smith, C. N.; Kesler, S. E.; Blum, J. D.; Rytuba, J. J. Isotope geochemistry of mercury in source rocks, mineral deposits and spring deposits of the California coast ranges, USA. *Earth. Planet. Sc. Lett.* **2008,** *269,* 399-407.

(30) Stetson, S. J.; Gray, J. E.; Wanty, R. B.; Macalady, D. L. Isotopic variability of mercury in ore, mine-waste calcine, and leachates of mine-waste calcine from areas mined for mercury. *Environ. Sci. Technol,* **2009,** *43,* 7331-7336.

(31) Epov, V. N.; Berail, S.; Jimenez-Moreno, M.; Perrot, P.; Pecheyran, C.; Amouroux, D.; Donard, O. F. X. Approach to measure isotopic ratios in species using multicollector-ICPMS coupled with chromatography. *Anal. Chem.* **2010,** *82,* 5652-5662.

(32) Kritee, K.; Barkay, T.; Blum, J. D. Mass dependent stable isotope fractionation of mercury during mer mediated microbial degradation of monomethylmercury. *Geochim. Cosmochim. Acta.* **2009,** *73,* 1285-1296.

(33) Boudou, A.; Ribeyre, F. Experimental study of trophic contamination of Salmo gairdneri by two mercury compounds- HgCl2 and CH3HgCl- Analysis at the organism and organ levels. *Water. Air. Soil. Pollut.* **1985,** *26,* 137-148.

(34) Pickhardt, P. C.; Stepanova, M.; Fisher, N. S. Contrasting uptake routes and tissue distributions of inorganic and methylmercury in mosquitofish (Gambusia affinis) and redear sunfish (Lepomis microlophus). *SETAC* **2006,** *25,* 2132-2142.

(35) Wang, W. X.; Wong, R. S. K. Bioaccumulation kinetics and exposure pathways of inorganic mercury and methylmercury in a marine fish, the sweetlips Plectorhinchus gibbosus. *Mar. Ecol. Progr. Ser.* **2003,** *261,* 257-268.

(36) Mason, R. P.; Reinfelder, J. R.; Morel, F. M. M. Bioaccumulation of mercury and methylmercury. *Water. Air. Soil. Pollut.* **1995,** *80*, 915-921.

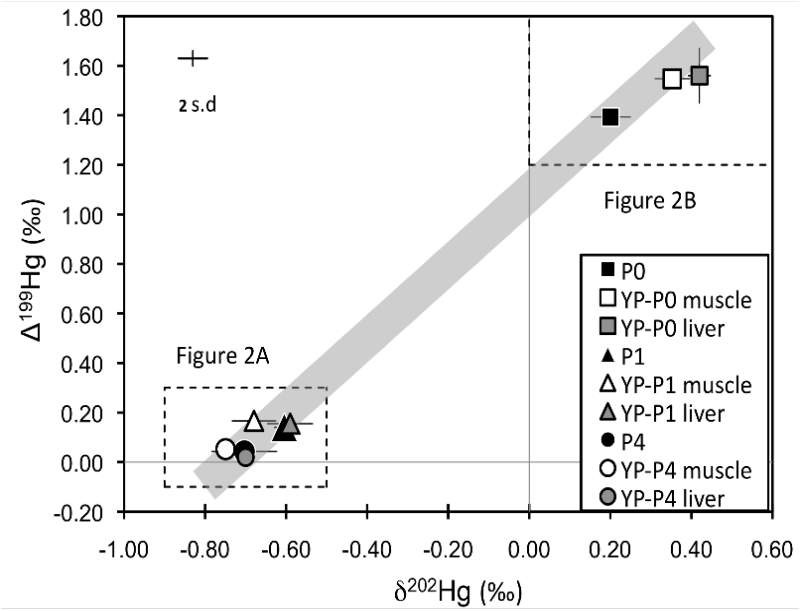

Figure 2.1 Plot of mean δ^{202}Hg and Δ^{199}Hg values from Experiment 1. The shaded line represents the mixing between 0.1 µg/g and 4.0 µg/g treatment pellets. Analytical uncertainly is indicated by the error bar (2 s.d.). Error bars on symbols are 1 s.d. of the mean of 3 food pellets, 2 liver tissues and 6 muscle tissues in each treatment. Dashed boxes show area of Figure 2.2A and 2.2B.

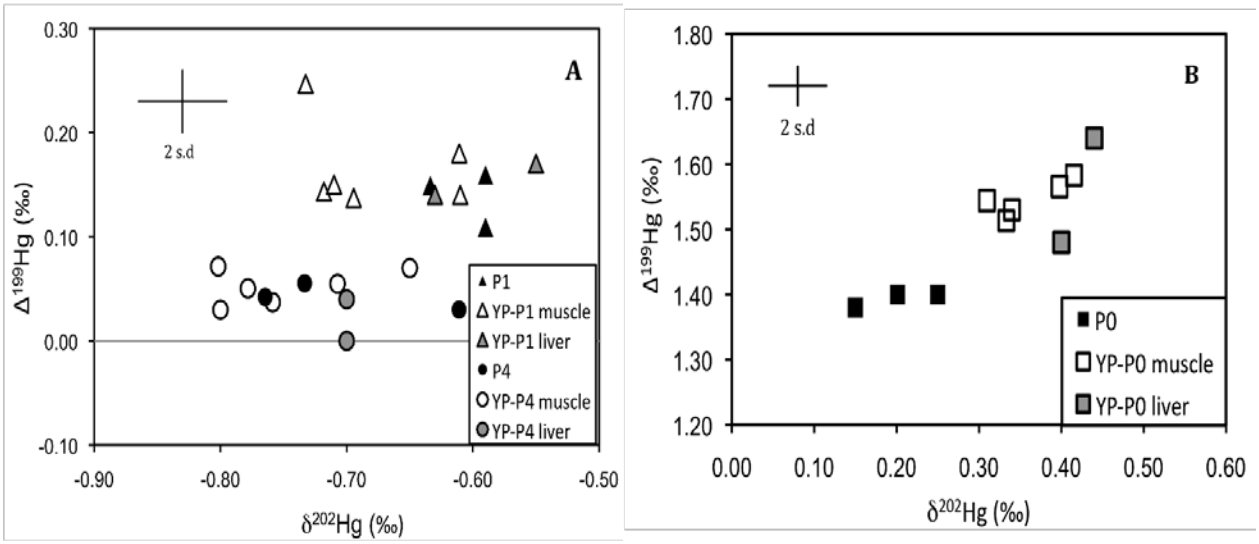

Figure 2.2 Plot of individual δ^{202}Hg and Δ^{199}Hg values from *Experiment 1*. (A) represents the 0.1 µg/g treatment and (B) represents the 1.0 and the 4.0 µg/g treatment. Each figure corresponds to the dashed boxes shown in Figure 1. Analytical uncertainty is indicated by the error bar (2 s.d.).

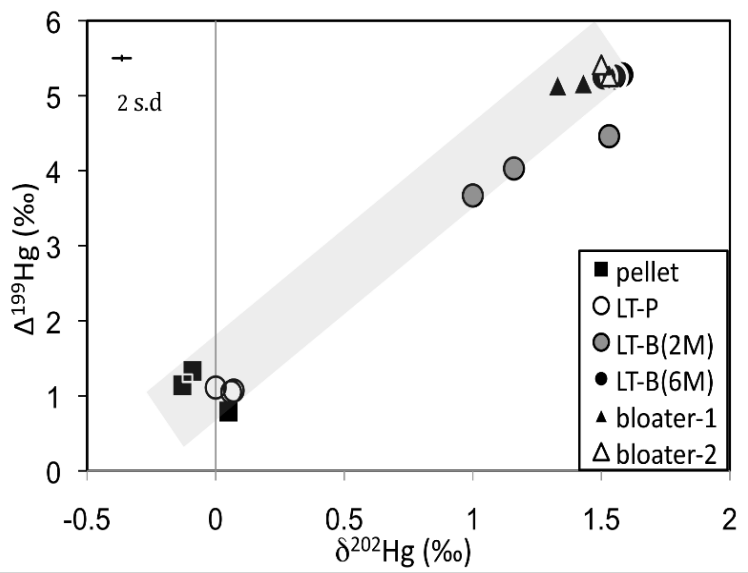

Figure 2.3 Plot of δ^{202}Hg and Δ^{199}Hg values from *Experiment 2*. The shaded line represents the mixing between the food pellets and bloater food source. Analytical uncertainty is indicated by the error bar (2 s.d).

2.4. Supporting Information

Supporting figures (Fig 2.S1A, B) and tables (Table 2.S1, S2). This material is available free of charge via the Internet at http://pubs.acs.org.

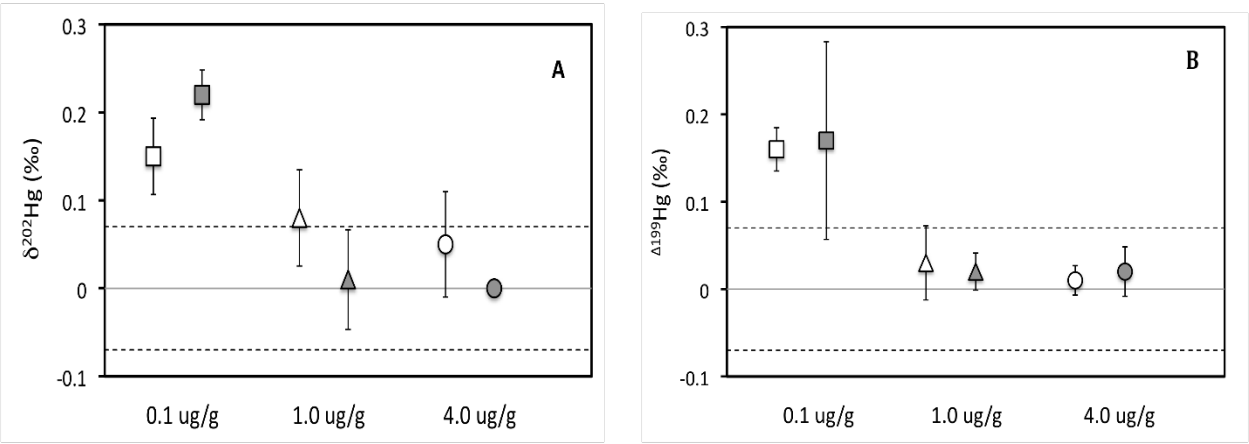

Figure 2.S1 δ^{202}Hg (A) and Δ^{199}Hg (B) differences between the mean food pellet and the mean yellow perch tissues (fish minus food). Open symbols represent the difference between the food pellet and the muscle tissues, and the shaded symbols are the difference between the food pellet and the liver tissues of YP-P0 (squares), YP-P1 (triangles), and YP-P4 (circles). Error bars on symbols are 1 s.d of the mean of 3 liver tissues and 6 muscle tissues in each treatment. Analytical uncertainty is indicated by the dash line (2 s.d).

Table 2.S1 THg concentrations (μg/g), and Hg isotopic compositions (‰) of the food pellet (P), muscle (M) and liver tissues (L) of YP-P0, YP-P1, and YP-P4 after 2-month feeding.

		THg (μg/g)	n	δ^{202}Hg (‰)	2sd	δ^{199}Hg (‰)	2sd	Δ^{201}Hg (‰)	2sd	Δ^{199}Hg (‰)	2sd
0.1 μg/g	P	0.0746	2	0.20	0.08	1.45	0.10	1.18	0.04	1.40	0.08
		0.0760	1	0.25		1.46		1.13		1.40	
		0.0763	1	0.15		1.42		1.14		1.38	
	M	0.218	2	0.42	0.12	1.69	0.14	1.29	0.10	1.58	
		0.206	2	0.33	0.06	1.60	0.06	1.26	0.04	1.51	0.10
		0.189	1	0.31		1.62		1.32		1.54	0.04
		0.213	2	0.40	0.06	1.67	0.02	1.30	0.02	1.57	
		0.206	2	0.34	0.12	1.62	0.18	1.32	0.08	1.53	0.04
		0.228	2	0.32	0.08	1.63	0.00	1.30	0.02	1.55	
	L	0.0200	1	0.44		1.75		1.50		1.64	
		0.0243	1	0.40		1.58		1.29		1.48	
1.0 μg/g	P	0.893	2	-0.63	0.04	-0.01	0.02	0.09	0.04	0.15	0.02
		0.920	2	-0.59	0.08	0.02	0.10	0.11	0.02	0.16	0.08
		1.041	2	-0.59	0.06	-0.04	0.04	0.06	0.04	0.11	0.02
	M	2.318	2	-0.72	0.02	-0.04	0.10	0.12	0.04	0.14	0.08
		2.037	2	-0.73	0.04	0.06	0.02	0.17	0.06	0.25	0.00
		2.573	2	-0.61	0.14	0.03	0.08	0.13	0.16	0.18	0.06
		2.876	2	-0.69	0.14	-0.04	0.02	0.13	0.02	0.14	0.02
		2.574	2	-0.61	0.12	-0.01	0.04	0.15	0.02	0.14	0.00
		2.882	2	-0.71	0.06	-0.03	0.10	0.09	0.16	0.15	0.08
	L	0.357	1	-0.55		0.03		0.10		0.17	
		0.313	1	-0.63		-0.02		0.13		0.14	
4.0 μg/g	P	4.10	2	-0.73	0.00	-0.13	0.02	0.03	0.08	0.06	0.02
		4.20	2	-0.76	0.06	-0.15	0.06	0.01	0.10	0.04	0.08
		4.18	2	-0.61	0.00	-0.12	0.02	-0.01	0.02	0.03	0.00
	M	12.3	2	-0.71	0.12	-0.12	0.04	0.01	0.02	0.06	0.02
		13.4	2	-0.76	0.18	-0.15	0.12	0.05	0.06	0.04	0.08
		13.0	2	-0.78	0.10	-0.15	0.06	0.07	0.16	0.05	0.04
		12.9	2	-0.80	0.02	-0.13	0.06	0.04	0.04	0.07	0.06
		15.0	2	-0.65	0.08	-0.09	0.12	0.00	0.10	0.07	0.10
		13.6	2	-0.80	0.22	-0.17	0.16	0.04	0.02	0.03	0.10
	L	3.46	2	-0.70	0.12	-0.18	0.06	-0.02	0.02	0.00	0.08
		4.08	2	-0.70	0.08	-0.13	0.00	0.04	0.04	0.04	0.02

Table 2.S2 THg concentrations (μg/g), Hg isotopic compositions (‰) of the food pellet (P), LT-P, bloater-1 (B1), bloater-2 (B2), LT-B(2M) and LT-B(6M).

	THg (μg/g)	n	δ^{202}Hg (‰)	2sd	δ^{199}Hg (‰)	2sd	Δ^{201}Hg (‰)	2sd	Δ^{199}Hg (‰)	2sd
P	0.0261	2	0.05	0.16	0.80	0.18	0.57	0.12	0.79	0.14
	0.0280	2	-0.09	0.02	1.31	0.30	1.04	0.06	1.33	0.32
	0.0261	2	-0.13	0.44	1.10	0.14	0.84	0.28	1.14	0.02
LT-P	0.106	1	0.07		1.08		0.67		1.07	
	0.112	2	0.00	0.02	1.12	0.02	0.78	0.16	1.11	0.00
	0.114	2	0.06	0.12	1.07	0.16	0.93	0.30	1.05	0.12
B1	0.311	2	1.43	0.04	5.53	0.02	4.04	0.02	5.17	0.00
	0.312	2	1.33	0.08	5.47	0.06	3.99	0.00	5.14	0.06
B2	0.467	2	1.50	0.00	5.79	0.04	4.22	0.18	5.41	0.04
	0.459	2	1.53	0.06	5.81	0.02	4.11	0.08	5.25	0.02
LT-B(2M)	0.166	1	1.53		4.84		3.53		4.46	
	0.119	1	1.00		3.92		2.85		3.67	
	0.128	1	1.16		4.32		3.19		4.03	
LT-B(6M)	0.297	2	1.55	0.08	5.64	0.20	4.09	0.02	5.25	0.08
	0.321	2	1.51	0.06	5.63	0.04	4.11	0.08	5.25	0.02
	0.329	2	1.58	0.12	5.68	0.04	4.12	0.06	5.28	0.00

CHAPTER 3

Application of mercury isotopes for tracing trophic transfer and internal distribution of mercury in marine fish feeding experiments

Abstract

We performed feeding experiments to investigate mercury (Hg) isotope fractionation during trophic transfer and internal distribution of total Hg (THg) in marine fish upon exposure to natural seafood. Young-of-the-year amberjack (*Seriola dumerili*) were fed with either blackfin tuna (*Thunnus atlanticus*) (2647 ng/g THg) or brown shrimp (*Farfantepenaeus aztecus*) (25.1 ng/g THg) for 80 and 50-days, respectively, and dissected for muscle, liver, kidney, brain, and blood. After 30 days of consuming tuna, Hg isotopes (δ^{202}Hg and Δ^{199}Hg) of the amberjack organs shifted to the tuna value (δ^{202}Hg= 0.55 ‰, Δ^{199}Hg= 1.54 ‰,), demonstrating the absence of Hg isotope fractionation. When amberjack were fed a shrimp diet, there was initial mixing of the amberjack organs toward the shrimp value (δ^{202}Hg= -0.48 ‰, Δ^{199}Hg= 0.32 ‰), followed by a cessation in further shifts in Δ^{199}Hg and a small shift in δ^{202}Hg. We attribute the failure of Δ^{199}Hg to reach the value of the shrimp diet to a reduction in Hg bioaccumulation from shrimp due to feeding inhibition, and the δ^{202}Hg shift to a small internal fractionation during excretion. Given that the feeding rate and Hg concentration of the diet can influence internal Hg isotope distribution, these parameters need to be considered in biosentinel fish studies.

3.1. Introduction

Monomethylmercury (MMHg) in aquatic environments is a major health concern due to its persistence, bioaccumulation and toxicity (*1*). Fish consumption is the most important pathway for human exposure to MMHg (*1*) and it is estimated that over 75% of the global fisheries product originates from marine environments (*2*). Despite the health risks posed to humans

consuming fish, there are still many unanswered questions about the sources, bioaccumulationand transport of MMHg to natural marine food webs as well as the internal processing of dietary Hg by marine organisms. Linking the bioaccumulated Hg in marine food webs to sources of Hg in the environment is a considerable challenge, in part, due to the complex biogeochemistry of Hg in the ocean. Mercury isotopic analyses of fish tissues are increasingly being used to infer sources of Hg to aquatic food webs and to provide evidence of biogeochemical pathways of Hg in aquatic systems (*3-6*). Lack of controlled experiments characterizing trophic transfer to marine food webs limits the interpretation of Hg isotopes in natural environments. In this study we performed feeding experiments to investigate Hg isotope fractionation during trophic transfer and internal distribution of total Hg (THg) in marine fish upon exposure to diets composed of naturally accumulated Hg from two distinct marine environments (estuarine and offshore).

Stable Hg isotopes can vary in the environment due to fractionation during reactions and by mixing of isotopically distinct reservoirs. Hg isotopes undergo two different types of fractionation. In mass-dependent fractionation (MDF), the degree of fractionation depends on the relative mass of the isotopes and is similar to other light stable isotope systems (such as nitrogen and carbon). Differences in MDF are reported as δ^{202}Hg in units of permil (‰) (*7*). Some of the environmental processes known to cause MDF include biotic methylation (*8*), demethylation (*9*), and photochemical reactions (*10*). Mass-independent fractionation (MIF) is thought to occur via the magnetic isotope effect (MIE) (*11*) and to a lesser extent the nuclear volume effect (NVE) (*12*) primarily in odd-mass number Hg isotopes. MIF is the deviation in isotope ratios from the theoretical prediction for MDF and is reported as Δ^{199}Hg and Δ^{201}Hg (‰) (*7*). Large magnitude MIF (>0.5‰) has only been documented during photochemical reduction and degradation of inorganic Hg (IHg) and MMHg (*10, 13*). Because Δ^{199}Hg and Δ^{201}Hg have been shown to be directly proportional to the degree of photochemical demethylation, they have been used to estimate the extent of MMHg photodegradation in many natural ecosystems (*3-5, 14*). The ratio of Δ^{199}Hg/Δ^{201}Hg may also be used to distinguish the degree of photochemical reduction and degradation of either IHg (Δ^{199}Hg/Δ^{201}Hg = 1.00) or MMHg (Δ^{199}Hg/Δ^{201}Hg = 1.36) (*10*). MIF of even-mass isotopes has also recently been reported in some atmospheric samples, but the mechanism producing this effect is not yet well understood (*15, 16*).

The fact that the odd-mass number Hg isotopes fractionate primarily via photochemical reactions makes then very useful as a tracer for monitoring MMHg during trophic transfer and bioaccumulation. A recent experimental study documented an absence of δ^{202}Hg and Δ^{199}Hg fractionation of MMHg during trophic transfer to juvenile freshwater fish (*17*). Other ecosystem level studies have also observed similar Δ^{199}Hg between closely linked prey and predators (e.g., pelagic sculpin and seal) and have suggested that Δ^{199}Hg is unlikely to fractionate via internal metabolic processes (*18*). Terrestrial plants such as lichens, rice and aspen tree foliage have also demonstrated an absence of Δ^{199}Hg fractionation during internal metabolic processes (*19-21*). Aside from the potential utilization of Δ^{199}Hg as a tracer, the influence of metabolic processes and the physiological state of fish on the fractionation of δ^{202}Hg needs to be further explored.

In this study, marine fish of the species *Seriola dumerili*, (common name greater amberjack, AJ) were exposed to diets of *Thunnus atlanticus* (common name blackfin tuna) and *Farfantepenaeus aztecus* (common name brown shrimp) in captivity. Amberjack are a marine reef-associated fish that are common in the northern Gulf of Mexico. They are known for their rapid growth rate and adaptability in captivity. At an early life stage they are often found in association with *Sargassum* patches where they feed on shrimp, small crabs and other small fishes. As they grow, they become aggressive predators and feed primarily on fishes (such as scad and blue runner) and invertebrates (*22*). Due to the difference in their trophic levels and feeding habitat, using tuna and shrimp as food sources allowed us to compare the effects on AJ of consuming high and low Hg food sources from the Gulf of Mexico. We monitored the rate of isotopic adjustment of various organs in the AJ to a changing diet and determined whether isotopic fractionation occurred between organs due to internal metabolic processes.

3.2. Material and methods

3.2.1. Experimental design

Young-of-the-year amberjacks (AJ) were caught in surface waters using sabike rig fishing lures and were fished around *Sargassum* weedlines formed in offshore waters of the Gulf of Mexico, located approximately 20 miles north of the Brutus Oil Rig (27’ 47.4286’’ N, 90’ 38.5115’’ W) and 165 miles southwest of New Orleans. The juvenile AJ were reared in a recirculating seawater system at the Louisiana University Marine Consortium marine center (LUMCON) from June to August of 2011. The tanks were maintained at temperatures of 22 to

30°C, pH of 8.0 to 8.8, and salinity of 23 to 30 ng/L throughout the experimental period. AJ were divided into two treatment tanks, each containing 25 individuals, and fed with either blackfin tuna (hereafter referred to as tuna) or brown shrimp (hereafter referred to as shrimp) to apparent satiation for a total of a 50- or 80-day period, respectively. The tuna were also caught near the Brutus Oil platform but at much greater depths (~1000 m) compared to AJ. The shrimp were caught in the bayous of Terrebonne Parish, LA (29’ 22.9968’’ N, 90’ 75.3281’’ W), located two miles to the west of LUMCON. The tuna and shrimp diets were prepared by removing the skin and exoskeleton respectively, and cutting only the muscle tissues into small pieces and freezing them for later use.

Three to five AJ were sacrificed at different time periods during the course of the feeding experiment (Table 1). On the day that AJ were first caught, five fish were randomly selected as a wild control (referred to as day 0). Three to five AJ were sacrificed each at day 10, 30, and 50 after consuming the tuna diet (referred to as AJ(T)). AJ that were fed with the shrimp diet (referred to as AJ(S)) were sacrificed at day 10, 30, 50, and 80.

Fish were measured for total length and wet weight prior to dissection and the extraction of muscle, liver, brain, kidney and blood at each time period. The dissection was performed by anesthetizing the fish with 1.5mL of a clove oil solution (10:1 ethanol to clove oil) diluted in 1 gallon of seawater. The caudal fin was removed to drain the blood into acid washed glass vials. Muscle, liver, brain and kidney were dissected using a stainless steel scalpel and scissors. For convenience, all components dissected in this study (muscle, liver, brain, kidney, and blood) will be referred to as “organs”. All the tools were thoroughly wiped with a paper wipe and cleaned with distilled water and alcohol between samples to avoid contamination. Each organ was placed in a pre-weighed plastic bag or acid washed glass vial to obtain wet weights. The organs were then frozen at -20 °C, freeze-dried, and further homogenized with mortar and pestle for Hg concentration and stable Hg isotope analyses at the University of Michigan (see below). All THg concentrations are reported based on dry weight except for blood.

3.2.2. Total mercury concentration analysis

Organs from individual fish generally did not contain enough Hg for isotopic analysis and, therefore, composite samples were made from the organs of the three to five individuals sacrificed at each time period. For muscle samples, both individual and composite samples were

analyzed since there was enough Hg in muscle to run individual fish. The THg concentrations were determined by Atomic Absorption Spectroscopy (AAS) following combustion at 800ºC using a Nippon Instruments MA-2000 Hg analyzer. Standard solutions of NIST SRM 3133 were used to obtain calibration curves and for quality assurance and quality control. The values of replicate analyses were always within 5%. Three standard reference materials, ERM CE 464 (average measured THg= 4232 µg/g, n=8) NRCC DOLT-2 (2193 µg/g, n=3) and NRCC DORM-3 (362 µg/g, n=8) were also analyzed along with the samples and agreed within 10% of certified values.

3.2.3. Methylmercury analysis

MMHg concentrations were analyzed for the shrimp and tuna diet as well as the muscle, liver, kidney and brain of AJ(S) at day 0 and 80 either at Wayne State University or the Metropolitan Council Environmental Services, St. Paul, Minnesota, using an aqueous distillation method (*23*). Briefly, the samples were digested with 4.6M nitric acid (HNO_3) at 60°C for 12hr and distilled at 140°C in Teflon distillation vessels. Distillates were added to 4.5M potassium hydroxide (KOH) and sodium tetraethylborate (NaTEB) for aqueous-phase derivitization and collection of Hg on Tenax traps. After the separation of Hg species using a gas chromatography column, MMHg and IHg were converted to Hg^0 and analyzed using Cold-Vapor Atomic Fluorescence Spectroscopy (CVAFS). Reagent blanks and standard reference material NRCC TORT-2 were included between samples for quality assurance. The reagent blanks showed no detectable MMHg and the recoveries of TORT-2 ranged between 91-107% (n= 8). The proportion of THg that occurs as MMHg is reported as %MMHg.

3.2.4. Mercury isotope analysis

Samples were weighed and loaded into ceramic boats with alternating layers of sodium carbonate and aluminum oxide powders that were baked out in a muffle furnace at 750°C overnight before use to assure low Hg blanks. The powders stabilize the combustion products and assure retention in the first stage of the furnace. The ceramic boats were loaded into an offline two-stage combustion furnace system. In the first combustion compartment, the samples were heated to 750°C over a 6-hour period to release all Hg (as Hg^0). Mercury-free oxygen was used to transport Hg^0 to the second combustion compartment maintained at 1000°C and

subsequently to an oxidizing "trap solution" of 1% $KMnO_4$ in 10% trace metal grade H_2SO_4, which was purged with Hg-free argon gas for 4 hours before use. To remove potential matrix components from samples, the trap solutions containing the oxidized Hg^{2+} were neutralized using hydroxylamine, reduced back to Hg^0 by addition of $SnCl_2$ and purged into another trap solution.

The procedural blanks were prepared by combusting only the combustion powders (without the sample) in a ceramic boat, transferring to a clean trap solution and measuring for THg before and after the transfer steps. The blanks had an average of 0.3±0.1 ng THg (*n*= 6). Measuring the THg concentrations of the trap solutions after both the combustion and transfer steps also allowed monitoring of the recoveries of THg during the combustion and transfer processes. The standard reference materials ERM CE 464 (n= 5) and NRCC DOLT-2 (n= 3) were also combusted and transferred in the same manner as the samples to monitor the recoveries of THg. The recoveries of the combustion and transfer steps of the samples and standard reference materials ranged between 97 and 106% and between 96 to 106%, respectively.

A Nu Instruments multi-collector inductively coupled plasma mass spectrometer (MC-ICP-MS) was used to measure Hg isotope ratios at the University of Michigan. The trap solutions were neutralized using hydroxylamine and diluted to between 1 and 5 ng/g, using the same neutralized trap solution matrix, to match the THg concentration of the sample to the standards. Hg was introduced to the MC-ICP-MS as Hg^0 by reducing Hg^{2+} to Hg^0 with $SnCl_2$, and separating Hg^0 from solution using a frosted glass tip phase separator. On-peak zero corrections were applied. Instrumental mass bias was corrected using an internal Tl standard (NIST SRM 997) and by bracketing each sample with NIST SRM 3133 matched to sample THg concentrations and matrix composition. MDF is reported as $\delta^{202}Hg$ in permil (‰) referenced to NIST SRM 3133:

$$\delta^{202}Hg = \{[(^{202}Hg/^{198}Hg)_{sample}/ (^{202}Hg/^{198}Hg)_{NIST3133}]-1\}*1000. \quad (1)$$

MIF represents the difference between the measured $\delta^{xxx}Hg$ value and the value predicted based on MDF and the $\delta^{202}Hg$ value. MIF is reported as $\Delta^{199}Hg$ and $\Delta^{201}Hg$ in permil (‰). The calculation is based on an approximation valid for δ <10‰ [7]:

$$\Delta^{199}Hg = \delta^{199}Hg - (\delta^{202}Hg * 0.252) \quad (2)$$

$$\Delta^{201}Hg = \delta^{201}Hg - (\delta^{202}Hg * 0.752) \quad (3)$$

Analytical uncertainty at 2 s.d. was estimated based on either replicate analysis of a standard solution (UM-Almáden) or on replicate analyses of procedural standards. In this study, we used ERM CE 464 to report analytical uncertainty since it had a larger uncertainty. UM-Almáden (n= 40) had mean values (±2 s.d.) of $\delta^{202}Hg$= -0.57±0.10 ‰, $\Delta^{201}Hg$= -0.03±0.06 ‰, and $\Delta^{199}Hg$= -0.02±0.06 ‰. Standard reference material ERM CE 464 (n=5) had mean values of $\delta^{202}Hg$= 0.65±0.10 ‰, $\Delta^{201}Hg$= 1.93±0.08 ‰, and $\Delta^{199}Hg$= 2.34±0.10 ‰; and DOLT-2 (n=3) had mean values of $\delta^{202}Hg$= -0.52±0.04 ‰, $\Delta^{201}Hg$= 0.59±0.06 ‰, and $\Delta^{199}Hg$= 0.70±0.08 ‰.

3.3. Results

AJ(T) and AJ(S) demonstrated a considerable variation in total body mass and fork length within each time period (Table 1). The total body mass and the fork length of AJ at day 0 varied by 2.6 and 1.4 fold, respectively, and the variation persisted to a similar extent over the course of the experiment. The experiment was not designed to monitor the changes in body mass and length over time. Instead, AJ with a variety of sizes were selected randomly for the determination of the internal Hg isotope distribution. Though the variability is too large to accurately estimate the growth rate, the fact that the composite and individual samples show similar THg concentrations and Hg isotope behaviors suggests that fish size does not significantly affect the internal distribution of Hg isotopes (see results below).

3.3.1. Total mercury concentrations in Amberjack

The average THg concentrations in the tuna and shrimp diets were 2647±66 ng/g (n= 3, 1 s.d) and 25.1±3.3 ng/g (n= 3, 1 s.d), respectively; similar to values reported in other studies from the Gulf of Mexico (*5*, *24*). Prior to the consumption of these diets (day 0), the AJ muscle, liver, kidney, brain and blood had THg concentrations of 75.1, 44.7, 49.9, 12.0 and 1.70 ng/g respectively. The individual sample of AJ muscle had THg concentration of 75.3 ng/g, which was similar to the composite sample. With consumption of either the tuna or shrimp diets in captivity, the THg concentration of AJ(T) and AJ(S) organs increased rapidly with time (Figure 1). To assess the extent of Hg bioaccumulation in each organ of AJ(T) and AJ(S) at different time periods, we calculated the bioaccumulation factor (BAF) (the ratio of THg concentration in

each organ to the THg concentration in the diet—tuna or shrimp) (Table 2). The AJ(T) and AJ(S) muscle demonstrated the highest BAF at day 10. After day 10, the highest BAF was observed in the kidney and the lowest BAF in the blood of AJ(T) and AJ(S). At the end of the experimental period (day 50 and 80, respectively), the THg concentrations in AJ(T) were ranked by decreasing order: kidney (4400 ng/g) > brain (3682 ng/g) > muscle (3201 ng/g composite, 3299 ng/g individual) >liver (2331 ng/g) >blood (277 ng/g) and THg concentrations in AJ(S) were ranked by decreasing order: kidney (235 ng/g) > muscle (215 ng/g composite, 187 ng/g individual) > liver (139 ng/g) > brain (63.7 ng/g) > blood (12.6 ng/g) (Figure 1). The THg concentrations in the AJ(S) liver, brain and blood decreased by 5%, 16%, and 22%, respectively, between day 50 and 80 (Figure 1). This was accompanied by a reduction of BAFs for the AJ(S) liver, brain and blood (Table 2).

3.3.2. Hg isotopic compositions in the diets

The δ^{202}Hg and Δ^{199}Hg values of Hg in the tuna were significantly higher compared to the shrimp diet (Figure 2a, 3a). The average isotopic composition of the tuna diet was δ^{202}Hg= 0.55±0.05 ‰ and Δ^{199}Hg= 1.54±0.01 ‰ (n=3, 1 s.d) and the shrimp diet was δ^{202}Hg= -0.48±0.05 ‰ and Δ^{199}Hg= 0.32±0.05 ‰ (n=3, 1 s.d). In the tuna virtually all of the THg was MMHg (>99%) and in the shrimp 80% of the THg was MMHg.

3.3.3. Hg isotopic compositions in Amberjack

The AJ muscle, liver and blood at day 0 displayed a range of δ^{202}Hg values from 0.38 to 0.59 ‰ and a range of Δ^{199}Hg values from 1.63 to 3.26 ‰. The brain and kidney could not be measured for Hg isotopes at day 0 due to the small amount of material. At day 0 the liver, brain, and kidney contained 41%, 47% and 39% of THg as MMHg (% MMHg), respectively. The muscle had >99% of THg as MMHg. We plotted percent of THg as MMHg (% MMHg) against Δ^{199}Hg for the AJ muscle, blood and liver to test whether the ratio of % MMHg to THg explained the observed Δ^{199}Hg variation in the AJ organs (Figure 4). The % MMHg in blood was estimated using values from the literature, which report approximately 90% of THg as MMHg in the blood of marine fish (*25, 26*). The % MMHg and Δ^{199}Hg of the AJ muscle, blood and liver demonstrated a strong correlation (r^2= 0.96). Although our estimate of the isotopic composition of IHg is based only on a simple linear extrapolation, it is likely that MMHg and IHg have

different Hg isotopic compositions and the extent of MMHg bioaccumulation in the various organs of the AJ explains the variation of Δ^{199}Hg at the start of the experiment.

3.3.4. Tuna treatment

Because of the difference in the Hg isotopic composition of AJ organs at day 0, and the different rate of Hg isotope re-equilibration of the organs to the new food source, two mixing lines were plotted: 1) between the tuna diet and the AJ muscle, and 2) between the tuna diet and the AJ blood at day 0 (Figure 2). The mixing lines are described by the equation $^{XXX}Hg_{mixture} = {}^{XXX}Hg_{tuna}\, f_{tuna} + {}^{XXX}Hg_{organ0}\, f_{organ0}$, where ^{XXX}Hg represents either δ^{202}Hg or Δ^{199}Hg, and f represents the fraction of THg concentration in either the tuna or the organs of AJ(T) at day 0. After 10 days of consuming the tuna diet, the isotopic compositions of AJ(T) composite samples of muscle, liver, kidney, brain, and blood shifted to values close to the tuna value. The isotopic composition of Hg in a single AJ(T) individual's muscle did not shift appreciably after 10 days (Figure 2). By day 30, the isotopic compositions of Hg in all organs including another individual's muscle had became nearly equal to the isotopic composition of the tuna diet. Only minor changes were observed in both δ^{202}Hg and Δ^{199}Hg of the AJ(T) organs (within the analytical uncertainty) at day 50.

3.3.5. Shrimp treatment

For AJ fed a shrimp diet, two mixing lines were plotted: 1) between the shrimp diet and the AJ muscle, and 2) between the shrimp diet and the AJ liver at day 0 (Figure 3). After consuming the shrimp diet for a 10-day period, the isotopic composition of Hg in the AJ liver, kidney and blood shifted towards the isotopic composition of the shrimp diet. After a 30-day period, we observed a cessation in the changes of Δ^{199}Hg and a small shift of δ^{202}Hg (+0.35 ‰) away from the mixing line for the liver, kidney and blood; they did not reach the isotopic composition of the shrimp diet. The brain of AJ(S), which did not have enough material to be analyzed for day 0 and 10, displayed an isotopic compositions similar to other organs after 30 days. From day 50 and to the end of the experimental period, the AJ organs showed only minor changes with time in δ^{202}Hg and Δ^{199}Hg (within the analytical uncertainty). The AJ(S) muscle (composite and individual) demonstrated a delayed response compared to other organs throughout the experimental period, and the isotopic composition of AJ(S) muscle did not shift away from the

mixing line until after day 50. At the end of the 80-day period, the liver and kidney contained 38%, and 22%, respectively, of their THg as MMHg. The muscle and brain contained entirely MMHg (>99%).

3.3.6. Photochemical degradation of Hg in the Gulf of Mexico

The experimentally determined $\Delta^{199}Hg/\Delta^{201}Hg$ ratio has been used to distinguish the extent of photochemical reduction of Hg(II) ($\Delta^{199}Hg/\Delta^{201}Hg$= 1.00±0.01) or photochemical degradation of MMHg ($\Delta^{199}Hg/\Delta^{201}Hg$= 1.34±0.04) [10]. We calculated the $\Delta^{199}Hg/\Delta^{201}Hg$ in AJ at day 0 prior to the consumption of either shrimp or tuna diet, and AJ(S) and AJ(T) after the feeding experiments. The $\Delta^{199}Hg/\Delta^{201}Hg$ in AJ at day 0, AJ(S) and AJ(T) were 1.24±0.04 (1 sd), 1.28±0.11 and 1.23±0.02, respectively. Values for the AJ in this study are lower than the experimental MMHg degradation value determined in freshwater experiments using riverine dissolved organic carbon by Bergquist and Blum [10] but consistent with other marine fish (including fish from the Gulf of Mexico) reported previously ($\Delta^{199}Hg/\Delta^{201}Hg$ of ~1.2) [3,5]. We suggest that the MIF observed in the fish tissues is due to photochemical degradation of MMHg prior to entry into the Gulf of Mexico marine food web.

3.4. Discussion

3.4.1. Hg isotopic compositions of the diets and of Amberjack before feeding

The tuna collected from the offshore region display significantly higher $\delta^{202}Hg$ and $\Delta^{199}Hg$ compared to the shrimp collected from the coastal region of the Gulf of Mexico. This suggests that the tuna and the shrimp obtain Hg from different sources, or that the Hg to which they are exposed has been fractionated by different biogeochemical processes. Previous studies that have reported spatial patterns of $\delta^{202}Hg$ and $\Delta^{199}Hg$ in fish and sediments suggested that Hg isotopes can be used to distinguish different Hg sources (*3, 5, 27*). Senn et al (*5*), in particular, found higher $\delta^{202}Hg$ and $\Delta^{199}Hg$ in offshore fish species compared to coastal fish species in the Gulf of Mexico and attributed this to the uptake of MMHg (by offshore food webs) that was subjected to a higher degree of photochemical degradation than MMHg taken up by coastal food webs. In fact, the isotopic compositions of Hg associated with coastal fishes ($\delta^{202}Hg$= -0.54±0.32 ‰ and $\Delta^{199}Hg$= 0.53±0.11 ‰) and offshore species such as the blackfin tuna ($\delta^{202}Hg$= 0.41±0.18 ‰ and

Δ^{199}Hg= 1.75±0.48 ‰) and juvenile yellowfin tuna (δ^{202}Hg= 0.54±0.15 ‰ and Δ^{199}Hg= 2.39±0.30 ‰) in the Gulf of Mexico (*5*) are in excellent agreement with the isotopic composition of the shrimp and tuna diets used in our study.

Within the offshore region where both AJ and tuna were collected, the tuna and the AJ organs at day 0 demonstrated a similar range of δ^{202}Hg but considerably different Δ^{199}Hg, with tuna displaying lower Δ^{199}Hg compared to the average Δ^{199}Hg of the AJ organs (muscle, liver, blood). Recent studies have shown increasing Δ^{199}Hg in organisms occupying decreasing water column depth in both lakes (*14*) and marine environments (*28*). Sherman and Blum (*6*) also observed a relationship between secchi depth (a measure of light penetration) and Δ^{199}Hg values among multiple lakes in Florida such that the fish inhabiting lakes with greater light penetration displayed higher Δ^{199}Hg values. Given that juvenile AJ were caught in the surface waters and adult tuna at much greater depths, the differences in the feeding depth and thus the degree of photochemical demethylation in the water column may explain the within habitat variation of Δ^{199}Hg among AJ and tuna. The similar range of δ^{202}Hg in the tuna and the AJ organs is consistent with the offshore region of the Gulf of Mexico receiving the same source of Hg prior to being subjected to photochemical degradation in different parts of the water column.

Variability was observed in Δ^{199}Hg among the AJ organs at day 0 (Figure 4). One explanation for this could be changes in the Δ^{199}Hg of food sources prior to capture of AJ, coupled with differences in the residence time of Hg in different organs. However, a strong correlation between % MMHg and Δ^{199}Hg of the AJ organs suggests that a difference in Δ^{199}Hg between MMHg and IHg in food sources (*17*), and a varying extent of MMHg versus IHg bioaccumulation in different organs may also provide an explanation for the Δ^{199}Hg variability in the specific organs of the AJ.

3.4.2. Tuna treatment

When AJ consumed the tuna diet, which had 35 times higher THg concentration compared to the initial AJ muscle and was composed mainly of MMHg, there was a dramatic shift in the Hg isotopic composition of the AJ(T) organs towards the tuna value within 10 days of the beginning of the feeding experiment. The isotopic composition of all AJ(T) organs nearly equaled the isotopic composition of the tuna diet within 30 days of consuming the tuna. A

previous study in which food pellets spiked with MMHg were fed to juvenile yellow perch, and bloater (86% MMHg) was fed to lake trout, also demonstrated direct transfer of the Hg isotopic composition of the food to fish (*17*) and attributed this to the rapid assimilation and trophic transfer of MMHg. Similarly, in this study, the uptake of a naturally high MMHg tuna diet, which led to the rapid increase in THg concentrations in the AJ(T) organs, appears to have caused rapid re-equilibration of the Hg isotopic composition of the internal organs to the new food source.

It is interesting to note the similarity in the patterns of the Hg isotope distribution between organs that we observe, and previous studies from the literature. Pharmacokinetic studies have documented rapid transfer of MMHg to the visceral organs (liver, kidney, spleen, gill) via blood and a much slower turnover of Hg in the muscle (25, 29, 30), which is what we observed in our feeding experiments (Figure 2). A number of radiotracer studies that exposed both adult freshwater and saltwater fish to experimental diets spiked with MMHg suggested that it requires approximately ~30 days for MMHg to be detected in fish muscle (29, 30), which is consistent with our study. Thus, with the demonstrated efficient assimilation of high MMHg diets, we can expect to observe an absence of Hg isotope fractionation in major fish organs upon internal distribution and trophic transfer of a high-MMHg diet.

3.4.3. Shrimp treatment

Amberjack fed with shrimp, which had a THg concentration 105 times lower than the tuna food source, displayed substantially different patterns of internal distribution of Hg isotopes. During the first 10 days of the feeding experiment, increases in the THg concentrations of the AJ(S) organs were accompanied by mixing of the Hg isotopic compositions between the values of the AJ(S) organs and the shrimp diet, indicating that bioaccumulation of shrimp-Hg was taking place without isotope fractionation. After the 30-day period however, there was a cessation in further shifts in Δ^{199}Hg toward the shrimp value and a small shift in δ^{202}Hg by ~0.35 ‰ in the AJ(S) organs away from the mixing line. We attribute the cessation of changes in Δ^{199}Hg to the reduction in the feeding rate of AJ(S), and the small shift of δ^{202}Hg to a small internal fractionation of δ^{202}Hg.

As discussed in the previous section, Δ^{199}Hg is the best indicator for monitoring the trophic transfer of MMHg and mixing of two isotopically distinct reservoirs of Hg, because internal

metabolic processes are unlikely to cause any fractionation of Δ^{199}Hg (*9*, *17*). The fact that Δ^{199}Hg of the AJ(S) organs ceased to mix with the shrimp diet and displayed only minor changes after the 30-day period suggest that the Hg associated with the shrimp was no longer effectively being transferred to the AJ(S). We suggest that this is most likely caused by the stress-related feeding inhibition behavior among AJ(S). After 30 days of the feeding experiment, AJ(S) began to refuse the shrimp diet and reached mortality close to the end of the experiment. Thus, given the low THg concentration in the shrimp diet and decrease in the feeding rate of AJ(S), the bioaccumulation of shrimp-Hg may have been too small to cause a measureable additional shift in the Δ^{199}Hg of AJ(S) organs.

It may be possible that with different isotopic compositions of IHg and MMHg, a shift in the differential uptake and excretion of these two Hg species could lead to the observed δ^{202}Hg shift in the AJ(S) organs. However, in order for such a large shift to occur via the uptake or excretion of IHg the shrimp diet would need to contain a large proportion of THg as IHg, which is not what we observe. While we can assume that the isotopic composition of the AJ(S) muscle at day 80 reflects the isotopic composition of bioaccumulated MMHg (> 99% THg as MMHg), this isotopic composition cannot be used to estimate the isotopic composition of IHg in the shrimp diet given the potential fractionation of δ^{202}Hg during internal metabolism and uptake (*8*, *9*). Kritee et al (*9*) observed a kinetic fractionation of δ^{202}Hg, but not in Δ^{199}Hg, during the microbial demethylation of MMHg such that the reactant (MMHg) became enriched in heavier δ^{202}Hg compared to the product (IHg). A number of studies have shown evidence for microbial transformation of Hg species in the intestines of fish (*31*) and in aquatic sediments (*32*). Thus, one possible scenario is that there is microbial demethylation of MMHg in the AJ(S) intestines followed by preferential trophic transfer of the remaining (higher δ^{202}Hg) MMHg to the internal organs of AJ(S), with excretion of the low δ^{202}Hg IHg-product from the body. This somewhat speculative scenario will require testing with further experiments.

With reduction in the feeding rate, it is possible that remobilization of fat and protein from liver and muscle tissues during starvation (*33*) may have facilitated the excretion of MMHg, leading to the small fractionation of δ^{202}Hg in the AJ(S) organs. Though we do not have physiological evidence to support remobilization from the AJ(S) organs, decrease in the THg concentrations and BAFs in the liver, brain, and blood after day 50 indicate that the Hg

bioaccumulation began to slow and excretion may have been enhanced in AJ(S). In fact, the reduction in THg concentrations in the visceral organs followed by the redistribution of Hg to the storage organs (muscle and kidney) has been observed repeatedly in Hg elimination studies in fish (*29, 34*), which is consistent with what we observed in the AJ(S) organs with time. If this is the case, we expect that MMHg with lower δ^{202}Hg, which is generally more reactive (*9*), would be preferentially excreted while the heavier Hg isotopes remain in the organs, thus leading to the enrichment of δ^{202}Hg in the AJ(S) organs during the excretion. As a side note, Laffont et al (*35*) reported an enrichment of δ^{202}Hg by 2 ‰ in human hair compared to a dietary source of MMHg from fish, which implies that internal processes in mammals can in some instances lead to the fractionation of δ^{202}Hg.

In summary, it appears that the consumption of a low-Hg shrimp diet and changes in the physiological state allowed the detection of incomplete turnover and mixing of MMHg in the AJ(S) organs and a small internal fractionation of δ^{202}Hg. This is in contrast to the experiments reported herein for a high-Hg tuna diet and for a previous study of freshwater fish (*17*), which reported an absence of δ^{202}Hg and Δ^{199}Hg fractionation during trophic transfer and the complete re-equilibration of the AJ(T) organs upon exposure to a high-MMHg diet. It is important to emphasize that the major differences between the experiments is the THg concentration in the diet and the feeding rate of the fish. Thus, our study suggests that while the active consumption of a high-MMHg diet results in rapid turnover in all organs of fish to the isotopic composition of a new food source through efficient MMHg assimilation, reduction in Hg bioaccumulation and feeding rate caused by changes in the physiological state of fish can lead to incomplete shift of Hg isotopes to a new food source.

3.4.4. Application of Hg isotopes in natural marine systems

The behavior of stable Hg isotopes during the trophic transfer and internal distribution of Hg in marine fish has been explored in this study. Previous studies using radiotracers offered quantitative estimates of the extent of trophic transfer and assimilation of dietary Hg in various species of fish (*36, 37*). The application of stable Hg isotopes provides unique insight into the sources of Hg to fish and the processes of trophic transfer of Hg in fish consuming natural diets. The ability to identify sources and monitor the process of Hg trophic transfer has the potential to aid in understanding of ecologically relevant Hg biogeochemical processes in natural marine

ecosystems. For instance, transport of coastal MMHg to the open ocean via bioadvection and horizontal trophic transfer has been suggested to play an important role in providing MMHg to open ocean food webs (*38*). However, distinguishing the relative importance of coastal versus offshore MMHg sources to marine food webs has been limited using previous techniques. Given that the Hg source can be monitored with stable Hg isotopes in fish tissues, we can now to distinguish the relative importance of Hg sources in marine food webs.

The finding that the physiological state of fish and the THg concentration in their diet can influence the Hg isotopic equilibration of various organs and tissues indicates that these parameters need to be taken into consideration when using Hg isotopes in fish to identify sources and biogeochemical processes in natural marine systems. For instance, while species feeding at high trophic levels and consuming high-MMHg diets are expected to reflect the dominant MMHg source of their respective marine environment, the identification of Hg sources in species that do not actively ingest food during certain seasons or life cycles may be difficult due to the slow transition of Δ^{199}Hg from a new diet and the potential fractionation of δ^{202}Hg. Even if the fish depend exclusively on high-MMHg diets, the fact that various ecological factors such as fish size, trophic position, habitat and food sources can influence the THg concentrations in aquatic organisms (*39, 40*) indicate that prey-predator relationships need to be well constrained before selecting a biosentinel fish species to monitor Hg pollution. Moreover, the utilization of Hg isotopes may be more applicable to sites that are severely impacted by a single point source, as demonstrated in studies using Hg isotopes in sediments (*27*). More research is required to understand how internal processes such as demethylation and excretion lead to the small observed fractionation of δ^{202}Hg. Nevertheless, we suggest that using stable Hg isotope techniques to trace Hg sources and trophic transfer in marine food webs has the potential to become a regular and important part of biomonitoring and ecological risk assessment.

Acknowledgments

We thank M. Johnson for operation of the MC-ICP-MS. C. Hammerschimdt at Wayne State University, S. Balogh and Y. Nollet at Metropolitan Council Environmental Services, St. Paul, MN, and M.T.K. Tsui at University of Michigan provided MMHg analyses.

Reference

(1) Mergler, D.; Anderson, H. A.; Chan, L. H. M.; Mahaffey, K. R.; Murray, M.; Sakamoto, M.; Stern, A. H. Methylmercury exposure and health effects in humans: A worldwide concern. *Ambio.* **1992,** *36,* 3-11.

(2) Sunderland, E. M. Mercury exposure from domestic and imported estuarine and marine fish in the U.S. seafood market. *Environ. Health. Persp.* **2007,** *115,* 235-242.

(3) Gehrke, G. E.; Blum, J. D.; Slotton, D. G.; Greenfield, B. K. Mercury isotope link mercury in San Francisco Bay forage fish to surface sediments. *Environ. Sci. Technol.* **2011,** *45,* 1264-1270.

(4) Point, D.; Sonke, J. E.; Day, R. D.; Roseneau, D. G.; Hobson, K. A.; Vander Pol, S. S.; Moors, A. J.; Pugh, R. S.; Donard, O. F. X.; Becker, P. R. Methylmercury photodegradation influenced by sea-ice cover in Arctic marine ecosystems. *Nature Geosci.* **2011,** *4,* 188-194.

(5) Senn, D. B.; Chesney, E. J.; Blum, J. D.; Bank, M. S.; Maage, A.; Shine, J. P. Stable isotope (N, C, Hg) study of methylmercury sources and trophic transfer in the Northern Gulf of Mexico. *Environ. Sci. Technol.* **2010,** *44,* 1630-1637.

(6) Sherman, L. S.; Blum, J. D. Mercury stable isotopes in sediments and largemouth bass from Florida lakes, USA. *Sci. Total. Environ.* ISSN 0048-9697. DOI 10.1016/j.scitotenv. **2012,** *09.* 038.

(7) Blum, J. D.; Bergquist, B. A. Reporting of variations in the natural isotopic composition of mercury. *Anal. Bioanal. Chem.* **2007,** *388,* 353-359.

(8) Rodriguez-gonzalez, P.; Epov, V. N.; Bridou, R.; Tessier, E.; Guyoneud, R.; Monperrus, M.; Amouroux, D. Species-specific stable isotope fractionation of mercury during Hg(II) methylation by an anaerobic bacteria (*Desulfobulbus propionicus*) under dark conditions. *Envrion. Sci. Technol.* **2009,** *43,* 9183-9188.

(9) Kritee, K.; Barkay, T.; Blum, J. D. Mass dependent stable isotope fractionation of mercury during mer mediated microbial degradation of monomethylmercury. *Geochim et Cosmochim Acta.* **2009,** *73,* 1285-1296.

(10) Bergquist, B. A.; Blum, J. D. Mass-dependent and -independent fractionation of Hg isotopes by photoreduction in aquatic systems. *Science* **2007,** *318,* 417-420.

(11) Schauble, E. A. Role of nuclear volume in driving equilibrium stable isotope fractionation of mercury, thallium, and other very heavy elements. *Geochim et Cosmochim Acta.* **2007,** *71,* 2170-2189.

(12) Buchachenko, A. L.; Ivanov, V. L.; Roznyatovskii, V. A.; Vorob'ev, A. K.; Ustynyuk, Y. A. Inversion of the sign of the magnetic isotope effect of mercury in photolysis of substituted dibenzylmercury. *Dokl. Phys. Chem.* **2008,** *420,* 85-87.

(13) Zheng, W.; Hintelmann, H. Mercury isotope fractionation during photoreduction in natural water is controlled by its Hg/DOC ratio. *Geochim et Cosmochim Acta.* **2009,** *27,* 6704-6715.

(14) Gantner, N.; Hintelmann, H.; Zheng, W.; Muir, D. C. Variations in stable isotope fractionation of Hg in food webs of Arctic lakes. *Environ. Sci. Technol.* **2009,** *43,* 9148-9154.

(15) Chen, J. B.; Hintelmann, H.; Feng, X. B.; Dimock, B. Unusual fractionation of both odd and even mercury isotopes in precipitation from Peterborough, ON, Canada. *Geochim et Cosmochim Acta.* **2013,** *90,* 33-46.

(16) Gratz, L. E; Keeler, G. J.; Blum, J. D.; Sherman, L. S. Isotopic composition and fractionation of mercury in Great Lakes precipitation and ambient air. *Environ. Sci. Technol.* **2010,** *44,* 7764-7770.

(17) Kwon, S. Y.; Blum, J. D.; Carvan, M. J.; Basu, N.; Head, J. A.; Madenjian, C. P.; David, S. R. Absence of fractionation of mercury isotopes during trophic transfer of methylmercury to freshwater fish in captivity. *Environ. Sci. Technol.* **2012,** *46*(14), 7527-7534.

(18) Perrot, V.; Pastukhov, M. V.; Epov, V. N.; Husted, S.; Donard, O. F. X.; Amouroux, D. Higher mass-independent isotope fractionation of methylmercury in the pelagic food web of Lake Baikal (Russia). *Environ. Sci. Technol.* **2012,** *46,* 5902-5911.

(19) Demers, J. D.; Blum, J. D.; Zak, D. R. Mercury isotopes in a forested ecosystem: Implications fr air-surface exchange dynamics and the global mercry cycle. *Global Biogeochem. Cy.* **2013,** *27,* 1-17.

(20) Estrade, N.; Carignan, J.; Donard, O. F. X. Isotope tracing of atmospheric mercury sources in an urban area of Northeastern France. *Environ. Sci. Technol.* **2010,** *44,* 6062-6067.

(21) Yin, R.; Feng, X.; Meng, B. Stable mercury isotope variation in rice plants (*Oryza sativa* L.) from the Wanshan mercury mining district, SW China. *Environ. Sci. Technol.* **2013,** *47,* 2238-2245.

(22) Badalamenti, F.; D'Anna, G.; Lopiano, L.; Scilipoti, D.; Mazzola, A. Feeding habits of young-of-the-year greater amberjack *Seriola dumerili* (Risso, 1810) along the N/W Sicilian Coast. *Sci. Mar.* **1995,** *59*(3-4), 317-323.

(23) Hammerschmidt, C. R.; Fitzgerald, W. F. Methylmercury in freshwater fish linked to

atmospheric mercury deposition. *Environ. Sci. Technol.* **2006,** *40*, 7764−7770.

(24) Zook, E. G.; Powell, J. J.; Hackley, B. M.; Emerson, J. A.; Brooker, J. R.; Knobl, G. M. Jr. National marine fisheries service preliminary survey of selected seafoods for mercury, lead, cadmium, chromium, and arsenic content. *J. Agric. Food Chem.* **1976,** *24* (1), 47-53.

(25) de Oliveira Ribeiro, C. A.; Rouleau, C.; Pelletier, E.; Audet, C.; Tjalve, H. Distribution kinetics of dietary methylmercury in the Arctic Charr (*Salvelinus alpinus*). *Environ. Sci. Technol.* **1999,** *33*, 902-907.

(26) Riisgard, H. U.; Hansen, S. Biomagnification of mercury in a marine grazing food-chain: algal cells *Phaedodactylum trichornutum*, mussels *Mytilus edulis* and flounder *Platichthys flesus* studied by means of a stepwise reduction-CVAA method. *Mar. Ecol. Prog. Ser.* **1990,** *62*, 259-270.

(27) Foucher, D.; Ogrinc, N.; Hintelmann, H. Tracing mercury contamination from the Idrija mining region (Slovenia) to the Gulf of Trieste using Hg isotope ratio measurements. *Environ. Sci. Technol.* **2009,** *43,* 33-39.

(28) Blum, J. D.; Popp, B. N.; Johnson, M. W.; Drazen, J. C.; Choy, A. Mercury isotope constraints on depth of methylation and degree of photo-degradation of methylmercury in the Central Pacific Ocean. AGU Annual Meeting, December. San Francisco, CA. **2012.**

(29) Lerner, J. J.; Mason, R. P. Methylmercury uptake and distribution kinetics in sheepshead minnows, *Cyprinodon variegates*, after exposure to CH_3Hg-spiked food. *Environ. Toxicol. Chem.* **2004,** *23,* 2138-2146.

(30) McCloskey, J. T.; Schultz, I. R.; Newman, M. C. Estimating the oral bioavailbility of methylmercury to channel catfish (*Ictalurus punctatus*). *Environ. Sci. Technol.* **1998,** *17*, 1524-1529.

(31) Rudd, J. W.; Furutani, A.; Turner, M. A. Mercury methylation by fish intestinal contents. *Appl. Environ. Microbiol.* **1980,** *40,* 777-782.

(32) Pak, K. R.; Bartha, R. Mercury methylmation and demethyation in anoxic lake sediments and by strictly anaerobic bacteria. *Appl. Environ. Microbiol.* **1998,** *64,* 1013-1017.

(33) Tseng ,Y. C.; Hwang, P. P. Some insights into energy metabolism for osmoregulation in fish. *Comp. Biochem. Phys. C.* **2008,** *148,* 419-429.

(34) Van Walleghen, J. L. A.; Blanchfield, P. J.; Hintelmann, H. Elimination of mercury by yellow perch in the wild. *Environ. Sci. Technol.* **2007,** *41*, 5895-5901.

(35) Laffont, L.; Sonke, J. E.; Maurice, L.; Monrroy, S. L.; Chincheros, J.; Amouroux, D.; Behra, P. Hg speciation and stable isotope signature in human hair as a tracer for dietary and occupational exposure to mercury. *Environ. Sci. Technol.* **2011,** *45*(23), 9910-9916.

(36) Pickhardt, P. C.; Stepanova, M.; Fisher, N. S. Contrasting uptake routes and tissue distribution of inorganic and methylmercury in mosquitofish (*Gambusia affinis*) and redear sunfish (*Lepomis microlophus*). *Environ. Toxicol. Chem.* **2006,** *25,* 2132-2142.

(37) Wang, W. X.; Wong, R. S. K. Bioaccumulation kinetics and exposure pathways of inorganic mercury and methylmercury in a marine fish, the sweetlips *Plectorhinchus gibbosus. Mar. Ecol. Prog. Seri.* **2003,** *261,* 257-268.

(38) Hammerschmidt, C. R.; Fitzgerald, W. F. Methylmercury cycling in sediments on the continental shelf of southern New England. *Geochim et Cosmochim Acta.* **2006,** *70,* 918-930.

(39) Chumchal, M. M.; Manbright, K. D. Ecological factors regulating mercury contamination of fish from Caddo Lake, Texas, USA. *Environ. Toxicol. Chem.* **2009,** *28,* 962-972.

(40) Swanson, H. K.; Kidd, K. A. Mercury concentrations in arctic food fishes reflect the presence of anadromous arctic charr (*Salvelinus alpinus*), species, and life history. *Environ. Sci. Technol.* **2010,** *44,* 3286-3292.

Table 3.1 List of average organ mass (g, wet weight), total body mass (g, wet weight), and total fork length (mm) of AJ(S) and AJ(T) at different time periods. The numbers in parentheses represent the number of individual AJ in each treatment (n).

	Day 0	**Day 10**		**Day 30**		**Day 50**		**Day 80**
	(5)	Shrimp (5)	Tuna (5)	Shrimp (5)	Tuna (5)	Shrimp (3)	Tuna (3)	Shrimp (5)
Liver	0.80±0.32	0.95±0.41	1.5±0.25	2.3±1.4	3.9±2.1	2.2±1.2	12±2.8	2.0±1.9
Kidney	0.22±0.12	0.20±0.07	0.35±0.16	0.65±0.27	0.30±0.06	0.44±0.15	0.78±0.15	0.78±0.75
Brain	0.43±0.13	0.32±0.20	0.44±0.12	0.42±0.11	0.40±0.12	0.48±0.11	0.56±0.17	0.47±0.39
Blood	2.9±1.4	3.3±1.0	4.3±0.92	3.7±2.09	3.5±0.51	2.1±0.91	3.2±1.3	2.1±1.7
Total mass	162±72	165±60	229±59	223±71	197±29	292±88	377±66	337±111
Fork length	22±3.3	21±2.7	24±2.8	23±2.0	22±2.4	30±2.7	30±1.7	27±2.7

Table 3.2 List of BAFs of AJ(S) and AJ(T) at different time periods.

	Day 10		**Day 30**		**Day 50**		**Day 80**
	Shrimp	Tuna	Shrimp	Tuna	Shrimp	Tuna	Shrimp
Muscle	3.77	0.19	4.77	0.79	7.39	1.21	8.56
Liver	2.49	0.18	4.02	1.00	5.84	0.88	5.52
Kidney	3.21	0.16	5.26	1.14	8.49	1.66	9.38
Brain	0.94	0.09	2.17	0.52	2.96	1.39	2.54
Blood	0.18	0.003	0.44	0.08	0.64	0.10	0.50
Whole fish	NA	NA	4.38	0.43	4.85	1.07	5.68

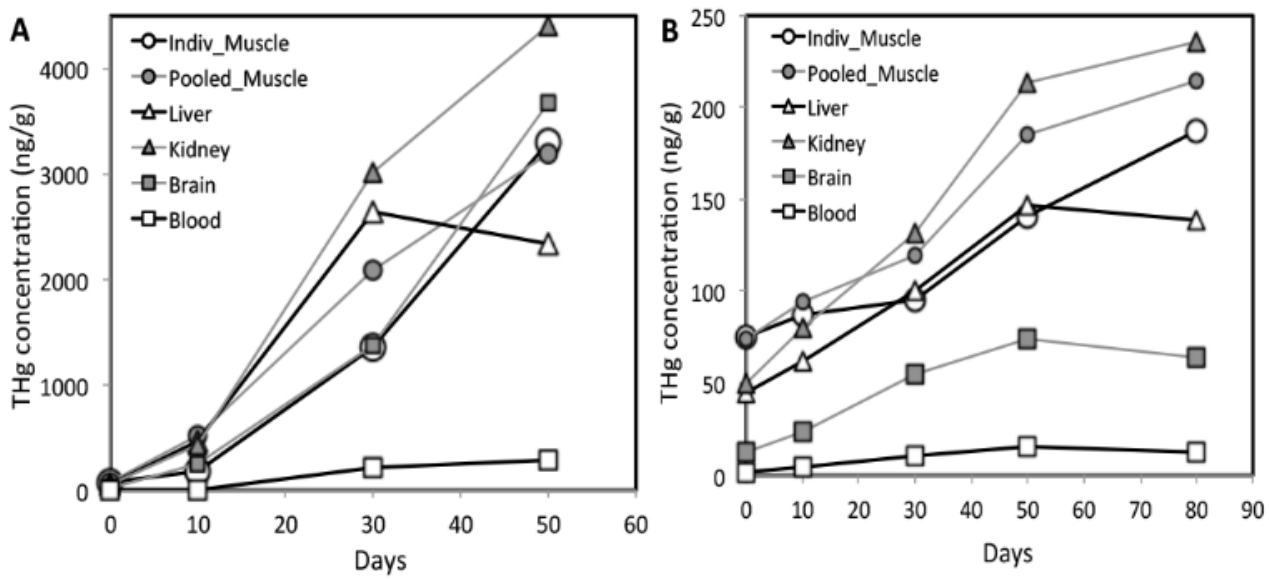

Figure 3.1 Total Hg (THg) concentrations (ng/g, dry weight) of the organs of A) Amberjack fed a tuna diet and B) Amberjack fed a shrimp diet at different time periods. THg concentrations of the blood are reported in wet weight.

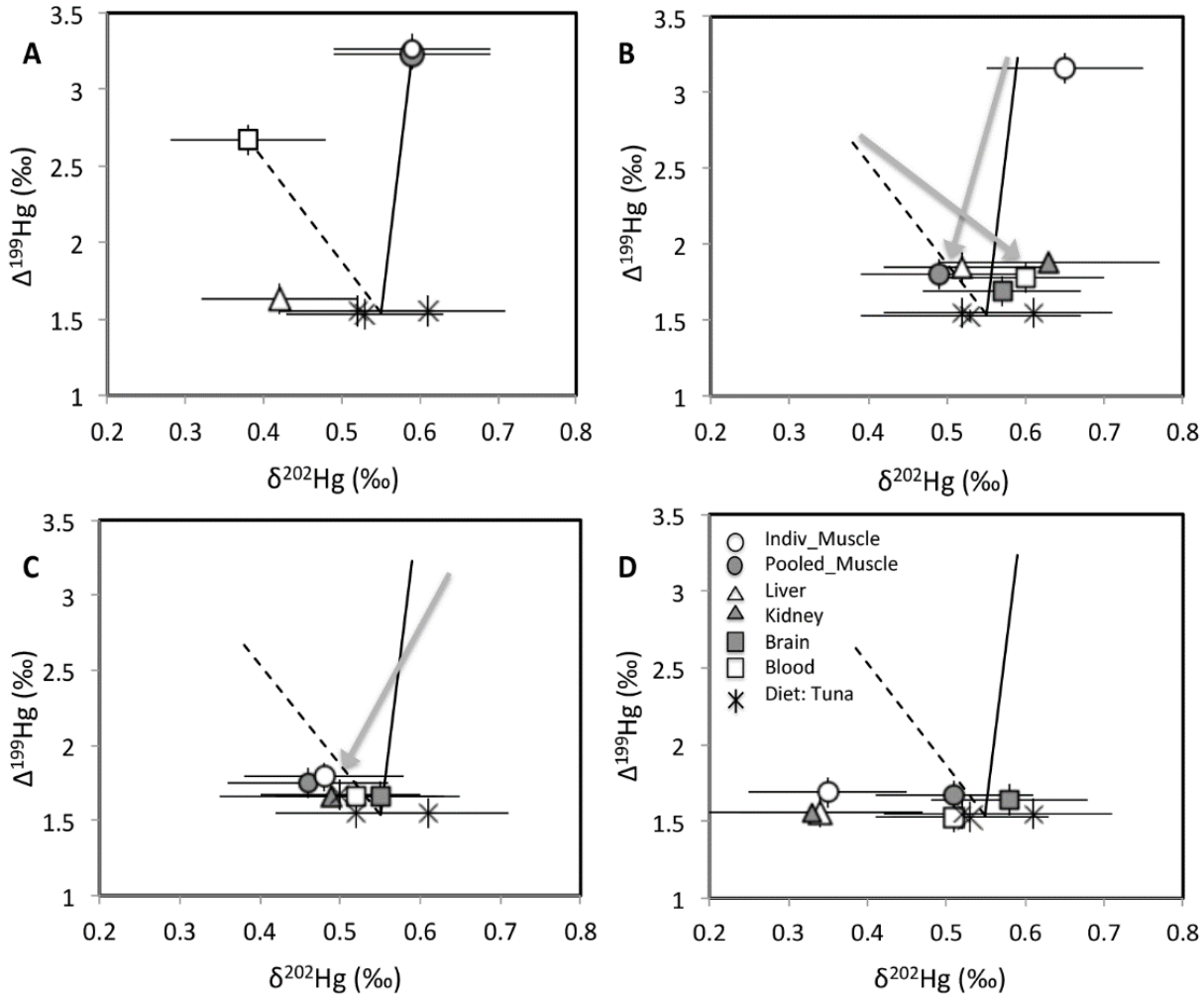

Figure 3.2 Plot of δ^{202}Hg and Δ^{199}Hg values of Amberjack fed a tuna diet at A) day 0, B) day 10, C) day 30, and D) day 50. The solid line represents the mixing line between the tuna diet and the AJ muscle at day 0 and the dotted line represents the mixing line between the tuna diet and the AJ blood at day 0. The grey arrows represent the shift in the Hg isotopic composition of each organ from the previous time period. Analytical uncertainty is indicated by the error bar (2 s.d).

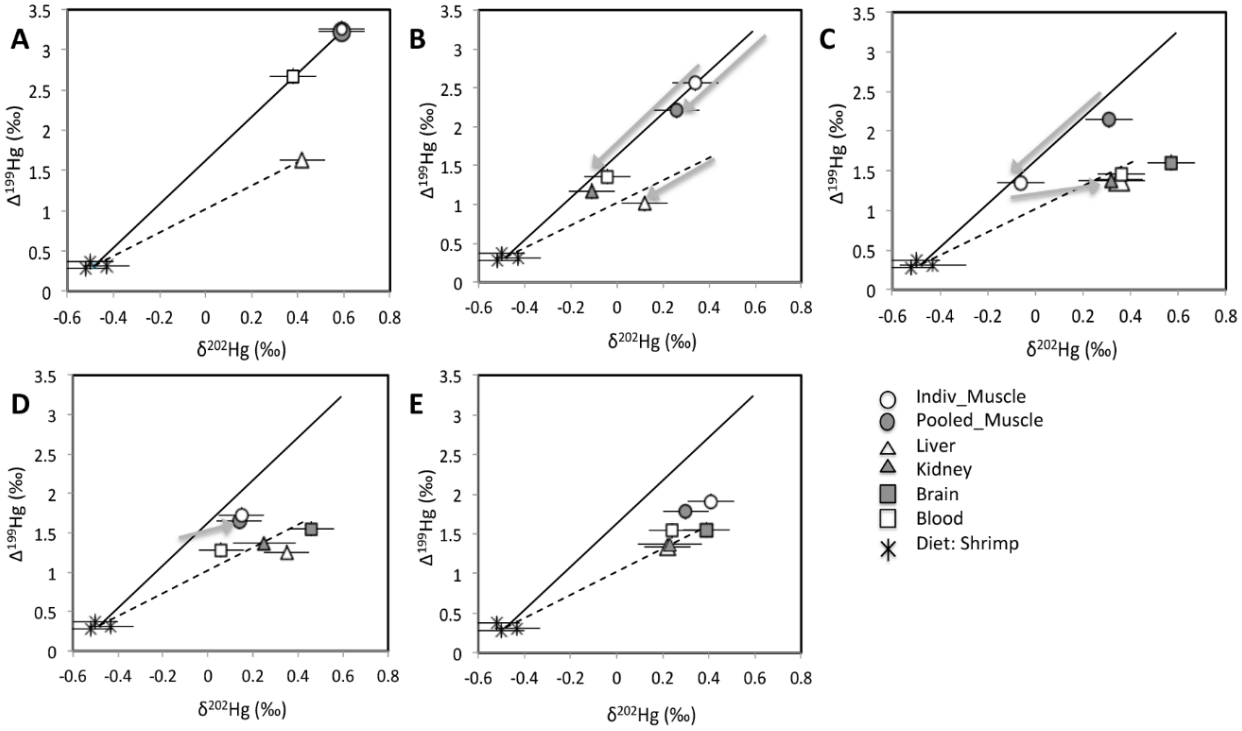

Figure 3.3 Plot of δ^{202}Hg and Δ^{199}Hg values of Amberjack fed a shrimp diet at A) day 10, B) day 30, C) day 50, D) day 80, and E) day 80 with shrimp-IHg and shrimp-MMHg. The solid line represents the mixing line between the shrimp diet and the AJ muscle at day 0 and the dotted line represents the mixing line between the shrimp diet and the AJ liver at day 0. The grey arrows represent the shift in the Hg isotopic composition of each organ from the previous time period. Analytical uncertainty is indicated by the error bar (2 s.d).

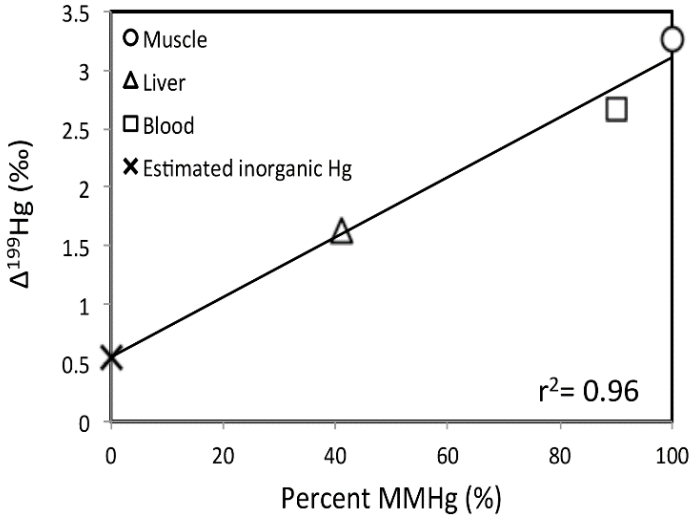

Figure 3.4 Plot of percent MMHg (% MMHg) and Δ^{199}Hg of the Amberjack organs at day 0. The Δ^{199}Hg of the inorganic Hg is extrapolated from the best-fit line of the muscle, liver, and blood of AJ.

CHAPTER 4

Mercury isotope study of sources and exposure pathways of methylmercury in estuarine food webs in the Northeastern U.S.

Abstract

We measured mercury (Hg) isotope ratios in sediments and various estuarine organisms (green crab, blue mussel, killifish, eider) to investigate methylmercury (MMHg) sources and exposure pathways in five Northeast coast (USA) estuaries. The mass independent Hg isotopic compositions (MIF; Δ^{199}Hg) of the sediments were linearly correlated with the sediment 1/Hg concentrations (Δ^{199}Hg: r^2=0.77, $p<0.05$), but the mass dependent isotope compositions (MDF; δ^{202}Hg) were not (r^2=0.26, p=0.16), reflecting inputs of anthropogenic Hg sources with varying δ^{202}Hg. The estuarine organisms all display positive Δ^{199}Hg values (0.21 to 0.98 ‰) indicating that MMHg is photo-degraded to varying degrees (5-12%) prior to entry into the food web. The δ^{202}Hg and Δ^{199}Hg values of most organisms can be explained by a mixture of MMHg and inorganic Hg from sediments. At one contaminated site mussels have anomalously high δ^{202}Hg, indicating exposure to a second pool of MMHg compared to sediment, crabs and fish. Eiders have similar Δ^{199}Hg as killifish but much higher δ^{202}Hg, suggesting that there is an internal fractionation of δ^{202}Hg in birds. Our study shows that Hg isotopes can be used to identify multiple anthropogenic inorganic Hg and MMHg sources and determine the degree of photo-degradation of MMHg in estuarine food webs.

4.1. Introduction

Monomethylmercury (MMHg) is a toxic and bioaccumulative organometallic compound that poses serious health risks to both humans and wildlife (*1*). Humans are primarily exposed to MMHg via the consumption of marine fish and shellfish, with over 90% of marine fisheries products originating from estuarine and open ocean areas (*2*, *3*). Many estuarine organisms

currently contain elevated MMHg levels, which can cause health problems in humans (*4, 5*), but there is considerable uncertainty concerning the relative importance of the sources and exposure pathways of MMHg to estuarine food webs.

Sediments have long been suggested as the dominant MMHg source to estuarine food webs. Estuarine sediments act as an important sink for Hg, receiving Hg via atmospheric deposition (*6*), industrial runoff (*7*) and riverine input (*8*), and provide geochemical conditions that promote biotic methylation (*9*). Past studies have also reported strong linkages between total Hg (THg) concentrations in sediments and THg in estuarine forage fish in San Francisco Bay (*10, 11*). In contrast, Chen et al (*12, 13*) recently documented a strong positive association between pelagic forage fish (*Fundulus heteroclittus* and *Menidia menidia*) MMHg concentrations and water column particulate MMHg concentrations, but not with sediments, across multiple estuaries on the Northeast coast, USA. Based on this observation, the authors suggested that the MMHg accumulated into water column particulates may be a more dominant MMHg source to pelagic organisms than sediment MMHg. Monomethylmercury can enter the water column via diffusion, advection and resuspension from sediments (*14*). Inflowing fluvial and tidal waters have been suggested as important external MMHg sources to pelagic food webs in the Bay of Fundy (*15*) and the Hudson River estuary (*16*), with coastal sediments being a less important source. At Chesapeake Bay (*17*) and Long Island Sound (*8*), both sediments and external sources were found to be important MMHg sources to these systems. Given these diverse sources, tools that can differentiate MMHg sources and exposure pathways are expected to help highlight the most important biogeochemical processes affecting MMHg in estuarine food webs.

Studies of the natural abundance of Hg isotopes have enhanced understanding of the sources and biogeochemical processing of Hg in natural environments. Mercury isotopes undergo mass-dependent fractionation (MDF, reported as δ^{202}Hg) and mass-independent fractionation (MIF, reported as Δ^{199}Hg and Δ^{201}Hg) (*18*). While MDF has been documented in various environmentally relevant reactions such as biotic methylation (*19*), demethylation (*20*), thiol-ligand exchange (*21*) and photochemical reactions (*22*), MIF in natural systems is thought to occur primarily in odd-mass number isotopes via photochemical reduction and degradation of inorganic Hg (IHg) and MMHg. Recently, Δ^{199}Hg has been applied as a biological and ecological tracer for understanding processes such as bioaccumulation and trophic transfer (*23, 24*) as well as transfers of MMHg between ecosystems (*25*). The ratio of Δ^{199}Hg/Δ^{201}Hg has also

become a valuable tool for distinguishing between photochemical reduction of IHg ($\Delta^{199}Hg/\Delta^{201}Hg$=1.00) and degradation of MMHg ($\Delta^{199}Hg/\Delta^{201}Hg$=1.2-1.4) (*22*).

Mercury isotope ratios have recently been used to provide insight into the sources and exposure pathways of MMHg to diverse marine food webs (*10, 24, 26, 27*). Based on these studies, we can make predictions as to how Hg isotope ratios might be useful for understanding the sources and biogeochemical processing of MMHg in estuaries. For instance, high positive $\Delta^{199}Hg$ values have been documented in pelagic fish (> 1‰) compared to coastal fish (< 1‰), indicating that MMHg that has been subjected to extensive photochemical degradation in the open ocean water column is the dominant MMHg source to pelagic food webs (*26, 27*). In shallow coastal environments it has been suggested that MMHg produced in the sediment, that has undergone relatively little photochemical degradation, enters the base of the food web (*27*). In another relevant study, Gehrke et al (*10*) documented relatively low $\Delta^{199}Hg$ values (< 1‰) in intertidal forage fish (i.e. topsmelt and silverside) that feed on epibenthic invertebrates across the San Francisco Bay Estuary. Fish $\delta^{202}Hg$ values were found to be consistently higher by 0.6 ‰ compared to nearby sediments at multiple sites, which led to the conclusion that the fractionation imparted during production and degradation pathways of MMHg in the sediment or during trophic transfer was responsible for these $\delta^{202}Hg$ offsets. Fish feeding experiments (*23, 24*), have now documented an absence of Hg isotope fractionation during trophic transfer of MMHg to fish, and therefore the isotopic offset is thought to provide insight into the biogeochemical pathways of MMHg prior to introduction to the food web. We also expect that the isotopic offset between fish and sediments may differ between sites that vary in Hg biogeochemical cycling, as well as between different feeding guilds among estuarine organisms.

In this study, we investigated the sources and exposure pathways of MMHg in food webs from five estuaries located across the northeastern coast of the USA. Sediments and organisms from these sites have been previously studied for IHg and MMHg concentrations by Chen et al (*12, 13*). The Northeast coast of the USA is one of the most productive marine ecosystems in the world and supports valuable commercial and recreational fisheries. In the last century, this area has become severely impacted by an increase in population, industrial activity, and emission of anthropogenic pollutants including Hg (*28*). Here we characterize the Hg isotopic compositions of estuarine sediments across sites on the Northeast coast to identify Hg sources in these regions. The sources and exposure pathways of MMHg were evaluated across food webs consisting of

epibenthose (green crab; *Carcinus maenas*, killifish; *Fundulus heteroclittus*), filter feeders (blue mussel; *Mytilus edulis*, ribbed mussels; *Geukensia demissa*), and consumers (common eider; *Somateria mollissima*). We determined the Hg isotopic composition of the estuarine organisms and estimated the isotopic composition of MMHg to identify the dominant MMHg source and exposure pathway to the estuarine food webs. The MMHg isotopic compositions were compared across sites and between feeding guilds (i.e. groups of species that exploit the same resources) to assess potential spatial and ecological variability in MMHg sources. To our knowledge, this is the first attempt to use Hg isotope ratios to compare MMHg sources to varying marine feeding guilds across multiple ecosystems.

4.2. Materials and Methods

4.2.1. Site description

We sampled five estuarine sites along the northeastern coast of the USA (Maine; ME, Massachusetts; MA, Rhode Island, RI; Connecticut, CT, New Jersey; NJ) in the summers of 2008 and 2010 (Fig S1). All sites were adjacent to coastal marsh habitats except for Bold Point, RI (BOLD), which was located in an unvegetated area of the Providence River Estuary. The Webhannet Estuary in Wells, ME (WELLS) and Buzzards Bay, MA (BUZZ) are characterized by sandy beaches and are sparsely populated. Both sites receive primarily atmospherically deposited Hg from non-point sources and the inputs are relatively small compared to the other Northeast coast sites (*29*). BOLD is situated in urbanized Providence, RI, and receives some atmospheric point source Hg from local waste incinerators (10% of the total Hg budget) (*29*). BOLD is impacted by local wastewater treatment facilities (21% of Hg input) and industrially impacted rivers (69% of Hg input) (*30*). Barn Island, CT (BARN) is located in the southeastern tip of Connecticut and also receives Hg via local wastewater treatment facilities and industrially impacted rivers—the Connecticut River (59% of Hg input) and the East River (25% of Hg input) (*8*). Mill Creek, NJ (MILL) is impacted by the Hackensack River, which has been heavily contaminated by landfills, and a Hg recovery plant that discharged 30-400 tons of Hg including elemental Hg, mercuric oxide, and other forms of oxidized Hg by-products during its operation between 1929 and 1974 (*31*).

4.2.2. Sampling & analysis

The estuarine sediments were measured for THg and MMHg concentrations at the University of Connecticut Department of Marine Sciences and were reported previously (*13*) (n=9). Four types of biota were analyzed for this study: green crabs (*Carcinus maenas*) (n=6), blue mussels (*Mytilus edulis*) (n=5) or ribbed mussels (*Geukensia demissa*) (n=2), killifish (*Fundulus*) (n=9), and eider (*Somateria*) (n=5) (referred to as crab, mussel, fish, and bird hereafter). The methods for sampling and processing of the sediments and aquatic biota are described in Chen et al (*13*). The aquatic biota were measured for stable nitrogen and carbon isotopic composition at the Stable Isotope Laboratory, Dartmouth College to characterize the trophic positions and feeding guilds. THg and MMHg analyses were conducted for most samples at the Trace Element Analysis Laboratory, Dartmouth College. These results were previously reported in Chen et al (*13*). Additional samples of mussels (n=4) and crabs (n=3) were measured for THg concentrations at the University of Michigan. These samples were freeze-dried prior to removing the shells, and homogenized in a zirconium grinding mill (Retsch, Mixer Mill MM 301). The mussels and crabs were measured for THg using Atomic Absorption Spectroscopy (AAS) following combustion of samples at 800^{o}C using a Nippon Instruments MA-2000 Hg analyzer. Standard reference material NIST-3133 was used to generate calibration curves and for quality control. Standard reference material TORT-3 (n=4) was analyzed as an external standard and agreed within 5% of certified values.

Samples of bird blood were collected near WELLS and BUZZ between January and April 2010 (Fig S1). The birds were captured using floating mist nets and the blood samples were collected by following the standard tissue collection protocol described in Evers et al (*32*). The blood samples were drawn non-lethally by venipuncture from either the cutaneous ulnar or tarsal vein using needles and syringes. The blood samples were stored in either clean heparinized capillary tubes or microtainers. The samples were sealed on both ends with Critocaps®, placed in 10 cc plastic vacutainers, and frozen at -25°C prior to the analyses for THg concentrations at the Wildlife Mercury Research Lab at the Biodiversity Research Institute, Maine, USA. The THg concentrations were determined using a direct Hg analyzer (DMA 80, Milestone Incorporated) following the USEPA Method 7473 (US EPA 2007). The standard reference materials DOLT-4 and DORM-4 were used to generate calibration curves and for quality control. DOLT-4 (n=5) and DORM-3 (n=5) were analyzed with samples and agreed within 10% of certified values. The

relative standard deviations of duplicate analyses of samples were within 5%. The THg concentrations of sediments and aquatic biota are reported in dry weight and the aquatic biota represent whole body tissues. The bird blood analyses are reported in wet weight (*32*).

4.2.3. Hg isotope analysis

The sediment and biota samples were measured for stable Hg isotopic composition at the University of Michigan. Blood samples were thawed and oven-dried at 50-60°C in acid washed ceramic boats. Samples of aquatic biota were weighed and loaded into ceramic boats with sodium carbonate and aluminum oxide powders. Offline two-stage combustion furnace systems were used to release Hg (as Hg^0) from the samples. The ceramic boats were loaded into the first combustion compartment and heated to 750°C over a 6-hour period. Released Hg^0 was directed to the second combustion compartment (1000°C) via a stream of Hg-free oxygen and subsequently oxidized in a trap solution (1% $KMnO_4$ in 10% trace metal grade H_2SO_4). The solutions containing Hg^{2+} were neutralized with hydroxylamine, reduced back to Hg^0 with $SnCl_2$ and purged into a new trap solution to remove combustion product matrix components from the sample.

Procedural blanks were prepared in the same manner as the samples (but with no sample placed in the ceramic boat) and measured for THg before and after the transfer steps. The procedural blanks had an average THg of 0.2±0.1 ng (n=6). The THg concentrations of the samples as well as the standard reference materials ERM CE 464 (n=3), TORT-2 (n=1) and MESS-3 (n=2) were measured before and after the transfer step to monitor the recoveries of THg during the combustion and transfer processes. The recoveries of the combustion and transfer steps of the samples and standard reference materials ranged between 89 to 100%, and 92 to 106%, respectively.

Stable Hg isotope ratios were measured using a Nu Instruments multi-collector inductively coupled plasma mass spectrometer (MC-ICP-MS). The trap solutions were neutralized using hydroxylamine. To match the THg concentration of the sample to the standard, the trap solutions containing the sample were diluted to between 1 and 5 ng/g using the same neutralized trap solution matrix. Hg was introduced to the MC-ICP-MS as Hg^0 by reducing Hg^{2+} in solution with $SnCl_2$, and separating Hg^0 using a frosted glass tip phase separator. On-peak zero corrections were applied. Instrumental mass bias was corrected using an internal Tl standard (NIST SRM

997) and by bracketing each sample with NIST SRM 3133 matched to sample THg concentrations and matrix composition. MDF is reported as δ^{202}Hg in permil (‰) referenced to NIST SRM 3133 (*18*):

$$\delta^{202}Hg = \{[(^{202}Hg/^{198}Hg)_{sample}/ (^{202}Hg/^{198}Hg)_{NIST3133}]-1\}*1000. \quad (1)$$

MIF represents the difference between the measured δ^{xxx}Hg value and the value predicted based on MDF and the δ^{202}Hg value (*18*). MIF is reported as Δ^{199}Hg and Δ^{201}Hg in permil (‰). The calculation is based on an approximation valid for δ <10‰:

$$\Delta^{199}Hg = \delta^{199}Hg - (\delta^{202}Hg * 0.252) \quad (2)$$

$$\Delta^{201}Hg = \delta^{201}Hg - (\delta^{202}Hg * 0.752) \quad (3)$$

Analytical uncertainty at 2 s.d. is estimated based on either replicate analysis of a standard solution (UM-Almáden) and on replicate analyses of standard reference materials. We used ERM CE 464 to report analytical uncertainty since it had a larger uncertainty. UM-Almáden (n= 30) had mean values (±2 s.d.) of δ^{202}Hg= -0.57±0.06 ‰, Δ^{201}Hg= -0.04±0.04 ‰, and Δ^{199}Hg= -0.02±0.05 ‰. Standard reference material ERM CE 464 (n=3) had mean values of δ^{202}Hg= 0.66±0.08 ‰, Δ^{201}Hg= 1.91±0.06 ‰, and Δ^{199}Hg= 2.31±0.09 ‰; TORT-2 (n=1) had values of δ^{202}Hg= 0.10 ‰, Δ^{201}Hg= 0.57 ‰, and Δ^{199}Hg= 0.79 ‰; and MESS-3 (n=2) had mean values of δ^{202}Hg= -1.81±0.08 ‰, Δ^{201}Hg= -0.05±0.05 ‰, and Δ^{199}Hg= 0.01±0.03 ‰.

4.3. Results & Discussion

4.3.1. Hg concentrations and isotopic compositions in the sediments

The THg concentrations of the Northeast coast sediments are quite low at BUZZ (5.70 ng/g) and WELLS (9.43 ng/g) and higher at the other three sites (BARN, BOLD, MILL) (42.0 to 2961 ng/g) (Table S1). Due to the low THg values at the BUZZ and WELLS sites (typical of uncontaminated sites) (*33, 34*), we designate WELLS and BUZZ as “background sites” and due to the relatively higher values at BOLD, BARN, and MILL we designate them as “contaminated

sites." The contaminated sites are associated with Hg point sources (see site description) and have at least 6 times higher THg concentration compared to the background sites.

Overall, the sediments displayed ranges of δ^{202}Hg values between -0.89 ‰ and -0.38 ‰, and Δ^{199}Hg values between -0.04 ‰ and 0.19 ‰, and were within the range of values reported previously in other coastal marine sediments (*7, 27, 35, 36*). We plotted 1/THg concentration against δ^{202}Hg and Δ^{199}Hg to linearize mixing relationships and to characterize the Hg isotopic compositions of the sediments in relation to the Hg contamination. We observed a weak negative (r^2=0.26, p=0.16) and significant positive (r^2=0.77, p<0.05) relationship between 1/THg concentration and δ^{202}Hg and Δ^{199}Hg, respectively (Fig 1). The Δ^{199}Hg values of the sediments were distinct between the background and contaminated sites with the contaminated sediments exhibiting uniform Δ^{199}Hg≈0 ‰, and slightly elevated Δ^{199}Hg in the background sediments. The sediments displayed ranges of negative δ^{202}Hg values and were less well correlated with the sediment THg concentrations.

The fact that the Δ^{199}Hg values of the Northeast coast sediments are correlated with the THg concentrations suggests that these sediments reflect inputs from multiple Hg sources associated with the Northeast coast estuaries. When we compared the background sediments to the contaminated sediments, the sites designated as "background" displayed negative δ^{202}Hg values with Δ^{199}Hg values that were distinctly positive compared to the contaminated sediments. Coastal and marine sediments from other studies that were characterized as background, or those that are pre-anthropogenic in age, display low THg concentrations, negative δ^{202}Hg and slightly elevated Δ^{199}Hg (*7, 35-37*). The background sediments from this study are consistent with the δ^{202}Hg and Δ^{199}Hg values reported in those previous studies. The positive Δ^{199}Hg values in the background sediments are likely the result of fractionation caused during partial photochemical reduction of IHg, which may occur either through deposition of photochemically reduced IHg from surface water (*38*), periodic exposure of surface sediments to sunlight during tidal fluctuation of water levels (1-2 m) (*7, 37*), or deposition of photochemically reduced IHg from rain water (*38*). Photochemical reduction of IHg has been used to explain the positive Δ^{199}Hg values documented in shallow and relatively undisturbed marshes (~ 0.66 ‰) (*37*) and coastal and intertidal sediments (~ 0.08 ‰) (*7, 27*) and we suggest that positive Δ^{199}Hg values may be imparted in background sediments without the mixing of anthropogenic Hg sources.

In the contaminated sediments, we observed similar ranges of negative δ^{202}Hg values but uniform Δ^{199}Hg≈0 ‰, reflecting the dominance of anthropogenic Hg sources in these sediments (*7, 35, 36, 39*). Various industrial Hg sources have been characterized by wide ranges of negative δ^{202}Hg and zero Δ^{199}Hg values (*22, 39, 40*), and the input of industrial Hg sources likely explains the low Δ^{199}Hg values, high THg concentrations, and wide ranges in δ^{202}Hg values observed in the contaminated sediments. The range of δ^{202}Hg values for the contaminated sites that are impacted by local industrial Hg sources (BARN, BOLD; -0.60 to -0.82 ‰) were also consistent with values for Hg^0 used in gold mining in the San Francisco Bay Estuary (-0.59 to -0.78 ‰) (*7*). Thus, the Hg isotopic compositions and the THg concentrations of the sediments appear to be consistent with the presence of multiple anthropogenic Hg sources in these regions.

4.3.2. Hg concentrations and isotopic compositions in biota

The THg concentrations of the estuarine biota increase in the order: crabs (55.3±24 ng/g) < fish (138±188 ng/g) < mussels (145±52 ng/g) < bird blood (863±724 ng/g) (Table S1). The fraction of THg that is in the form of MMHg (referred to as % MMHg hereafter) for the aquatic biota increases in the order: mussels (57.9±4.5%) < crabs (83.7±3.0%) < fish (91.4±5.9%) and these values follow the same order as δ^{15}N values (7.4±1.0 ‰, 10.3±3.0 ‰, 11.3±3.2 ‰; Table S1), representing the approximate trophic position. The % MMHg values of the birds were estimated from Wayland et al (*42*), who reported over 98% MMHg in blood. The increasing % MMHg with trophic position (δ^{15}N) is consistent with the pattern of MMHg biomagnification documented in many aquatic food webs (*43, 44*). We designate the feeding guilds of the estuarine biota based on the δ^{13}C values and the detailed feeding behaviors are shown in Table S1 and Chen et al (*12, 13*). The δ^{15}N (13.2 ‰) and δ^{13}C (-17.4 ‰) values for the birds (Table S1) were estimated from Hobson et al (*45*) who measured the same species in the Arctic. This estimate was adequate for approximating the relative trophic position and feeding guild of these birds, which suggests a slightly higher trophic position compared to the fish measured in this study.

Across the Northeast coast estuarine study sites, we observed wide ranges of δ^{202}Hg values but relatively narrow ranges of Δ^{199}Hg values in the estuarine biota (Table S1). At each study site the δ^{202}Hg and Δ^{199}Hg values of the estuarine biota displayed an increasing trend with trophic position—following the order mussels, crabs, fish, and birds (Fig 2a,b). Similar trends have

previously been attributed to the varying extent of MMHg bioaccumulation with trophic position (*23*, *24*). We plotted % MMHg against δ^{202}Hg and Δ^{199}Hg of the sediment and aquatic biota (without the birds) and observed significant positive relationships with Δ^{199}Hg ($p<0.05$) across all sites; (WELLS; $r^2=0.86$, BUZZ; $r^2=0.70$, BOLD; $r^2=0.72$, BARN; $r^2=0.89$) and of δ^{202}Hg at all sites except BOLD; (WELLS; $r^2=0.68$, $p<0.05$, BUZZ; $r^2=0.71$, $p<0.05$, BOLD; $r^2=0.52$, $p=0.08$, BARN; $r^2=0.80$, $p<0.05$). Due to the significant positive relationships observed at most sites, the Hg isotopic composition reflecting the bioaccumulated MMHg was estimated using a linear regression of % MMHg against δ^{202}Hg and Δ^{199}Hg. The δ^{202}Hg and Δ^{199}Hg values estimated for MMHg demonstrated relatively narrow ranges across the Northeast coast estuarine food webs; -0.22 to 0.28 and 0.39 ‰ to 1.00 ‰, respectively (Fig 2a,b). At sites where birds were measured (proximity to WELLS and BUZZ), the birds (containing >98% MMHg) demonstrated similar Δ^{199}Hg but much higher δ^{202}Hg compared to the fish (containing >90% MMHg) measured at the same locations (bird δ^{202}Hg; 0.59 to 1.39 ‰, fish δ^{202}Hg; -0.34 to 0.23 ‰). At BOLD, the mussels displayed significantly higher δ^{202}Hg values compared to other aquatic biota.

Overall, we find strong evidence for an increasing trend in the δ^{202}Hg and Δ^{199}Hg values of the sediments and estuarine biota with % MMHg (trophic position) in the Northeast coast estuarine food webs. This trend has also been documented in other aquatic food webs (*27*, *46-48*). While metabolic fractionation was previously proposed as a potential mechanism (*46*), recent fish feeding experiments showed that metabolic fractionation does not occur during trophic transfer to fish (*23*, *24*). Instead, the differences in Hg isotopic composition between MMHg and IHg and the varying extent of MMHg versus IHg bioaccumulation with trophic position provide a consistent explanation for the Hg isotopic composition variability in food webs. Thus, the absence of MDF and MIF during MMHg trophic transfer implies that the estuarine biota mainly reflect the isotopic composition of MMHg incorporated at the base of the food web. The anomalously high δ^{202}Hg values observed in the WELLS and BUZZ birds and the BOLD mussels suggest that these organisms may be accumulating MMHg from an additional source. Below we assess the dominant MMHg source and exposure pathways in the Northeast coast estuarine food webs using the Hg isotopic composition estimated for MMHg and provide an explanation for the δ^{202}Hg values found in the birds and the BOLD mussels.

4.3.3. Sources and biogeochemical pathways of MMHg

The Northeast coast estuarine biota analyzed in this study collectively displayed moderately positive Δ^{199}Hg values (0.2 to 1.0 ‰) (Table S1). This suggests that the bioaccumulated MMHg was subjected to photochemical degradation prior to incorporation into the estuarine food web. In fish, which have consistently high % MMHg and for which we have isotope data at each site, we found lower Δ^{199}Hg in the contaminated sites (0.56±0.15 ‰) compared to the uncontaminated sites (0.90±0.06 ‰). This indicates that the fish at the contaminated sites are either exposed to MMHg that was subjected to a lesser degree of photochemical degradation compared to those found at the uncontaminated sites or MMHg that originated from anthropogenic IHg sources from the sediments which have low Δ^{199}Hg (≈0 ‰). The slope of Δ^{199}Hg/ Δ^{201}Hg has been used to distinguish between photochemical degradation and reduction of MMHg versus IHg in natural aquatic ecosystems[22]. We plotted Δ^{199}Hg against Δ^{201}Hg for all estuarine biota, and used a York regression to estimate the slope of Δ^{199}Hg/ Δ^{201}Hg, which is 1.22±0.07 (r^2=0.90, $p<0.05$). This slope is consistent with the slopes reported in other marine fish (~1.2) exposed to photochemically degraded MMHg from their respective environments (*10, 26, 27, 41, 49, 50*). On a Δ^{199}Hg versus δ^{202}Hg diagram we plot values for sediments and biota and the experimentally derived slopes representing the expected changes in the MMHg isotopic composition caused by photochemical degradation of MMHg (Δ^{199}Hg=4.79±0.33 * δ^{202}Hg at 10mg/L DOC) (*11*) (Fig 3; dotted lines). These slopes are derived from previously published MMHg photochemical degradation experiments that employed aquatic solutions spiked with MMHg and DOC, and natural sunlight (*22*), and are only rough estimates since experimental conditions were different from those in the natural setting we studied. Based on values for fish, we estimate that MMHg is photochemically degraded to varying degrees ranging from 5-12 % across the Northeast coast sites prior to entering the food webs.

The δ^{202}Hg values for MMHg prior to photochemical degradation were estimated following the approach of Gehrke et al (*10*) and Sherman and Blum (*51*) and were all higher than the corresponding δ^{202}Hg values of THg measured in the sediments. Given that the sediment is mainly composed of IHg, we suggest that MMHg that is bioaccumulated is mass dependently fractionated compared to the IHg in the sediment. This has been observed in previous studies (*11, 51*) and has been attributed to the net effect of microbial Hg methylation and demethylation, which has increased δ^{202}Hg values prior to photochemical degradation. The degree of the offset

in δ^{202}Hg between the MMHg (before photo-degradation) and IHg are somewhat variable across the sites but generally consistent with previous studies. An alternate explanation for this offset in δ^{202}Hg between IHg and MMHg is that it is caused by introduction of MMHg from a different source than the local sediment, which has higher δ^{202}Hg (e.g. methylation in upstream marshes).

The proportion of MMHg photochemical degradation estimated here is comparable with many shallow coastal regions (*10, 27*) and high turbidity lakes (*51*), but much lower than open ocean environments (*26, 27*). The simplest explanation for the source of the MMHg to which estuarine biota are exposed is that it is derived from the IHg in sediments and has subsequently undergone small amounts of photochemical degradation in the water column, perhaps becoming attached to particles and subsequently redeposited to the sediment. In a study of fish and sediment in the Gulf of Mexico it was observed that the Hg isotopic composition of coastal fish was consistent with exposure to sediment-derived MMHg that had undergone small amounts of photochemical degradation, whereas open ocean fish had much higher Δ^{199}Hg values indicative of much higher degrees of photo-degradation (*27*). Day et al (*49*) also found ranges of Δ^{199}Hg values in the eggs of epipelagic seabirds with the individuals feeding near shallow coastal embayments displaying significantly lower Δ^{199}Hg values compared to those feeding on open ocean species.

The positive offsets in δ^{202}Hg between IHg (in sediment) and MMHg (in biota) are consistent with previous studies suggesting that the local sediments may be the primary site for MMHg production prior to photochemical degradation in the water column and bioaccumulation in the food webs. It has been shown that microbial methylation causes the fractionation of δ^{202}Hg, leading to lower δ^{202}Hg in the product-MMHg compared to the reactant (*19*). A portion of Hg that has been methylated could subsequently be microbially demethylated, resulting in higher δ^{202}Hg values in the remaining MMHg (*20*), and the net effect of these processes provides an explanation for the δ^{202}Hg values in the sediments. Large positive offsets in δ^{202}Hg have been documented in estuarine sediments (*10*), and to a lesser extent in rocky streambeds (*25*) where MMHg production in sediments is less likely to occur. The site-specific variation in the offsets in δ^{202}Hg suggests that the relative degree of fractionation due to microbial methylation versus demethylation differs across the Northeast coast study sites. The demethylation activities in these

regions are poorly understood but Schartup et al (*52*) recently documented variable methylation rates in sediment across the Northeast coast estuarine sites.

While our results are consistent with the previous findings that suggested sediments as the primary site for MMHg production, it is possible that MMHg derived from various external sources may also play an important role in the Northeast coast estuarine food webs. Methylmercury produced within wetlands and river watersheds have been shown to supply significant amounts of MMHg to aquatic ecosystems in the Northeast USA (*15, 17, 29, 53*). Chen et al (*14*) recently documented a lack of relationship between MMHg concentrations in sediments and in the water column across the same sites of the Northeast coast estuaries that we studied and suggested that sediments may be a minor contributor to MMHg found in water column. Given that the MMHg flux via sedimentation exceeds that due to resuspension at our study sites (*13*), it is possible that external MMHg sources deposited in the sediment via settling particles may provide a viable alternative explanation for the observed offsets in δ^{202}Hg between IHg (sediment) and the bioaccumulated MMHg. It is difficult to make a clear differentiation between in situ mass dependent fractionation of sediment-produced MMHg versus mixing of external MMHg sources in this study. Further investigation will be required to characterize the isotopic composition of various external MMHg sources and biogeochemical processes affecting MMHg production in sediments.

In summary, our results are consistent with either the production of MMHg from IHg in sediments or derivation of MMHg externally with deposition to the sediments. This MMHg is then subjected to a small amount of photodegradation in the water column before entering the food web and being passed to the various organisms at the study sites (with one exception described below). The use of Hg isotope ratios in this study provides additional insight into the sources and exposure pathways of MMHg studied by Chen et al (*12, 13*) in the same Northeast coast estuarine food webs. Chen et al (*12, 13*) documented a strong positive association between pelagic fish (silverside, killifish) MMHg concentrations and water column particulate MMHg concentrations, but not with sediment MMHg concentrations. Mussels and crabs did not show significant correlations with sediment and water column concentrations of MMHg. Based on these observations, it was suggested that while sediments may be the main repository for Hg, sediment MMHg concentrations are not an accurate predictor for MMHg bioaccumulation in estuarine biota. The authors also argued that the MMHg exposure via the water column may be

the result of either complex interactions between water and sediment MMHg or input of external MMHg sources from offshore. Given that the estuarine biota studied demonstrate different feeding behaviors and variable MMHg uptake routes, the consistent MMHg isotopic composition observed in various feeding guilds from each study location suggest that there may be extensive MMHg cycling between the sediment and water column via deposition and resuspension cycles without significant changes in the Hg isotopic compositions of the MMHg. In other words, even if the fish derive MMHg primarily from the water column, the MMHg in the water column may be isotopically similar to the small proportion of MMHg in the sediments.

4.3.4. Ecological variability in MMHg sources

While it appears that most aquatic organisms in this study acquire sediment-associated MMHg via trophic transfer, the high positive δ^{202}Hg values found in the WELLS and BUZZ birds and the BOLD mussels suggest that these organisms are exposed to a different (or additional) MMHg source that has considerably higher δ^{202}Hg values (Fig 2). Considering the mussels first, the main difference between the BOLD mussels and the mussels sampled in the other Northeast coast estuaries is that while the other mussels have a Hg isotopic composition consistent with a mixture of IHg and MMHg from the sediment, this pattern was observed only for Δ^{199}Hg, but not δ^{202}Hg in the BOLD mussels (Fig 2). Thus we infer that the BOLD mussels may be exposed to an additional MMHg source, possibly from the water column, due to their active filter feeding mechanism. The δ^{13}C values confirm that they feed on both pelagic and benthic resources (*12, 13*), which is clearly different from the crabs and fish that depend dominantly on benthic and epibenthic resources closely associated with the sediments.

We have identified two different scenarios that might explain how the BOLD mussels are exposed to Hg with anomalously high positive δ^{202}Hg values. First, to achieve high positive δ^{202}Hg values, the sediment-associated MMHg would have to be subjected to additional non-photochemical degradation and accompanying fractionation, causing the remaining MMHg to shift to higher δ^{202}Hg values. We speculate that resuspension of sediment-associated MMHg followed by microbial demethylation (*20*) in the water column (*15*) could produce MMHg with high positive δ^{202}Hg that is available for uptake by the mussels. BOLD is characterized by the highest TSS and particulate MMHg concentrations (*13*), and this region may be particularly susceptible to additional biogeochemical processing of Hg in the water column. Second, it is also

possible that the BOLD mussels were exposed to a second, and possibly unrelated external MMHg source that either has high δ^{202}Hg values inherited from an anthropogenic source or has undergone extensive microbial demethylation prior to being released into the estuary. BOLD is surrounded by an unvegetated area and diverse point sources of Hg, which may expose this site to extensive runoff of industrial Hg sources (*29, 53*). Moreover, based on recent evidence that suggests inflowing fluvial MMHg can serve as an important external MMHg source to pelagic food webs (*17*), we presume that exposure to an externally derived MMHg source may be a viable alternate explanation for the high δ^{202}Hg in the BOLD mussels.

In the birds, we documented similar Δ^{199}Hg but much higher δ^{202}Hg compared to fish from the same sites, which are the highest trophic level aquatic organisms measured in this study (Fig 2). It is possible that the high δ^{202}Hg MMHg is caused by the differences in food sources obtained from their respective sampling habitats compared to those of WELLS and BUZZ (Fig S1) or by their selective feeding behavior given that they feed dominantly on benthic invertebrates including mussels (*54*). Thus, if we assume that the birds analyzed in this study feed primarily on mussels, we might expect a significant positive relationship between % MMHg and δ^{202}Hg, and between % MMHg and Δ^{199}Hg of the sediments, mussels and birds due to the trophic transfer of MMHg. We plotted % MMHg against the δ^{202}Hg and Δ^{199}Hg values of the sediments, mussels and birds and observed significant positive relationships at WELLS (δ^{202}Hg; r^2=0.87, $p<0.05$, Δ^{199}Hg= 0.93, $p<0.05$) and BUZZ (δ^{202}Hg; r^2=0.99, $p<0.05$, Δ^{199}Hg; r^2=0.97, $p<0.05$). However, the trophic transfer of MMHg from the sediment, to mussels, to birds would indicate that the crabs and fish are exposed to a different MMHg source than the mussels, and this is not what we observed, except at the BOLD site. Moreover, given that the species of bird analyzed in this study have a relatively large feeding habitat (~60 km^2) (*55*), the small difference in the feeding habitat probably cannot account for the high δ^{202}Hg in the birds. Instead, we attribute the high δ^{202}Hg values in the birds to an internal metabolic fractionation of δ^{202}Hg. While metabolic fractionation of δ^{202}Hg has not been observed in fish (*23, 24*), internal demethylation has been proposed to occur in the liver of many species of bird (*56, 57*) and this may lead to the fractionation of δ^{202}Hg in birds. Previous studies have documented 1-2 ‰ higher δ^{202}Hg values in birds (egg contents), and in mammals including seals, whales, and human hair

compared to their respective diets (*39, 46, 47, 58, 59*) and attributed this pattern to the kinetic fractionation of δ^{202}Hg via internal demethylation.

Our study demonstrates that the measurement of Hg isotope ratios provides new insight into sources and exposure pathways of MMHg in estuarine food webs. Past studies that utilized Hg isotope ratios to decipher MMHg sources and exposure pathways in coastal food webs have only examined fish, and over smaller coastal regions (*10*, *27*). We found evidence for multiple Hg sources across the Northeast coast sediments, and the MMHg associated with the sediments appears to serve as the dominant MMHg source to the estuarine food webs. There has been a long-standing debate over the relative importance of MMHg derived from sediment or from the water column as a source to estuarine organisms. Complex biogeochemical processes affecting Hg bioavailability between sediment and water column however make it difficult to trace the dominant MMHg sources in the estuarine food webs based on Hg concentration alone. This study suggests that MMHg associated with sediments probably acts as the dominant source to many estuarine organisms, but that certain feeding guilds and certain localities are more susceptible to accumulating additional external MMHg sources. While further investigation is necessary to characterize various external MMHg sources, our study demonstrates that the measurement of Hg isotope ratios can be a valuable tool for deciphering MMHg sources and exposure pathways in diverse aquatic food webs and assessing the ecological variability of MMHg sources.

Acknowledgement

The authors would like to thank M. Johnson for the MC-ICP-MS operation, L. Savoy and other BRI staff for eider sample collection, D. Bugge, J. Williams, G. Bernier, T. Hollweg and K. Labrum for collection of aquatic samples, and P. Balcom, B. Jackson and V. Taylor for mercury analysis. The project described was supported in part by NIH Grant Number P42 ES007373 from the National Institute of Environmental Health Sciences.

References

(1) Mergler, D.; Anderson, H. A.; Chan, L. H. M.; Mahaffey, K. R.; Murray, M.; Sakamoto, M.; Stern, A. H. Methylmercury exposure and health effects in humans: A worldwide concern. *Ambio.* **2007**, *36*, 3-11.

(2) Ryther, J. H. Photosynthesis and fish production in the sea. *Science* **1969,** *166,* 72-76.

(3) Sunderland, E. M. Mercury exposure from domestic and imported estuarine and marine fish in the U.S. seafood market. *Environ Health Persp.* **2007,** *115,* 235-242.

(4) Baeyens, W.; Leermakers, M.; Papina, T.; Saprykin, A.; Brion, N.; Noyen, J.; De Geiter, M.; Elskens, M.; Goyens, L. Bioconcentration and biomagnification of mercury and methylmercury in North Sea and Scheldt Estuary fish. *Arch. Environ. Contam. Toxicol*. **2003,** *45,* 498– 508.

(5) Kawaguchi, T.; Porter, D.; Bushek, D.; Jones, B. Mercury in the American oyster Crassostrea virinica in South Carolina, USA, and public health concerns. *Marine Pollut. Bull.* **1999,** *38,* 324-327.

(6) Engle, M. A.; Tate, M. T.; Krabbenhoft, D. P.; Shauer, J. J.; Kolker, A.; Shanley, J. B.; Bothner, M. H. Comparison of atmospheric mercury speciation and deposition at nine sites across central and eastern North America. *J. Geophys. Res. Atmos.* **2010,** *115*, 1-13.

(7) Gehrke, G. E.; Blum, J. D.; Marvin-DiPasquale, M. Sources of mercury to San Francisco Bay surface sediment as revealed by mercury stable isotopes. *Geochim et Cosmochim Acta.* **2009a,** *75,* 691-705.

(8) Balcom, P. H.; Fitzgerald, W. F.; Vandal, G. M.; Lamborg, C. H.; Rolfhus, K. R.; Langer, C. S.; Hammerschmidt, C. R. Mercury sources and cycling in the Connecticut River and Long Island Sound. *Mar. Chem.* **2004,** *90,* 53-74.

(9) Benoit, J. M.; Gilmour, C. C.; Heyes, A.; Mason, R. P.; Miller, C. L. Geochemical and biological controls over methylmercury production and degradation in aquatic ecosystems. *In Biogeochemistry of Environmentally Important Trace Elements*; Cai, Y., Braids, O. C., Eds.; American Chemical Society: Washington DC **2003**, *835,* 262-297.

(10) Gehrke, G. E.; Blum, J. D.; Slotton, D. G.; Greenfield, B. K. Mercury isotope link mercury in San Francisco Bay forage fish to surface sediments. *Environ. Sci. Technol.* **2011,** *45,* 1264-1270.

(11) Greenfield, B. K.; Jahn, A. Mercury in San Francisco Bay forage fish. *Environ. Pollut.* **2010,** *158,* 2716-2724.

(12) Chen, C. Y.; Dionne, M.; Mayes, B. M.; Ward, D. M.; Sturup, S.; Jackson, B. P. Mercury bioavailability and bioaccumulation in estuarine food webs in the Gulf of Maine. *Environ. Sci. Technol.* **2009**, *43,* 1804-1810.

(13) Chen, C. Y.; Borsuk, M. E.; Bugge, D. M.; Hollweg, T.; Balcom, P. H.; Ward, D. M.; Williams, J.; Mason, R. P. Benthic and pelagic pathways of methylmercury bioaccumulation in estuarine food webs of the Northeast United States. *Plos. One*. **2014**, *9*, 1-11.

(14) Hammershmidt, C. R.; Fitzgerald, W. F. Sediment-water exchange of methylmercury determined from shipboard benthic flux chambers. *Mar. Chem.* **2008,** *109*, 86-97.

(15) Sunderland, E. M.; Dalziel, J.; Heyes, A.; Branfireun, B.A.; Krabbenhoft, D. P.; Gobas, F. A. P. C. Response of a Macrotidal Estuary to Changes in Anthropogenic Mercury Loading between 1850 and 2000. *Environ. Sci. Technol.* **2010**, *44*, 1698-1704.

(16) Mason, R. P.; Lawson, N. M.; Lawrence, A. L.; Leaner, J. J.; Lee, J. G.; Sheu, G. R. Mercury in the Chesapeake Bay. *Mar. Chem.* **1999,** *65*, 77-96.

(17) Balcom, P. H.; Hammerschmidt, C. R.; Fitzgerald, W. F.; Lamborg, C. H. O'Conner, J. S. Seasonal distributions and cycling of mercury and methylmercury in the waters of New York/New Jersey Harbor Estuary. *Mar. Chem.* **2008,** *109*, 1-17.

(18) Blum, J. D.; Bergquist, B. A. Reporting of variations in the natural isotopic composition of mercury. *Anal. Bioanal. Chem.* **2007,** *388*, 353-359.

(19) Rodriguez-gonzalez, P.; Epov, V. N.; Bridou, R.; Tessier, E.; Guyoneud, R.; Monperrus, M.; Amouroux D. Species-specific stable isotope fractionation of mercury during Hg(II) methylation by an anaerobic bacteria (*Desulfobulbus propionicus*) under dark conditions. *Envrion. Sci. Technol.* **2009,** *43*, 9183-9188.

(20) Kritee, K.; Barkay, T.; Blum, J. D. Mass dependent stable isotope fractionation of mercury during mer mediated microbial degradation of monomethylmercury. *Geochim et Cosmochim Acta*. **2009,** *73*, 1285-1296.

(21) Wiederhold, J. C.; Cramer, C. J.; Daniel, K.; Infante, I.; Bourdon, B.; Kretzschmar, R. Equilibrium mercury isotope fractionation between dissolved Hg(II) species and thiol-bound Hg. *Environ. Sci. Technol.* **2010,** *44*, 4191-4197.

(22) Bergquist, B. A.; Blum, J. D. Mass-dependent and -independent fractionation of Hg isotopes by photoreduction in aquatic systems. *Science* **2007,** *318*, 417-420.

(23) Kwon, S. Y.; Blum, J. D.; Carvan, M. J.; Basu, N.; Head, J. A.; Madenjian, C. P., David, S. R. Absence of fractionation of mercury isotopes during trophic transfer of methylmercury to freshwater fish in captivity. *Environ. Sci. Technol.* **2012,** *46*, 7527-7534.

(24) Kwon, S. Y.; Blum, J. D.; Chirby, M. A.; Chesney, E. J. Application of mercury isotopes for tracing trophic transfer and internal distribution of mercury in marine fish feeding experiments. *Environ. Toxicol. Chem.* **2013,** *23*, 2322-2330.

(25) Tsui, M. T. K.; Blum, J. D.; Kwon, S. Y.; Finlay, J. C.; Balogh, S. J.; Nollet, Y. H. Sources and transfers of methylmercury in adjacent river and forest food webs. *Environ. Sci. Technol.* **2012,** *46,* 10957-10964.

(26) Blum, J. D.; Popp, B. N.; Drazen, J. C.; Choy, C. A.; Johnson, M. W. Methylmercury production below the mixed layer in the North Pacific Ocean. *Nat. Geosci.* **2013,** *6,* 879-884.

(27) Senn, D. B.; Chesney, E. J.; Blum, J. D.; Bank, M. S.; Maage, A.; Shine, J. P. Stable isotope (N, C, Hg) study of methylmercury sources and trophic transfer in the Northern Gulf of Mexico. *Environ. Sci. Technol.* **2010,** *44,* 1630-1637.

(28) Long, E. R.; Robertson, A.; Wolfe, D. A.; Hameedi, J. W.; Sloane, G. M. Estimates of the spatial extent of sediment toxicity in major US estuaries. *Environ. Sci. Technol.* **1996,** *30,* 3585-3592.

(29) Driscoll, C. T.; Han, Y. J.; Chen, C. Y.; Evers, D. C.; Lambert, K. F.; Holsen, T. M.; Kamman, N. C.; Munson, R. K. Mercury contamination in forest and freshwater ecosystems in the northeastern United States. *BioSci.* **2007,** *57,* 17-28.

(30) Vandal, G. M.; Fitzgerald, W. F. A preliminary mercury budget for Narragansett Bay (Rhode Island, USA). *Water Air Soil Pollut.* **1995,** *80,* 679-682.

(31) Cardona-Marek, T.; Schaefer, J.; Ellickson, K.; Barkay, T.; Reinfelder, J. R. Mercury speciation, reactivity, and bioavailability in a highly contaminated estuary, Berry's Creek, New Jersey Meadowlands. *Environ. Sci. Technol.* **2007,** *41,* 8268−8274.

(32) Evers, D. C.; Burgess, N.; Champoux, L.; Hoskins, B.; Major, A.; Goodale, W.; Taylor, R.; Roppenga, R.; Daigle, T. Patterns and interpretation of mercury exposure in freshwater avian communities in northeastern North America. *Ecotoxicol.* **2005,** *14,* 193-222.

(33) Kannan, K.; Smith Jr, R. G.; Lee, R. F.; Windom, H. L.; Heitmuller, P .T.; Macauley, J. M.; Summer, J. K. Distribution of total mercury and methyl mercury in water, sediment, and fish from south Florida estuaries. *Arch. Environ. Contam. Toxicol.* **1998,** *34,* 109-118.

(34) Sunderland, E. M.; Gobas, F. A. P. C.; Heyes, A.; Branfireun, B. A.; Bayer, A. K.; Cranston, R. E.; Parson, M. B. Speciation and bioavailability of mercury in well-mixed estuarine sediments. *Mar. Chem.* **2004**, *90,* 91-105.

(35) Donovan, P. M.; Blum, J. D.; Yee, D.; Gehrke, G. E.; Singer, M. B. An isotopic record of mercury in San Francisco Bay sediment. *Chem. Geo.* **2013**, *349-350,* 87-98.

(36) Foucher, D.; Ogrinc, N.; Hintelmann, H. Tracing mercury contamination from the Idrija mining region (Slovenia) to the Gulf of Trieste using Hg isotope ratio. *Environ. Sci. Technol.* **2009**, *43,* 33-39.

(37) Das, R.; Bizimis, M.; Wilson, A. M. Tracing mercury seawater vs. atmospheric inputs in a pristine SE USA salt march system: Mercury isotope evidence. *Chem. Geo*. **2012,** *336,* 50-61.

(38) Gratz, L. E.; Keeler, G. J.; Blum, J. D.; Sherman, L. S. Isotopic composition and fractionation of mercury in Great Lakes precipitation and ambient air. *Environ. Sci. Technol.* **2010,** *44,* 7754-7770.

(39) Mil-Homens, M.; Blum, J.; Canario, J.; Caetano, M.; Costa, A. M.; Lebreiro, S. M.; Trancoso, M.; Richter. T.; de Stigter. H.; Johnson, M.; Branco, V.; Cesario, R.; Mouro, F.; Mateus, M.; Boer, W.; Melo, Z. Tracing anthropogenic Hg and Pb input using stable Hg and Pb isotope ratios in sediments of the central Portuguese Margin. *Chem. Geo.* **2012,** *336,* 62-71.

(40) Gehrke, G. E.; Blum, J. D.; Meyers, P. A. The geochemical behavior and isotopic composition of Hg in a mid-Pleistocene western Mediterranean sapropel. *Geochim et Cosmochim Acta.* **2009,** 73, 1651-1665.

(41) Laffont, L.; Sonke, J. E.; Maurice, L.; Monrroy, S. L.; Chincheros, J.; Amouroux, D.; Behra, P. Hg speciation and stable isotope signature in human hair as a tracer for dietary and occupational exposure to mercury. *Environ. Sci. Technol.* **2011**, *45,* 9910-9916.

(42) Wayland, M.; Garcia-Fernandez, A. J.; Neugebauer, E.; Gilchrist, H. G. Concentrations of cadmium, mercury and selenium in blood, liver and kidney of common eider ducks from the Canadian arctic. *Environ. Monit. Assess.* **2001,** *71,* 255-267.

(43) Mason, R. P.; Sullivan, K. A. Mercury in Lake Michigan. *Environ. Sci. Technol.* **1997**, *31,* 942-947.

(44) Watras, C. J.; Bloom, N. S. Mercury and methylmercury in individual zooplankton: Implications for bioaccumulation. *Limol. Oceanogr.* **1992**, *37,* 1313-1318.

(45) Hobson , K. A. Trophic relationships among high Arctic seabirds: insights from tissue-dependent stale-isotope models. *Mar. Ecol. Prog. Ser.* **1993,** *95,* 7-18.

(46) Das, R.; Salters, V. J. M.; Odom, A. L. A case for in vivo mass-independent fractionation of mercury isotopes in fish. *Geochem. Geophys. Geosyst.* **2009,** *10,* Q11012.

(47) Gantner, N.; Hintelmann, H.; Zheng, W.; Muir, D. C. Variations in stable isotope fractionation of Hg in food webs of Arctic lakes. *Environ. Sci. Technol.* **2009,** *43,* 9148-9154.

(48) Perrot, V.; Pastukhov, M. V.; Epov, V. N.; Husted, S.; Donard, O. F. X.; Amouroux, D. Higher mass-independent isotope fractionation of methylmercury in the pelagic food web of Lake Baikal (Russia). *Environ. Sci. Technol.* **2012,** *46,* 5902-5911.

(49) Day, R. D.; Roseneau, D. G.; Berail, S.; Hobson, K. A.; Donard, O. F. X.; Vander Pol, S. S.; Pugh, R. S.; Moors, A. J.; Long, S. E.; Becker, P. R. Mercury stable isotopes in seabird eggs reflect a gradient from terrestrial geogenic to oceanic mercury reservoirs. *Environ. Sci. Technol.* **2012,** *46,* 5327-5335.

(50) Point, D.; Sonke, J. E.; Day, R. D.; Roseneau, D. G.; Hobson, K. A.; Vander Pol, S. S.; Moors, A. J.; Pugh, R. S.; Donard, O. F. X.; Becker, P. R. Methylmercury photodegradation influenced by sea-ice cover in Arctic marine ecosystems. *Nat. Geosci.* **2011**, *4,* 188-194.

(51) Sherman, L. S.; Blum, J. D. Mercury stable isotopes in sediments and largemouth bass from Florida lakes, USA. *Sci. Tot. Environ.* **2013,** *448,* 163-175.

(52) Schartup, A. T.; Mason, R. P.; Balcom, P. H.; Hollweg, T. A.; Chen, C. Y. Methylmercury production in estuarine sediments: Role of organic matter. *Environ. Sci. Technol.* **2012,** *47,* 695-700.

(53) Dennis, I. F.; Clair, T. A.; Driscoll, C. T.; Kamman, N.; Chalmercs, A.; Shanley, J.; Norton, S. A.; Kahl, S. Distribution patterns of mercury in lakes and rivers of northeastern North America. *Ecotoxicol.* **2005,** *14,* 113-123.

(54) Guillemette, M.; Ydenberg, R.C.; Himmelman, J.H. The role of energy intake rate in prey and habitat selection of common eiders *Somateria mollissima* in winter: a risk-sensitive interpretation. *J. Animal Ecol*. **1992,** *61,* 599-610.

(55) Merkel, F. R.; Mosbech, A.; Sonne, C.; Flagstad, A.; Falk, K.; Jamieson, S. E. Local movements, home ranges and body condition of Common Eider *Somateria mollissima* wintering in southwest Greenland. *Ardea.* **2006,** *94,* 639-650.

(56) Eagles-Smith, C.A.; Ackerman, J.T.; Yee, J.; Adelsbach, T.L. Mercury demethylation in waterbird livers: Dose-response thresholds and differences among species. *Environ. Toxicol. Chem*. **2009,** *28,* 568-577.

(57) Kim, E.Y.; Murakami, T.; Saeki, K.; Tatsukawa, R. Mercury levels and its chemical form in tissues and organs of seabirds. *Arch. Environ. Contam. Toxicol.* **1996,** *30,* 259-266.

(58) Li, M.; Sherman, L. S.; Blum, J. D.; Granjean, P.; Mikkelsen, B.; Sunderland, E. C.; Weihe, P.; Shine, J. Assessing sources of human methylmercury exposure using stable mercury isotopes. *Environ. Sci. Technol.* **2014,** DOI 10.1021/es500340r.

(59) Sherman, L. S.; Blum, J. D.; Franzblau, A.; Basu, N. New insight into biomarker of human mercury exposure using naturally occurring mercury stable isotopes. *Environ. Sci. Technol*. **2013,** *47,* 3403-3409.

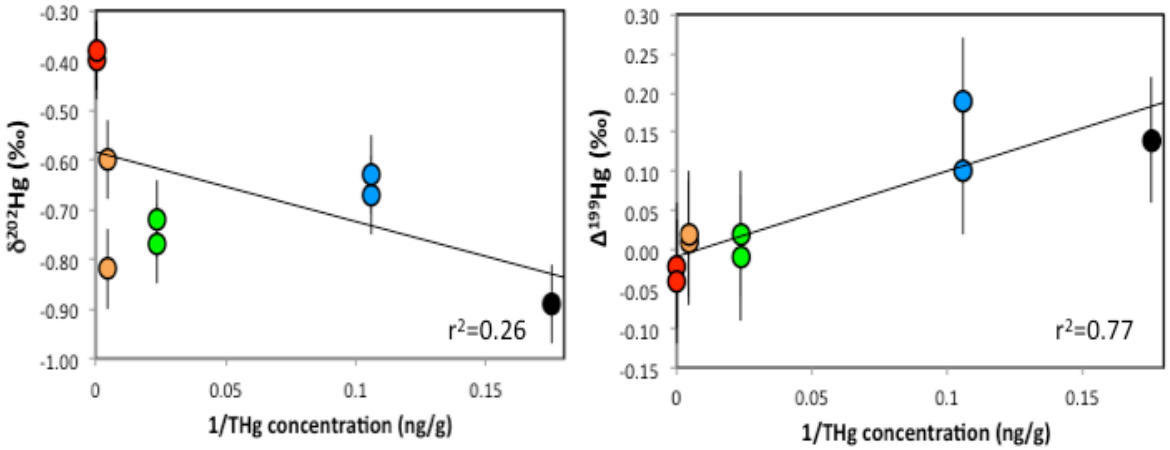

Figure 4.1 Plot of 1/THg concentration (ng/g) versus δ^{202}Hg and Δ^{199}Hg values of the Northeast coast estuary sediments. Each site is represented with different colors; BUZZ (black), WELLS (blue), BARN (green), BOLD (orange), and MILL (red). The solid lines represent linear regressions. Analytical uncertainty is indicated by the error bar (2 s.d).

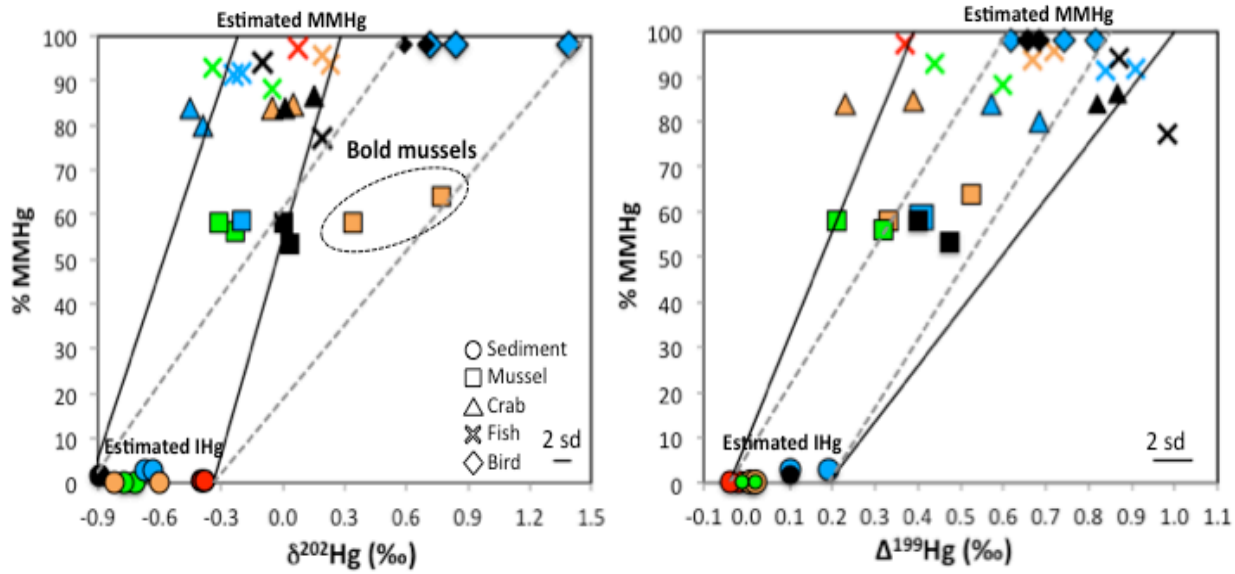

Figure 4.2 Plot of % MMHg versus δ^{202}Hg (a) and Δ^{199}Hg values (b) of estuarine sediments and biota. Each site is represented by a different color; BUZZ (black), WELLS (blue), BARN (green), BOLD (orange), and MILL (red). The solid lines represent the range of estimated MMHg isotopic composition needed to explain sediments, crabs and fish. The dotted lines represent the range of estimated MMHg isotopic composition needed to explain mussels from BOLD and birds from BUZZ and WELLS. The "estimated MMHg" and "estimated IHg" represent the ranges of Hg isotopic composition extrapolated for 100% MMHg and 100% IHg, respectively, based on the linear regression of % MMHg vs δ^{202}Hg and Δ^{199}Hg. Analytical uncertainty is indicated by the error bar (2 s.d).

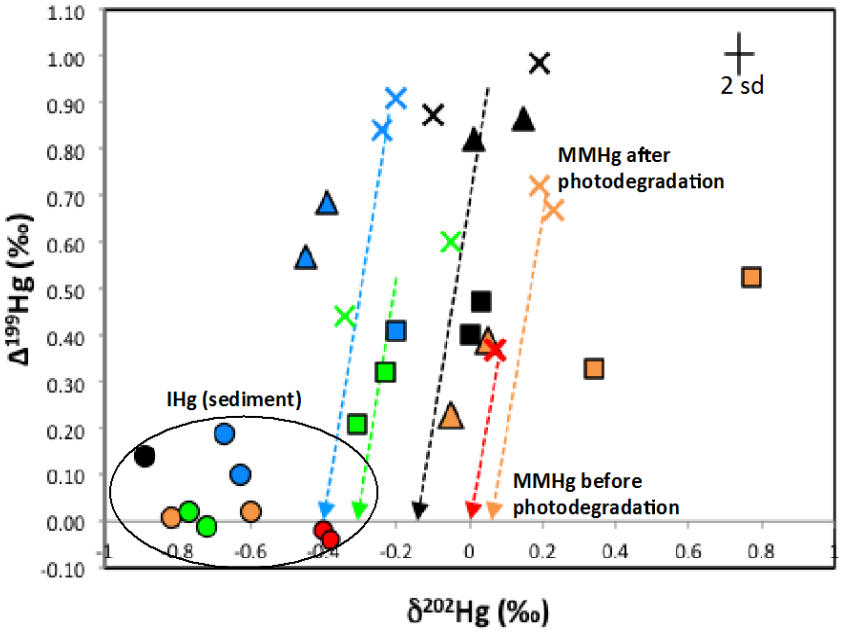

Figure 4.3 Plot of δ^{202}Hg and Δ^{199}Hg values of all sediments and estuarine biota. Each site is represented with different colors; BUZZ (black), WELLS (blue), BARN (green), BOLD (orange), and MILL (red). Symbols are the same as Figure 2. The arrows represent the experimentally derived photochemical degradation slope for MMHg. Analytical uncertainty is indicated by the error bar (2 s.d).

4.4. Supporting Information

Supporting figure (Fig 4.S1) and table (Table 4.S1). This material is available free of charge via the Internet at http://pubs.acs.org.

Figure 4.S1 Map of the Northeast coast, USA representing the sampling locations (Maine; ME, Massachusetts; MA, Rhode Island, RI; Connecticut, CT, New Jersey; NJ). Aquatic biota were sampled at sites indicated in black circles. Birds were sampled at three locations in ME and MA and are represented with white circles. This map has been modified from nationalatlas.gov.

Table 4.S1 THg concentrations (ng/g), % MMHg, stable carbon and nitrogen values and Hg isotope ratios of all sediment and estuarine biotas.

	THg (ng/g)	% MMHg	$\delta^{15}N$ (‰)	$\delta^{13}C$ (‰)	$\delta^{202}Hg$ (‰)	$\Delta^{201}Hg$ (‰)	$\Delta^{199}Hg$ (‰)
Sediment							
WELLS, ME	9.43	2.96			-0.67	0.09	0.19
	9.43	2.96			-0.63	0.02	0.10
BUZZ, MA	5.70	1.74			-0.89	0.17	0.10
BOLD, RI	221	0.20			-0.82	0.01	0.01
	221	0.20			-0.60	0.01	0.02
BARN, CT	42.0	0.13			-0.72	0.15	-0.01
	42.0	0.13			-0.77	0.18	0.02
MILL, NJ	2962	0.32			-0.40	0.01	-0.02
	2962	0.32			-0.38	0.02	-0.04
Mussel	*Filter feeder; particulate organic matter*						
WELLS, ME	109	58.7	6.16	-19.60	-0.20	0.09	0.41
BUZZ, MA	187	53.4	8.43	-18.67	0.03	0.02	0.47
	169				0.00	0.23	0.40
BOLD, RI	192	63.9	7.80	-18.97	0.77	0.06	0.52
	61.2				0.34	0.27	0.33
BARN, CT	190	56.1	7.08	-20.08	-0.23	0.04	0.32
	113				-0.31	0.12	0.21
average	*146*	*58.0*	*7.37*	*-19.33*	*0.06*	*0.12*	*0.38*
Crab	*Epibenthic consumer; benthic microalgae, benthic invertebrates*						
WELLS, ME	68.1	80.0	9.37	-16.78	-0.39	0.03	0.68
	26.4				-0.45	0.45	0.57
BUZZ, MA	58.3	86.5	7.83	-14.72	0.15	0.05	0.87
	84.6				0.01	0.72	0.82
BOLD, RI	68.3	84.6	13.54	-18.26	0.05	0.03	0.39
	25.8				-0.05	0.45	0.23
average	*55.3*	*83.7*	*10.25*	*-16.59*	*-0.11*	*0.29*	*0.59*
Fish	*Epibenthic/water column consumer; zooplankton, microalgae, benthic invertebrates, detritus*						
WELLS, ME	67.4	91.7	8.99	-14.87	-0.20	0.70	0.91
	25.5	91.3	7.80	-14.95	-0.24	0.75	0.84
BUZZ, MA	96.5	77.3	9.84	-16.12	0.19	0.77	0.98
	122	94.1	11.68	-16.38	-0.10	0.73	0.87
BOLD, RI	79.4	95.8	15.70	-16.07	0.19	0.54	0.72
	45.2	93.8	15.78	-16.58	0.23	0.63	0.67
BARN, CT	120	93.1	10.02	-16.13	-0.34	0.33	0.44
	54.5	88.1	7.80	-17.14	-0.05	0.46	0.60
MILL, NJ	631	97.3	13.91	-24.02	0.07	0.29	0.37
average	*138*	*91.4*	*11.28*	*-16.92*	*-0.03*	*0.58*	*0.71*
Bird	*Epibenthic and water column consumer; bivalves, mollusks, crustaceans, fish*						

WELLS, ME	208[SA]				0.71	0.59	0.74
	363[SA]				0.84	0.63	0.82
	453[SC]				1.39	0.46	0.62
BUZZ, MA	1755[PL]				0.70	0.46	0.66
	1536[PL]				0.59	0.51	0.68
average	*863*	*(98)*	*(13.2)*	*(17.4)*	*0.85*	*0.53*	*0.70*

Detailed feeding strategies are found in Chen et al[12,13].
Values in bracket are derived from Wayland et al[42], and Hobson et al[45].
SA, SC, and PL refer to Saco Bay, ME, Scarborough Marsh, ME, and Plum Island Sound, MA, respectively.

CHAPTER 5

Isotopic study of mercury sources and transfer between a freshwater lake and adjacent forest food web

Abstract

Studies of monomethylmercury (MMHg) sources and biogeochemical pathways have been extensive in aquatic ecosystems but limited in forest ecosystems. Increasing evidence suggests that there is significant mercury (Hg) exchange between aquatic and forest ecosystems. We use Hg stable isotope ratios (δ^{202}Hg and Δ^{199}Hg) to investigate the relative importance of MMHg sources and assess Hg transfer pathways between Douglas Lake and adjacent forests located at the University of Michigan Biological Station, USA. We characterize Hg isotopic compositions of basal resources and use linear regression of % MMHg versus δ^{202}Hg and Δ^{199}Hg to estimate Hg isotope values for inorganic mercury (IHg) and MMHg in the aquatic and adjacent forest food webs. In the aquatic ecosystem, we found that lake sediment represents a mixture of IHg pools deposited via watershed runoff and precipitation. The δ^{202}Hg and Δ^{199}Hg values estimated for IHg are consistent with other studies that measured forest floor (i.e., soil, leaf litter) in temperate forests. The Δ^{199}Hg value estimated for MMHg in the aquatic food web indicates that MMHg is subjected to ~20% photochemical degradation prior to bioaccumulation. In the forest ecosystems, we found a significant negative relationship between total Hg concentration and both δ^{202}Hg and Δ^{199}Hg of terrestrial soil, riparian soil, and even bulk lake sediment. This suggests that IHg input from watershed runoff provides an important Hg transfer pathway between the forest and aquatic ecosystems. We measured Δ^{199}Hg values for high trophic level insects and compared these insects at multiple distances perpendicular to the lake shoreline. The Δ^{199}Hg values correspond to the % canopy cover, suggesting that terrestrial MMHg is subjected to varying extents of photochemical degradation and the extent may be controlled by sunlight exposure. Our study demonstrates that the use of Hg isotopes adds important new

insight into the relative importance of MMHg sources and complex Hg transfer pathways across ecosystem boundaries.

5.1. Introduction

Transformation of inorganic mercury (IHg) to monomethylmercury (MMHg) in aquatic environments can result in high MMHg levels in fish and cause negative health impacts for wildlife and humans that consume fish (*1*). MMHg is a toxic and bioaccumulative organometallic compound, which can accumulate to elevated levels in high trophic level organisms via biomagnification (*2*). Previous studies of MMHg sources and biogeochemical pathways in aquatic ecosystems have been extensive, but studies in terrestrial ecosystems have been more limited. A number of recent studies have reported elevated MMHg levels in terrestrial organisms such as spiders (*3-5*), birds (*6, 7*) and bats (*8, 9*) collected across North American forests. The MMHg levels in these organisms have been linked to reproductive failure, physiological alteration, and neurological deficit (*6, 7*). Understanding MMHg sources and exposure pathways are key to reduction of MMHg levels in both aquatic and terrestrial ecosystems.

Biogeochemical processes governing in situ MMHg production and degradation as well as external inputs of MMHg can determine the exposure and fate of MMHg in ecosystem food webs. Increasing evidence also suggests that complex ecological processes governing Hg transfer across ecosystem boundaries may impact recipient ecosystems that are subsidized with energy and nutrients. For instance, terrestrial ecosystems may produce MMHg in situ from microbial methylation of IHg in forest soil and wetlands (*10, 11*) or receive external inputs from rainwater and fog (*12, 13*). Another potentially important MMHg source to terrestrial ecosystems is through transfer from aquatic ecosystems by emergent insects that spend a part of their lifecycle in aquatic environments and provide important energy and nutrient subsidies to terrestrial ecosystems (*4*). Using mesocosm ponds, Tweedy et al. (*5*) documented a positive relationship between MMHg levels in riparian spiders and the emergent insect flux (i.e. microcaddisfly and chironomids). Cristol et al. (*3*) observed higher total Hg (THg) concentrations in riparian spiders and birds that feed along streams contaminated with Hg compared to those at a reference site at South River, Virginia, and attributed this to either MMHg flux mediated by emergent insects or in situ MMHg production in floodplains. Conversely, IHg associated with terrestrial resources as

well as MMHg produced both internally and externally can be transported back to aquatic ecosystems through watershed runoff (*14*) or movements of organisms (*15*). Given the presence of multiple sources and complex biogeochemical processes governing Hg transfer between ecosystem boundaries, tools that can provide direct linkages between source and receptor should help elucidate dominant MMHg sources to aquatic and terrestrial ecosystems.

Here we use Hg isotopic compositions to assess MMHg sources and biogeochemical pathways in a freshwater lake and an adjacent forest food web. Mercury stable isotopes can undergo both mass dependent (MDF) and mass-independent fractionation (MIF). Mass-dependent fractionation is reported as δ^{202}Hg (in ‰; *16*) and occurs via multiple environmentally relevant processes including microbial methylation (*17, 18*), demethylation (*19*), thiol-ligand exchange (*20*), and photochemical reduction (*21, 22*). Mass-independent fractionation (MIF), reported as Δ^{199}Hg and Δ^{201}Hg (in ‰; *16*), occurs predominantly via photochemical degradation of MMHg and photoreduction of IHg (*21*). Consequently, Δ^{199}Hg has been used as a conservative tracer for understanding biological processes such as bioaccumulation and trophic transfer (*23-25*). The ratio of Δ^{199}Hg/Δ^{201}Hg has also been used for distinguishing between photochemical reduction of IHg (Δ^{199}Hg/Δ^{201}Hg=1.00) and photodegradation of MMHg (Δ^{199}Hg/Δ^{201}Hg=1.2-1.4) in natural ecosystems (e.g., *26*).

In combination with traditional ecological isotope tracers (i.e., δ^{13}C and δ^{15}N), the measurement of Hg isotopic composition has proven its utility for distinguishing between sources and identifying biogeochemical processing of MMHg in diverse ecosystems (*28-30*). For example, Senn et al. (2010) characterized coastal and pelagic food webs in the Gulf of Mexico, USA. Large positive Δ^{199}Hg values (> +1‰) were measured in pelagic organisms, which exhibited marine δ^{13}C signatures (~ -15 ‰). This indicated that MMHg subjected to extensive photochemical degradation in the pelagic water column was the dominant MMHg source to pelagic food webs. Coastal organisms were characterized by small positive Δ^{199}Hg (< +1‰) and terrestrial δ^{13}C signatures (~ -20 ‰), suggesting that MMHg produced in the coastal sediment had undergone small amounts of photochemical degradation. In another study, Tsui et al. (*25*) observed distinct ranges in δ^{202}Hg (estimated for MMHg) between stream, riparian, and upland forest food webs consisting of macroinvertebrates in northern California, USA. Based on this evidence, it was suggested that MMHg associated with precipitation, which had higher δ^{202}Hg

values (-0.5 to +0.5 ‰), might be the dominant source to forest food webs, in contrast to MMHg produced by microbial methylation in the stream (-1.7 to -1.4 ‰). In the riparian food web, the δ^{202}Hg estimated for MMHg displayed intermediate values between stream and upland forest food webs, suggesting the potential importance of emergent insects as mediators of the MMHg flux to adjacent forest ecosystems. Given the clear linkages between δ^{13}C and Hg isotope values, we suggest that the analysis of Hg isotope ratios should shed light on the relative importance of MMHg sources and biogeochemical processes governing Hg transfer between ecosystems.

In this study, we investigate the sources and biogeochemical pathways of MMHg in the littoral zone of Douglas Lake, Michigan and adjacent forest ecosystems, and assess the importance of Hg transfer between Douglas Lake and adjacent forests. The study site is on the property of the University of Michigan Biological Station (UMBS), which is relatively undeveloped and is well characterized in terms of ecology and environmental conditions. The UMBS is dominated by temperate forests and includes ~11 km of shoreline along Douglas Lake, which receives Hg primarily by long-range atmospheric transport (*12, 31*). Douglas Lake hosts diverse assemblages of emergent insects such as mayflies and dragonflies. Here, we characterize Hg isotopic compositions in the basal resources and various assemblages of aquatic and forest organisms consisting of macroinvertebrates, birds, bats, and fish. The δ^{13}C and δ^{15}N values were determined to assess the energy sources and feeding guilds, and the relative trophic position of the organisms, respectively. The isotopic compositions representing IHg and MMHg were estimated by analyzing organisms with a range of % MMHg, an approach previously applied to a northern California watershed (*25, 32*). The estimated IHg and MMHg isotopic compositions were used to identify the dominant MMHg sources in the aquatic and forest food webs, and assess the importance of Hg transfer between ecosystems.

5.2. Materials & Methods

5.2.1. Sample collection and processing

We collected basal resources and diverse assemblages of macroinvertebrates, birds, bats, and fish in the littoral zone of Douglas Lake and in the riparian and forest adjacent to Douglas Lake near the Grapevine Point Trail at the UMBS (Fig 1). Douglas Lake is a kettle lake located near the northern tip of the Michigan's lower peninsula (45°33'31.15"N, 84°40'39.35"W). The lake covers a surface area of 13.7 km^2 and has an average depth of 9 m. Douglas Lake is

characterized as mesotrophic, with sand and fine gravel as the dominant substrates. The surrounding watershed covers an area of 52 km^2 and is composed of sandy terraces with *Populus tremuloides* (aspen), and *Quercus rubra* (red oak) as the dominant overstory trees in the forest. Basic water quality parameters were obtained from the Douglas Lake Buoy Data during the aquatic sampling period of May-June, 2013 (Table 1).

In the littoral zone of Douglas Lake, we sampled surface sediment, aquatic detritus, macroinvertebrates, and fish within 4 m of the shoreline at water depths of 0.5-1 m (Table 2). All samples were collected in early May 2013, prior to the seasonal emergence of aquatic insects. Surface sediment (0-5 cm) were collected at 4 different locations (10 m apart) with acid-washed scoops or clean centrifuge tubes. At each location, approximately 50mL of sediment was collected. Samples of aquatic detritus composed mostly of decaying deciduous foliage were collected with gloved hands and rinsed thoroughly with distilled water prior to storage. Aquatic macroinvertebrates were collected by scraping sandy bottoms with a trawl, and juvenile fish were captured using seine nets. All biota samples were emptied into clean trays, separated by species using alcohol-cleaned stainless steel forceps, and placed into clean centrifuge tubes for later processing.

In the riparian zone and the forest near Grapevine Point Trail, we sampled soil, leaf litter, macroinvertebrates, birds, and bats (Table 2). All samples were collected in mid to late July 2013, after emergence of aquatic insects. Forest macroinvertebrates were sampled in four different locations, in a transect perpendicular to the Douglas Lake shoreline, at distances of 0-5, 5-10, 10-30 and 30-60m (Fig 1). Approximately 30 clean plastic cups were installed as pitfall traps along each transect. Macroinvertebrates were collected from the traps and sorted by species twice a day using alcohol-cleaned stainless steel forceps. Basal resources including soil (O-horizon; 0-5cm depth) and leaf litter were collected with clean gloved hands at two distances along the transects (0-5m and 30-60m). Hair and excrement samples were collected for *Myotis lucifugus* (brown bats) and *Turdus migratorius* (American robins). Bat hair samples were obtained by installing a mist net near the nest to capture bats during the hours of feeding, after which hair was removed with alcohol-cleaned stainless steel scissors. Fresh excrement samples were obtained by placing aluminum foil under a single nest overnight. Samples of American Robin excrement were removed from multiple nests using clean stainless steel forceps.

All samples were placed in either clean plastic bags or clean centrifuge tubes prior to storage at -20°C. The frozen samples were transported to the University of Michigan for processing and analyses. Samples were freeze-dried and homogenized by combining multiple samples or individuals of the same species using an alumina ball mill, or an acid-cleaned glass mortar and pestle.

5.2.2. Stable C and N isotope analyses

Stable isotopic compositions of carbon and nitrogen ($\delta^{13}C$ and $\delta^{15}N$) were measured to estimate the influence of energy sources and trophic positions in the food web, respectively. Homogenized powders from each sample were weighed into tin capsules (average 1.2 mg), and analyzed using a Costech ECS 4010 elemental analyzer coupled to the inlet of a Finnigan Delta V Plus mass spectrometer in the Stable Isotope Laboratory at the University of Michigan. Isotope values are expressed in the standard $\delta^{15}N$ and $\delta^{13}C$ notation (‰) relative to international standards (atmospheric N_2 and PeeDee belemnite). An acetanilide standard was used to generate calibration curves. Analytical precision was quantified using several internationally calibrated standards; IAEA N_2, IAEA-600 Caffeine, IAEA-CH-6 Sucrose, and USGS 25 interspersed throughout every 13 samples. The analytical uncertainty of $\delta^{15}N$ and $\delta^{13}C$ were ±0.12 ‰ (1SD).

5.2.3. Hg and MMHg concentration and Hg stable isotope analyses

Total Hg concentrations (THg) were first determined by combustion and atomic absorption spectroscopy (AAS) using a Nippon Instruments MA-2000 Hg analyzer. Standard reference material NIST 3133 was used to generate calibration curves and to monitor quality control. The standard reference material TORT-2 (n= 7) was measured along with the samples and THg was measured as 90±4% (±1 s.d.) of the certified value. The MMHg concentrations were determined for a subset of basal resources and biota at the University of North Carolina at Greensboro. Samples were digested in 4.6 M HNO_3 at 60°C for 12 hours and the acid digests were neutralized with 4.6 M KOH, and added with 1% $Na_2B_4O_7$ for derivatization and collection of ethylated Hg species on Tenax traps. Ethylated Hg species were separated using a gas chromatography column, converted to Hg^0 on a pyrolytic trap, and analyzed via cold-vapor atomic fluorescence spectroscopy (AFS) using a Brooks Rand Model III Hg detector. Reagent blanks (n=2), SRM TORT-3 (n=4), and SRM DORM-4 (n=21) were analyzed along with the

samples for quality control. The reagent blank had no detectable MMHg and the average recoveries of SRM TORT-3 and SRM DORM-4 were 86% and 91%, respectively. The relative standard deviation of replicate samples ranged between 1.8 and 10 %.

The detailed procedure for measuring Hg stable isotope ratios is provided in Blum (*33*). Briefly, samples were loaded into ceramic boats with Na_2CO_3 and Al_2O_3 powders, and combusted in an offline two-stage combustion furnace to release Hg^0 from the samples. Released Hg^0 was captured into a trap solution (1% $KMnO_4$ in 10% trace metal grade H_2SO_4) using a flow of Hg-free oxygen. To remove combustion product matrix components from the sample, the solution was neutralized with NH_2OH and Hg was reduced back to Hg^0 with $SnCl_2$, and purged into a new trap solution. The blanks and recoveries of the combustion and transfer steps were monitored by measuring THg in the trap solutions of procedural blanks (powders in boats without samples), samples, and the standard reference materials TORT-2 (n=4) and MESS-3 (n=2). The THg in the trap solutions were determined by cold vapor atomic absorption spectroscopy (CV-AAS; Nippon MA-2000). The procedural blanks had an average THg of 0.16±0.05 ng (n=5). The recoveries of the combustion and transfer steps of all the samples and standard reference materials ranged between 90 to 108%, and 89 to 104%, respectively. The THg concentrations are reported based on the THg measured in the trap solutions and the mass of freeze-dried samples placed on the combustion furnace (Table 2).

Mercury stable isotope ratios were measured using a Nu Instruments multi-collector inductively coupled plasma mass spectrometer (MC-ICP-MS). Sample Hg was introduced to the MC-ICP-MS by continuously reducing Hg^{2+} in solution with 2% $SnCl_2$, and separating Hg^0 using a frosted glass tip phase separator. Instrumental mass bias was corrected using an internal Tl standard (NIST SRM 997) introduced to the gas flow as an aerosol and by bracketing each sample with NIST SRM 3133 matched to matrix composition and to sample THg concentrations within 10%. MDF is reported as $\delta^{202}Hg$ in permil (‰) referenced to NIST SRM 3133:

$$\delta^{202}Hg = \{[(^{202}Hg/^{198}Hg)_{sample}/ (^{202}Hg/^{198}Hg)_{NIST3133}]-1\}*1000 \quad (1)$$

MIF represents the difference between the measured δ^{xxx}Hg value and the value predicted based on MDF alone. MIF is reported as Δ^{199}Hg, Δ^{200}Hg, and Δ^{201}Hg in permil (‰). The calculation is based on an approximation valid for δ <10‰:

$$\Delta^{199}Hg = \delta^{199}Hg - (\delta^{202}Hg * 0.252) \quad (2)$$

$$\Delta^{200}Hg = \delta^{200}Hg - (\delta^{202}Hg * 0.5024) \quad (3)$$

$$\Delta^{201}Hg = \delta^{201}Hg - (\delta^{202}Hg * 0.752) \quad (4)$$

Analytical uncertainty at 2 s.d. is estimated based on replicate analysis of a standard solution (UM-Almáden) and replicate analyses of standard reference materials (TORT-2 and MESS-3). We used TORT-2 to report analytical uncertainty since it had a larger uncertainty. UM-Almáden (n= 46) had mean values (±2 s.d.) of δ^{202}Hg= -0.57±0.13 ‰, and Δ^{199}Hg= -0.04±0.09‰. Standard reference material TORT-2 (n=4) had mean values of δ^{202}Hg= 0.06±0.12‰, and Δ^{199}Hg= 0.75±0.11 ‰; and MESS-3 (n=2) had mean values of δ^{202}Hg= -2.18±0.07‰, and Δ^{199}Hg= 0.03±0.04 ‰.

5.3. Results & Discussion

5.3.1. MMHg biomagnification in the aquatic food web

The THg concentrations of basal resources in Douglas Lake had mean values of 4.26±0.04 ng/g and 26.3±0.3 ng/g in the sediment and aquatic detritus, respectively (Table 2). The THg concentrations of aquatic organisms ranged between 31.7 ng/g (dragonfly larvae) and 186 ng/g (shiner) (Table 2). The mean fraction of THg that is MMHg (% MMHg hereafter) increases in the order: mussel (32 %), mayfly (42 %), snail (46 %), dragonfly larvae (Aeshnidae; 67 %), water bug (80 %), dragonfly larvae (Erythemis; 84 %), yellow perch (~100 %), and shiner (~100 %) (Table 2). The % MMHg of crayfish was estimated from the literature (*34*, *35*), using reported values of >90% in freshwater crayfish found across New England and northern Californian streams. The increasing trend of % MMHg corresponds with increasing δ^{15}N values estimated by trophic position (r^2= 0.93, $p<0.05$). This is consistent with MMHg biomagnification trends documented in many aquatic food webs (*2*, *36*). The δ^{13}C values of the aquatic organisms displayed a range between -30.7 to -22.8 ‰ (Table 2). The δ^{13}C values observed in this study are

within the ranges of similar organisms utilizing allochthonous resources in freshwater lake systems (*37*).

The Hg isotopic compositions of the aquatic basal resources and organisms ranged between -2.05 and 0.12 ‰ for δ^{202}Hg, and between -0.12 and 2.52 ‰ for Δ^{199}Hg (Table 2). The δ^{202}Hg and Δ^{199}Hg values of the aquatic organisms displayed an increasing trend with increasing trophic position (δ^{15}N and % MMHg). Similar trends have been documented in many aquatic food webs including lakes (*29, 38*), streams and forests (*15, 25*), and marine ecosystems (*30, 39*). Fish feeding experiments indicate that the differences in the Hg isotopic composition with trophic position are not due to isotope fractionation of δ^{202}Hg or Δ^{199}Hg (*23, 24*). Instead, it represents mixtures of different proportions of IHg and MMHg, which have different isotopic compositions that were imparted before entry into the food web. As in our present study, others have used linear regressions of % MMHg versus Hg isotope values to estimate the isotopic composition representing the bioaccumulated MMHg and IHg in ecosystem food webs (*24, 25, 39*). Our regression of % MMHg versus δ^{202}Hg and Δ^{199}Hg values of the aquatic organisms (Figure 2a, b) did not include the sediment values in order to differentiate between the bulk IHg associated with the basal resources and the IHg attributable to bioaccumulation within the food web. Significant positive relationships ($p < 0.05$) with δ^{202}Hg ($r^2 = 0.77$) and Δ^{199}Hg values ($r^2 = 0.90$) (Figure 2a,b) indicate that the aquatic organisms represent varying mixtures of MMHg and IHg caused by preferential trophic transfer of MMHg. The estimated MMHg (100% MMHg) had δ^{202}Hg and Δ^{199}Hg values of -0.05 ‰ (± <0.01 ‰) and 2.05 ‰ (± <0.01 ‰), respectively. The estimated IHg (100% IHg) had δ^{202}Hg and Δ^{199}Hg values of -1.17 ‰ (± <0.01 ‰) and -0.33 ‰ (± <0.01 ‰), respectively. Bulk sediment had higher δ^{202}Hg and Δ^{199}Hg than values estimated for IHg in the food web (Figure 2).

5.3.2. Sources and biogeochemical processing of MMHg in the aquatic food web

Because our data show that the MMHg isotopic composition is preserved without fractionation during trophic transfer, we can use these values to provide insight into the sources and biogeochemical processing of MMHg prior to bioaccumulation. The positive Δ^{199}Hg value of the estimated MMHg indicates that MMHg has been subjected to photochemical degradation prior to entry into the food web and bioaccumulation. The slope of Δ^{199}Hg/ Δ^{201}Hg has been used to distinguish between photochemical degradation and reduction of MMHg and IHg in

aquatic ecosystems (*25, 28, 29, 38-41*). We used a York regression (*42*) to estimate the slope of $\Delta^{199}Hg/\ \Delta^{201}Hg$ for the aquatic organisms, and found a slope of 1.32±0.03 (r^2= 1.00, p <0.05) (Fig 3). This slope is consistent with the photochemical degradation of MMHg observed in freshwater lakes (*21, 28, 29, 38, 41*) and streams (*25*), and is greater than the slope observed in marine food webs (~1.2) (*27, 30, 40, 43-45)*.

We can also use Hg isotope values to infer the extent of biological and dark abiotic reactions to which MMHg was subjected prior to photochemical degradation. The $\delta^{202}Hg$ value prior to photochemical degradation was estimated using the approach first proposed by Gehrke et al. (*43*) by applying the experimentally derived slopes representing the expected changes in MMHg isotopic composition caused by photochemical degradation at varying DOC concentrations (*21*). This approach has been used to estimate $\delta^{202}Hg$ values for MMHg prior to photochemical degradation in many aquatic ecosystems (*25, 39-41, 43*). Using the DOC level in Douglas Lake during the aquatic sampling period (9.6-11.1 mg/L; Table 1), we employ the $\Delta^{199}Hg/\ \delta^{202}Hg$ slope of 4.79±0.33, which represents the change in MMHg isotopic composition at 10mg/L DOC. We note, however, that the Hg/DOC ratio of the experiments of Bergquist and Blum (*21*) were much higher than in natural systems. With this caveat, we estimate that MMHg had a $\delta^{202}Hg$ value of ~ -0.52 ‰ prior to ~20% photochemical degradation in the aquatic ecosystem (Fig 4). This value is higher than that of IHg estimated based on the linear regression of % MMHg versus Hg isotope values as well as the values for the sediment composed mainly of IHg. Based on this result, the simplest explanation for the $\delta^{202}Hg$ difference between the sediment (IHg) and the estimated MMHg is the combined effect of microbial methylation of IHg (*18*) and subsequent dark abiotic or microbial demethylation of MMHg in the sediment (*19*), causing the remaining MMHg to have a higher $\delta^{202}Hg$ value compared to the reactant IHg. Alternatively, the introduction of a small proportion of an external IHg source (i.e. terrestrial soil, precipitation), which has a different $\delta^{202}Hg$ value than the bulk sediment, could be preferentially methylated and subsequently demethylated to produce values estimated for MMHg.

Sediment near the sediment-water interface has been suggested as the dominant site for MMHg production in many freshwater lake systems (*46, 47*). It has been observed that $\delta^{202}Hg$ values estimated for MMHg from biota are typically higher than many lake and coastal sediments where microbial methylation and demethylation processes are active (*30, 39, 41, 43*).

Although our result is consistent with the previous findings that suggest sediment as the primary site for MMHg production, our study shows that only a fraction of the IHg in sediment may be available for production of MMHg. In this study, we estimated the isotopic composition of IHg in the food web by measuring organisms with a wide range of % MMHg values. The isotopic composition estimated for IHg, representing the bioaccumulated IHg, displayed a slightly lower δ^{202}Hg value and a significantly lower Δ^{199}Hg value compared to the values for the sediment. Based on this evidence, we speculate that there are two IHg pools in the sediment (e.g., *48*)—one that is preferentially methylated and bioaccumulated and the other representing the remainder of IHg in the bulk sediment.

To explain the estimated IHg isotope values, we suggest that IHg may be derived in part from runoff of terrestrial soil, which is consistent with the low δ^{202}Hg and Δ^{199}Hg values of the terrestrial soil measured in this study as well as forest floor from northeastern Wisconsin forests (*49, 50*) (Fig 5). Forest watersheds have been shown to supply significant amounts of IHg to freshwater lakes via watershed runoff (*51, 52*). Recent experimental studies have also shown that dissociation of IHg bound to soil organic matter can impart slightly higher δ^{202}Hg on the desorbed (soluble) fraction of IHg (*53*), and can provide IHg that is available for uptake by microbial cells (*54*). It is possible that bioaccumulated IHg is deposited to surface sediment via watershed runoff and is preferentially methylated, and subsequently demethylated to produce a higher δ^{202}Hg value in the estimated MMHg prior to photochemical degradation and bioaccumulation. A fraction of IHg that has been incorporated into microbial cells but has not yet undergone microbial methylation could then be passed to various organisms from the base of the food web. For the bulk sediment, a mixture of IHg derived from terrestrial soil and IHg deposited through precipitation, which has higher δ^{202}Hg and Δ^{199}Hg values than the local sediment, appears to be responsible for the positive Δ^{199}Hg values and the slightly higher δ^{202}Hg value compared to the estimated IHg (Fig 5). In fact, our bulk sediment values are within the ranges of δ^{202}Hg but higher in Δ^{199}Hg compared to many freshwater lake and stream sediments measured previously (*41, 55, 56*). Photochemical reduction of IHg from precipitation has been used to explain the positive Δ^{199}Hg values in shallow and relatively undisturbed sediments (*39, 56*), and we suggest that precipitation is likely responsible for the positive Δ^{199}Hg values documented in the Douglas Lake littoral bulk sediment.

The isotopic composition of IHg in the bulk sediment suggests that precipitation may be an important IHg source to the Douglas Lake food web in addition to IHg derived from the terrestrial soil (Fig 5). It has been suggested that inorganic Hg recently deposited through precipitation can be preferentially methylated and supply the dominant MMHg source to some North American freshwater lake food webs compared to a previously deposited IHg (*57-59*). Interestingly, we found consistent ranges of δ^{202}Hg values between the estimated MMHg in sediment prior to photochemical degradation and precipitation characterized as background or collected from North American regions that are unimpacted by point source Hg (Fig 4) (*49*, *60*). While this is speculative, it is possible that precipitation deposited to surface sediment via sorption to particles and that has undergone both microbial methylation and demethylation, could also provide a viable explanation for the observed δ^{202}Hg values that we estimate for MMHg prior to photochemical degradation.

In summary, our results are consistent with in situ MMHg production of IHg from an external source. This IHg may have originated from either watershed runoff of terrestrial soil or IHg deposited through precipitation. MMHg produced in the surface sediment was then subjected to a small amount of photochemical degradation before entering the food web. The MMHg production and bioaccumulation from the sediment is also consistent with the feeding behaviors and the habitat of the aquatic organisms collected in this study (Table 2). We can explain the small Hg isotopic variability in the linear regression of % MMHg versus Hg isotope values by the variation in feeding behaviors, which can expose certain aquatic organisms to additional MMHg sources. For instance, the mussel sample displayed a slightly higher than expected Δ^{199}Hg value considering its low trophic position (32% MMHg, δ^{15}N= 4.36 ‰) and its low δ^{202}Hg value, which is consistent with a mixture of IHg and MMHg (Fig 2a,b). It is possible that the mussel was exposed to MMHg subjected to additional photochemical degradation in the water column via particle re-suspension from the sediment. The mussel in this study displayed the most depleted δ^{13}C value, confirming its reliance on water column resources (i.e. phytoplankton, seston) via an active filter feeding mechanism. In contrast, the snail displayed a relatively high δ^{202}Hg value compared to the low Δ^{199}Hg value, which is consistent with a mixture of IHg and MMHg (Fig 2a,b). We suggest that the snail is exposed to MMHg that was subjected to additional microbial methylation and demethylation. Periphyton and algal mats have been shown to provide adequate microhabitats for microbial activity in freshwater lakes (*61, 62*).

The highest $\delta^{13}C$ value observed in the snail is consistent with its extensive grazing behavior on periphyton and microbe-rich substrates.

5.3.3. MMHg biomagnification in the riparian and forest food webs

The THg concentrations in the terrestrial basal resources were 7.97±0.23, 26.7±0.57 and 38.4±0.79 ng/g in the riparian soil, forest soil, and leaf litter, respectively (Table 2). The THg concentrations of the forest organisms ranged between 18.3 (moth) and 487 ng/g (millipede) (Table 2). The % MMHg increases in the order: worm (2 %), millipede (9 %), moth (19 %), dragonfly (44 %), beetle larvae (63 %), spider (97 %), and beetle (99%) (Table 2). The % MMHg values of the forest organisms displayed a significant positive relationship with the $\delta^{15}N$ values (r^2= 0.57, $p<0.05$), indicating that biomagnification of MMHg is taking place in the forest food web. The $\delta^{13}C$ values displayed a wide range, between -31.5 and -23.3 ‰, and overlapped with the ranges for the aquatic ecosystem (Table 2). This suggests that the aquatic and forest food webs may be relying on similar energy resources.

The terrestrial basal resources and organisms displayed a wide range in $\delta^{202}Hg$ (-2.25 to -0.35 ‰), and $\Delta^{199}Hg$ values (-0.22 to 1.80 ‰) (Table 2). These values also overlapped with the ranges of Hg isotope values observed in the aquatic ecosystem. Based on the biomagnification trend of MMHg, we plotted $\delta^{202}Hg$ and $\Delta^{199}Hg$ values against % MMHg of the forest organisms. Basal resources were excluded from the linear regression to differentiate between the IHg associated with the basal resources and the IHg that has bioaccumulated in the food web. We observed significant correlations with $\delta^{202}Hg$ (r^2= 0.59, $p<0.05$) and $\Delta^{199}Hg$ (r^2= 0.68, $p<0.05$) (Fig 6a,b). We estimate that MMHg (100% MMHg) has a $\delta^{202}Hg$ value of -0.34 (± <0.01 ‰) and a $\Delta^{199}Hg$ value of 1.36 ‰ (± <0.01 ‰). The estimated isotopic composition of IHg is $\delta^{202}Hg$= -1.34 (± <0.01 ‰) and $\Delta^{199}Hg$= -0.04 ‰ (± <0.01 ‰), which is consistent with values for the soil measured in this study as well as soil collected in other temperate forest (*25*, *49*).

Overall, the $\delta^{13}C$ and Hg isotope values displayed overlapping ranges between the aquatic and adjacent forest ecosystems. The isotopic compositions estimated for MMHg and IHg were similar between the two ecosystems (Fig 7). These results indicate that the forest organisms either share similar MMHg sources with the aquatic organisms (via emergent insect mediated MMHg flux) or receive similar IHg sources from terrestrial resources. Within the forest ecosystem, we observed a large isotopic variability within the same species of organisms (beetle

larvae, beetle, spider) measured at different distances (0-5, 5-10, 10-30, 30-60 meters) from the lakeshore (Fig 8a,b). The large Hg isotopic variability among the forest organisms indicates that MMHg is potentially subjected to varying extents of biogeochemical processes such as methylation, demethylation and photochemical degradation prior to bioaccumulation at different forest ecosystem positions. Below we assess the relative importance of MMHg sources and possible biogeochemical processes in the forest ecosystem, and provide an explanation for the large Hg isotopic variability among the forest organisms.

5.3.4. Hg transfer between aquatic and forest ecosystems

Our results contrast somewhat with Tsui et al. (*25*), who previously observed distinct δ^{202}Hg values for MMHg and a large offset in the estimated IHg and MMHg isotopic compositions between stream and upland forest food webs in northern California, USA. That study also observed intermediate δ^{202}Hg values in the riparian organisms and attributed them to the bioaccumulation of both forest- and stream-driven MMHg sources via emergent insect mediated MMHg flux to adjacent forest ecosystems. We assess the potential importance of emergent insect mediated MMHg flux to the adjacent forest food web at Douglas Lake by comparing δ^{202}Hg values for insects that have close to 100% MMHg (carnivores) and were measured at varying distances from the lake (beetle larvae, beetles, spiders) (Fig 8a). We did not observe significant or consistent changes in δ^{202}Hg with distance. The average THg and MMHg concentrations in the forest organisms were at least 2 times higher than the average THg and MMHg concentrations of the aquatic organisms. This indicates that even with a significant emergent insect mediated MMHg transfer from the aquatic ecosystem to the forest; the aquatic MMHg is unlikely to be the dominant MMHg source to the terrestrial macroinvertebrate communities, which is consistent with another recent study (*63*).

Emergent insect mediated MMHg flux to the forest ecosystem is perhaps only important to those animals that mainly consume emergent insects (Fig 4). In the bat hair (composed mainly of MMHg) (*8*), we documented a similar Δ^{199}Hg value but a much higher δ^{202}Hg compared to dragonfly larvae (Aeshinidae). The bat excrement, composed mainly of IHg, displayed similar Hg isotope values with the bulk lake sediment. Based on this, we propose that the anomalously high δ^{202}Hg value in the bat hair is caused by an internal metabolic fractionation of δ^{202}Hg upon bioaccumulation of MMHg from the aquatic ecosystem. Previous studies have documented 1-

2 ‰ higher δ^{202}Hg values, but identical Δ^{199}Hg values, in birds, and in mammals including seals, whales, and human hair compared to their respective diets, and attributed this to fractionation associated with internal demethylation of MMHg (*27, 29, 39, 44, 64, 65*). For bat excrement, the low Δ^{199}Hg value indicates that the bat excrement most likely reflects varying mixtures of bioaccumulated IHg and MMHg from the aquatic ecosystem rather than resulting from internal demethylation.

For the majority of forest organisms, the isotopic composition estimated for IHg strongly indicates that the aquatic and forest ecosystems share a similar IHg source (Fig 7). We observed a consistent increasing trend in δ^{202}Hg and Δ^{199}Hg values from terrestrial soil to riparian soil and finally to the bulk sediment (Fig 5), and found significant negative relationships between THg concentration and Hg isotope values for the terrestrial soil, riparian soil, and the bulk sediment (δ^{202}Hg; $p<0.05$, $r^2= 0.87$, Δ^{199}Hg; $p<0.05$, $r^2= 0.71$). Based on this evidence, it appears that IHg input via watershed runoff of terrestrial soil is responsible for the ranges of δ^{202}Hg and Δ^{199}Hg values among the riparian soil and sediment. The overlapping ranges of δ^{13}C values between the aquatic and forest ecosystems further supports the hypothesis that the organisms from two different ecosystems may be relying on similar energy resources in addition to IHg (Table 2). Overall, our study suggests that emergent insects play a less important role as an energy subsidy to the adjacent forest food webs compared to the northern California forests where rocky substrates dominate and energy resources for riparian and upland forest macroinvertebrates are insufficient during dry summer periods (*25*). Instead, the terrestrial ecosystem appears to supply important energy resources along with IHg to the riparian and subsequently to the aquatic ecosystem at our study site.

5.3.5. Sources and biogeochemical processing of MMHg in the riparian and forest food webs

The processes governing in situ MMHg production and photochemical degradation may be similar between the littoral and forest ecosystems based on the direction and the magnitude of the estimated isotopic composition of MMHg in our study site (Fig 7). The large Hg isotopic variability among the forest organisms indicates that MMHg derived from the forest ecosystem may be subjected to varying extents of photochemical degradation prior to bioaccumulation. In this study, we collected diverse assemblages of forest organisms at varying distances from the

lakeshore; each differing slightly in environmental characteristics. Among the insects that have ~100% MMHg and were measured at each location, we observed an overall decreasing trend in Δ^{199}Hg values with increasing distance from the lakeshore (Fig 8b). The lower Δ^{199}Hg values with increasing distance correspond with % canopy openness, which decreased systematically in the progression: 55, 24, 20, and 11%. We used the slope of Δ^{199}Hg/ Δ^{201}Hg to distinguish between photochemical degradation and reduction of MMHg and IHg, and found a slope of 1.21±0.03 (r^2= 0.98, p <0.05) (Fig 3). This slope suggests that MMHg is indeed photochemically degraded prior to bioaccumulation and that the extent of photochemical degradation may vary depending on the location within the forest.

Using the same method as in the aquatic ecosystem, we used the slope of Δ^{199}Hg/δ^{202}Hg= 4.79±0.33 to estimate the δ^{202}Hg value of MMHg prior to photochemical degradation in the forest ecosystem. These are only rough estimates, however, because photochemical degradation experiments were conducted in aqueous solutions and thus different conditions from those in the natural forest setting (*21*). We estimate that MMHg had a δ^{202}Hg value of ~ -0.62 ‰ prior to ~15% photochemical degradation in the forest ecosystem (Fig 9). This value is higher than the δ^{202}Hg value of IHg estimated based on the linear regression of % MMHg versus Hg isotope values as well as the values for the soil composed mainly of IHg.

We first discuss the potential importance of precipitation as a source of IHg to the forest ecosystem. We found consistent ranges of δ^{202}Hg values between the estimated MMHg prior to photochemical degradation and precipitation samples characterized as background in North American regions (*49, 60*). Nonetheless, we suggest that precipitation is unlikely to be an important IHg source to the forest ecosystem. We observed significantly lower Hg isotope values, particularly in Δ^{199}Hg, in the terrestrial basal resources including soil and leaf litter compared to precipitation, indicating that precipitation provides a relatively small IHg input to the forest ecosystem (Fig 5). Instead, we infer that IHg is microbially methylated and perhaps demethylated in the soil prior to photochemical degradation and bioaccumulation to the forest food web. The isotopic composition estimated for IHg based on the linear regression of % MMHg versus Hg isotope values was nearly identical to the Hg isotopic composition of the soil, indicating that soil is likely the dominant site for MMHg production and serves as the base of the food web (Fig 6a,b). Previous studies have also shown that deciduous foliage, which uptakes gaseous Hg from the atmosphere, is the dominant IHg input to terrestrial ecosystems rather than

precipitation (*49, 66, 67*). The highly negative δ^{202}Hg values in the leaf litter are thought to be the product of MDF during the uptake and subsequent oxidation of gaseous Hg within the foliage (*49*). As it decays, IHg associated with the foliage is sequestered into soil (*66*). We suggest that the combined effect of microbial methylation and subsequent demethylation of this sequestered IHg can produce a higher δ^{202}Hg value in the estimated MMHg prior to photochemical degradation.

5.4. Conclusion

The Hg isotope ratios measured in the basal resources as well as the aquatic and forest food webs suggest that both ecosystems may be subjected to similar biogeochemical processing of MMHg, which includes in situ MMHg production and photochemical degradation prior to bioaccumulation into the food webs. In addition to MMHg, the measurement of Hg isotope ratios in organisms with low % MMHg have allowed us to differentiate between the IHg associated with the basal resources and the IHg that has bioaccumulated into the food web. Many previous studies that characterized Hg isotope ratios in ecosystem food webs have simply assumed that the observed range in Hg isotopic composition was the result of MMHg incorporation that has undergone varying amounts of photochemical degradation prior to entry into the food web (*29, 39-41*). This is valid for studies of fish and other organisms that have a high % MMHg in their tissues, but not for food web items with low % MMHg. Further study is required to investigate the relative importance of IHg sources (i.e. precipitation and terrestrial soil) and differentiate its bioavailability for supplying the dominant MMHg source to the aquatic and forest ecosystems. Our study suggests that the use of Hg isotopes adds important new insight when deciphering complex Hg transfer pathways and delineating the presence of multiple IHg pools in natural ecosystems.

Acknowledgement

The authors would like to thank M Johnson for expert MC-ICP-MS operation, L Wingate and KC Lohmann for the stable carbon and nitrogen isotope analysis, A Fotis for canopy cover measurements, R Ross for biota processing, S Pruett-Jones, P Meyers, D Lim for biota sampling. This work was funded by an M-Cubed grant from the University of Michigan (contribution to

sample collection, analysis), and collaborative grants 1354811 and 1353850 to M Tsui and J Blum from the NSF Ecosystem Science Program (contribution to sample analysis)

References

(1) Mergler, D.; Anderson, H. A.; Chan, L. H. M.; Mahaffey, K. R.; Murray, M.; Sakamoto, M. et al. Methylmercury exposure and health effects in humans: A worldwide concern. *Ambio.* **2007,** *36*, 3-11.

(2) Mason, R. P.; Sullivan, K. A. Mercury in Lake Michigan. *Environ Sci Technol*. **1997,** *31*, 942-947.

(3) Cristol, D. A.; Brasso, R. L.; Condon, A. M.; Fovargue, R. E.; Friedman, S. L.; Hallinger, K. K. et al. The movement of aquatic mercury through terrestrial food webs. *Science*, **2008,** *320*, 335.

(4) Paetzold, A.; Smith, M.; Warren, P. H.; Maltby, L. Environmental impact propagated by cross-system subsidy: Chronic stream pollution controls riparian spider population. *Ecology,* **2011,** *92*, 1711-1716.

(5) Tweedy, B. N.; Drenner, R. W.; Chumchal, M. M.; Kennedy, J. H. Effects of fish on emergent insect-mediated flux of methylmercury acorss a gradient of contamination. *Environ Sci Technol*. **2013,** *47*, 1614-1619.

(6) Brasso, R. L.; Cristol, D. A. Effects of mercury exposure on the reproductive success of tree swallows (Tachycineta bicolor). *Ecotox.* **2008,** *17*, 133-141.

(7) Ever, D. C.; Savoy, L. J.; DeSorbo, C. R.; Yates, D. E.; Hanson, W.; Taylor, K. M. et al. Adverse effects from environmental mercury loads on breeding common loons. *Ecotox*, **2008,** *17*, 69-81.

(8) Evers, D. C.; Jackson, A. K.; Tear, T. H.; Osborne, C. E. Hidden risk: Mercury in terrestrial ecosystems of the Northeast. *Gorham: Maine.* **2012.**

(9) Wada, H.; Yates, D. E.; Evers, D. C.; Taylor, R. J.; Hopkins, W. A. Tissue mercury concentrations and adrenocortical responses of female big brown bats (*Eptesicus fuscus*) near a contaminated river. *Ecotox*, **2010,** *19*, 1277-1284.

(10) Selvendiran, P.; Driscoll, C. T.; Cushey, J. T.; Montesdeoca, M. R. Wetland influence on mercury fate and transport in a temperate forested watershed. *Environ Pollut*, **2008,** *154*, 46-55.

(11) St. Louis, V. L.; Rudd, J. W. M.; Kelly, C. A.; Beaty, K. G.; Bloom, N. S.; Flett, R. J. Importance of wetlands as sources of methyl mercury to boreal forest ecosystems. *Can J Fish Aquat Sci*. **1994,** *51*, 1065-1076.

(12) Hall, B. D.; Manolopoulos, H.; Hurely, J. P.; Schauer, J. J.; St. Louis, V. L.; Kenski, D. et al. Methyl and total mercury in precipitation in the Great Lakes region. *Atmos Environ.* **2005,** *39,* 7557-7569.

(13) Weiss-Penzias, P. S.; Ortiz, C. Jr; Acosta, R. P.; Heim, W.; Ryan, J. P.; Fernandez, D. et al. Total and monomethyl mercury in fog water from the central California coast. *Geophys Res Lett*. **2012,** *39,* 1-5.

(14) Jardine, T. D.; Kidd, K. A.; Rasmussen, J. B. Aquatic and terrestrial organic matter in the diet of stream consumers: implications for mercury bioaccumulation. *Ecol Appl*. **2012,** *22,* 843-855.

(15) Tsui, M. T. K.; Blum, J. D.; Finlay, J. C.; Balogh, S. J.; Nollet, Y. H.; Palen, W. J.; Power, M. E. Variation in terrestrial and aquatic sources of methylmercury in stream predators as revealed by stable mercury isotopes. *Environ Sci Technol.* **2014,** *48,* 10128-10135.

(16) Blum, J. D.; Bergquist, B. A. Reporting of variations in the natural isotopic composition of mercury. *Anal Bioanal Chem*. **2007,** *388,* 353-359.

(17) Perrot, V.; Bridou, R.; Pedrero, Z.; Guyoneaud, R.; Monperrus, M.; Amouroux, D. Identical Hg isotope mass dependent fractionation signature during methylation by sulfate-reducing bacteria in sulfate and sulfate-free environment. *Environ Sci Technol*. **2015,** DOI: 10.1021/es5033376

(18) Rodriguez-gonzalez, P.; Epov, V. N.; Bridou, R.; Tessier, E.; Guyoneud, R.; Monperrus, M. et al. Species-specific stable isotope fractionation of mercury during Hg(II) methylation by an anaerobic bacteria (Desulfobulbus propionicus) under dark conditions. *Envrion Sci Technol*. **2009,** *43,* 9183-9188.

(19) Kritee, K.; Barkay, T.; Blum, J. D. Mass dependent stable isotope fractionation of mercury during mer mediated microbial degradation of monomethylmercury. *Geochim et Cosmochim Acta*. **2009,** *73,* 1285-1296.

(20) Wiederhold, J. C.; Cramer, C. J.; Daniel, K.; Infante, I.; Bourdon, B.; Kretzschmar, R. Equilibrium mercury isotope fractionation between dissolved Hg(II) species and thiol-bound Hg. *Environ Sci Technol*. **2010,** *44,* 4191-4197.

(21) Bergquist, B. A.; Blum, J. D. Mass-dependent and -independent fractionation of Hg isotopes by photoreduction in aquatic systems. *Science,* **2007,** *318,* 417-420.

(22) Zheng, W.; Hintelmann, H. Mercury isotope fractionation during photoreduction in natural water is controlled by its Hg/DOC ratio. *Geochim et Cosmochim Acta.* **2009,** *73,* 6704-6715.

(23) Kwon, S. Y.; Blum, J. D.; Carvan, M. J.; Basu, N.; Head, J. A.; Madenjian, C. P. et al. Absence of fractionation of mercury isotopes during trophic transfer of methylmercury to freshwater fish in captivity. *Environ Sci Technol.* **2012,** *46,* 7527-7534.

(24) Kwon, S. Y.; Blum, J. D.; Chirby, M. A.; Chesney, E. J. Application of mercury isotopes for tracing trophic transfer and internal distribution of mercury in marine fish feeding experiments. *Environ Toxicol Chem*. **2013,** *23,* 2322-2330.

(25) Tsui, M. T. K.; Blum, J. D.; Kwon, S. Y.; Finlay, J. C.; Balogh, S. J.; Nollet, Y. H. Sources and transfers of methylmercury in adjacent river and forest food webs. *Environ Sci Technol*. **2012,** *46,* 10957-10964.

(26) Blum, J. D.; Sherman, L. S.; Johnson, M. W. Mercury isotopes in earth and environmental sciences. *Annu Rev Earth Planet Sci*. **2014,** *42,* 249-269.

(27) Day, R. D.; Roseneau, D. G.; Berail, S.; Hobson, K. A.; Donard, O. F. X.; Vander Pol, S. S. et al. Mercury stable isotopes in seabird eggs reflect a gradient from terrestrial geogenic to oceanic mercury reservoirs. *Environ Sci Technol.* **2012,** *46,* 5327-5335.

(28) Gantner, N.; Hintelmann, H.; Zheng, W.; Muir, D. C. Variations in stable isotope fractionation of Hg in food webs of Arctic lakes. *Environ Sci Technol*. **2009,** *43,* 9148-9154.

(29) Perrot, V.; Pastukhov, M. V.; Epov, V. N.; Husted, S.; Donard, O. F. X.; Amouroux, D. Higher mass-independent isotope fractionation of methylmercury in the pelagic food web of Lake Baikal (Russia). *Environ Sci Technol*. **2012,** *46,* 5902-5911.

(30) Senn, D. B.; Chesney, E. J.; Blum, J. D.; Bank, M. S.; Maage, A.; Shine, J. P. Stable isotope (N, C, Hg) study of methylmercury sources and trophic transfer in the Northern Gulf of Mexico. *Environ Sci Technol*. **2010,** *44,* 1630-1637.

(31) Keeler, G. J.; Dvonch, J. T. Atmospheric Mercury: A Decade of Observations in the Great Lakes. In: Pirrone N, Mahaffey KR, editors. Dynamics of Mercury Pollution on Regional and Global Scales: Atmospheric Processes and Human Exposures around the World. *Norwell: Springer Publishers.* **2005,** 611-36.

(32) Tsui, M. T. K.; Blum, J. D.; Kwon, S. Y.; Finlay, J. C.; Balogh, S. J.; Nollet, Y. H. Photodegradation of methylmercury in stream ecosystems. *Limnol Oceanogr.* **2013,** *58,* 13-22.

(33) Blum, J.D. Applications to stable mercury isotope biogeochemistry. In: Baskaran M, editor. *Handbook of environmental isotope geochemistry. Berlin, Germany: Springer;* **2011,** 229-246.

(34) Hothem, R. L.; Bergen, D. R.; Bauer, M. L.; Crayon, J. J.; Meckstroth, A. M. Mercury and trace elements in crayfish from Northern California. *Bull Environ Contam Toxicol.* **2007,** *79,* 628-632.

(35) Pennuto, C. M.; Lane, O. P.; Evers, D. C.; Tayloer, R. J.; Loukmas, J. Mercury in the Northern Crayfish, Orconectes virillis (Hagen), in New England, USA. *Ecotox.* **2005,** *14,* 149-162.

(36) Watras, C. J.; Bloom, N. S. Mercury and methylmercury in individual zooplankton: Implications for bioaccumulation. *Limol Oceanogr.* **1992,** *37,* 1313-1318.

(37) France, R. L. Critical examination of stable isotope analysis as a means for tracing carbon pathways in stream ecosystems. *Can J Fish Aquat Sci.* **1995,** *52,* 651-656.

(38) Das, R.; Salters, V. J. M.; Odom, A. L. A case for in vivo mass-independent fractionation of mercury isotopes in fish. *Geochem Geophys Geosyst.* **2009,** *10,* Q11012.

(39) Kwon, S. Y.; Blum, J. D.; Chen, C. Y.; Meattey, D. E.; Mason, R. P. Mercury isotope study of sources and exposure pathways of methylmercury in estuarine food webs in the Northeastern U.S. *Environ Sci Technol.* **2014,** *48,* 10089-10097.

(40) Blum, J. D.; Popp, B. N.; Drazen, J. C.; Choy, C. A.; Johnson, M. W. Methylmercury production below the mixed layer in the North Pacific Ocean. *Nat Geosci.* **2013,** *6,* 879-884.

(41) Sherman, L. S.; Blum, J. D. Mercury stable isotopes in sediment and largemouth bass from Florida lakes, USA. *Sci Tot Environ.* **2013,** *448,* 163-175.

(42) York, D. Least-squares fitting of a straight line. *Can J Phys.* **1966,** *44,* 1076–86.

(43) Gehrke, G. E.; Blum, J. D.; Slotton, D. G.; Greenfield, B. K. Mercury isotope link mercury in San Francisco Bay forage fish to surface sediment. *Environ Sci Technol.* **2011,** *45,* 1264-1270.

(44) Laffont, L.; Sonke, J. E.; Maurice, L.; Monrroy, S. L.; Chincheros, J.; Amouroux, D. et al. Hg speciation and stable isotope signature in human hair as a tracer for dietary and occupational exposure to mercury. *Environ Sci Technol*. **2011,** *45,* 9910-9916.

(45) Point, D.; Sonke, J. E.; Day, R. D.; Roseneau, D. G.; Hobson, K. A.; Vander Pol, S. S. et al. Methylmercury photodegradation influenced by sea-ice cover in Arctic marine ecosystems. *Nat Geosci*. **2011,** *4,* 188-194.

(46) Gilmour, C. C.; Henry, E. A. Mercury methylation in aquatic systems affected by acid deposition. *Environ Pollut.* **1991,** *71,* 131–69.

(47) Ullrich, S. M.; Tanton, T. W.; Abdrashitova, S. A. Mercury in the aquatic environment: a review of factors affecting methylation. *Crit Rev Environ Sci Technol.* **2001,** *31,* 241–93.

(48) Jonsson, S.; Skyllberg, U.; Nilsson, M. B.; Lundberg, E.; Andersson, A.; Björn, E. Differentiated availability of geochemical mercury pools controls methylmercury levels in estuarine sediment and biota. *Nat Commun*. **2014,** *5,* article 4624.

(49) Demers, J. D.; Blum, J. D.; Zak, D. R. Mercury isotopes in a forested ecosystem: Implications for air-surface exchange dynamics and the global mercury cycle. *Global Biogeochem Cy*. **2013,** *27,* 1-17.

(50) Zhang, H.; Yin, R.; Feng, X.; Sommar, J.; Anderson, C. W. N.; Sapkata, A. et al. Atmospheric mercury inputs in montane soils increase with elevation: evidence form mercury isotope signatures. *Scientific Reports*, **2013,** *3,* 1-8.

(51) Dennis, I. F.; Clair, T. A.; Driscoll, C. T.; Kamman, N.; Chalmercs, A.; Shanley, J. et al. Distribution patterns of mercury in lakes and rivers of northeastern North America. *Ecotoxicol.* **2005,** *14,* 113-123.

(52) Driscoll, C. T.; Han, Y. J.; Chen, C. Y.; Evers, D. C.; Lambert, K. F.; Holsen, T. M. et al. Mercury contamination in forest and freshwater ecosystems in the Northeastern United States. *BioSci*. **2007,** *57,* 17-28.

(53) Yin, R.; Feng, X.; Wang, J.; Bao, Z.; Yu, B.; Chen, J. Mercury isotope variations between bioavailable mercury fractions and total mercury in mercury contaminated soil in Wanshan Mercury Mine, SW China. *Chem Geol*. **2013,** *336,* 80-86.

(54) Mason, R. P.; Reinfelder, J. R.; Morel, F. M. M. Uptake, toxicity, and trophic transfer of mercury in a coastal diatom. *Environ Sci Technol*. **1996,** *30,* 1835-1845.

(55) Donovan, P. M.; Blum, J. D.; Yee, D.; Gehrke, G. E.; Singer, M. B. An isotopic record of mercury in San Francisco Bay sediment. *Chem Geo*. **2013,** *349-350,* 87-98.

(56) Gehrke, G. E.; Blum, J. D.; Marvin-DiPasquale, M. Sources of mercury to San Francisco Bay surface sediment as revealed by mercury stable isotopes. *Geochim et Cosmochim Acta*. **2009,** *75,* 691-705.

(57) Hammerschmidt, C. R.; Fitzgerald, W. F. Methylmercury in freshwater fish linked to atmospheric mercury deposition. *Environ Sci Technol*. **2006,** *40,* 7764–70.

(58) Harris, R. C.; Rudd, J. W. M.; Amyot, M.; Babiarz, C. L.; Beaty, K. G.; Blanchfield, P. J. et al. Whole-ecosystem study shows rapid fish-mercury response to changes in mercury deposition. *Proc Natl Acad Sci*. **2007,** *104,* 16586–91.

(59) Hintelmann, H. R.; Harris, A.; Heyes, J. P.; Hurley, C. A.; Kelly, D. P.; Krabbenhoft, S. et al. Reactivity and mobility of new and old mercury deposition in a boreal forest ecosystem during the first year of the METAALICUS study. *Environ Sci Technol*. **2002,** *36,* 5034– 5040.

(60) Gratz, L. E.; Keeler, G. J.; Blum, J. D.; Sherman, L. S. Isotopic composition and fractionation of mercury in Great Lakes precipitation and ambient air. *Environ Sci Technol*. **2010,** *44,* 7764-7770.

(61) Cleckner, L. B.; Gilmour, C. C.; Hurley, J. P.; Krabbenhoft, D. P. Mercury methylation in periphyton of the Florida Everglades. *Limnol Oceanogr*. **1999,** *44,* 1815–25.

(62) Desrosiers, M.; Planas, D.; Mucci, A. Mercury methylation in the epilithon of boreal shield aquatic ecosystems. *Environ Sci Technol*. **2006,** *40,* 1540–6.

(63) Bartrons, M.; Gratton, C.; Spiesman, B. J.; Vander Zanden, M. J. Taking the trophic bypass: aquatic-terrestrial linkage reduces methylmercury in a terrestrial food web. *Ecol Appl*. **2015,** *25,* 151–159.

(64) Li, M.; Sherman, L. S.; Blum, J. D.; Granjean, P.; Mikkelsen, B.; Sunderland, E. C. et al. Assesing sources of human methylmercury exposure using stable mercury isotopes. *Environ Sci Technol*. **2014,** *48,* 8800-8806.

(65) Sherman, L. S.; Blum, J. D.; Franzblau, A.; Basu, N. New insight into biomarker of human mercury exposure using naturally occurring mercury stable isotopes. *Environ Sci Technol*. **2013,** *47,* 3403-3409.

(66) Demers, J. D.; Driscoll, C. T.; Fahey, T. J.; Yavitt, J. B. Mercury cycling in litter and soil in different forest types in the Adirondack Region, New York, USA. *Ecol Appl*. **2007,** *17,* 1341-1351.

(67) Hall, B. D.; St. Louis, V. L. Methylmercury and total mercury in plant litter decomposing in upland forests and flooded landscape. *Environ Sci Technol.* **2004,** *38,* 5010-5021.

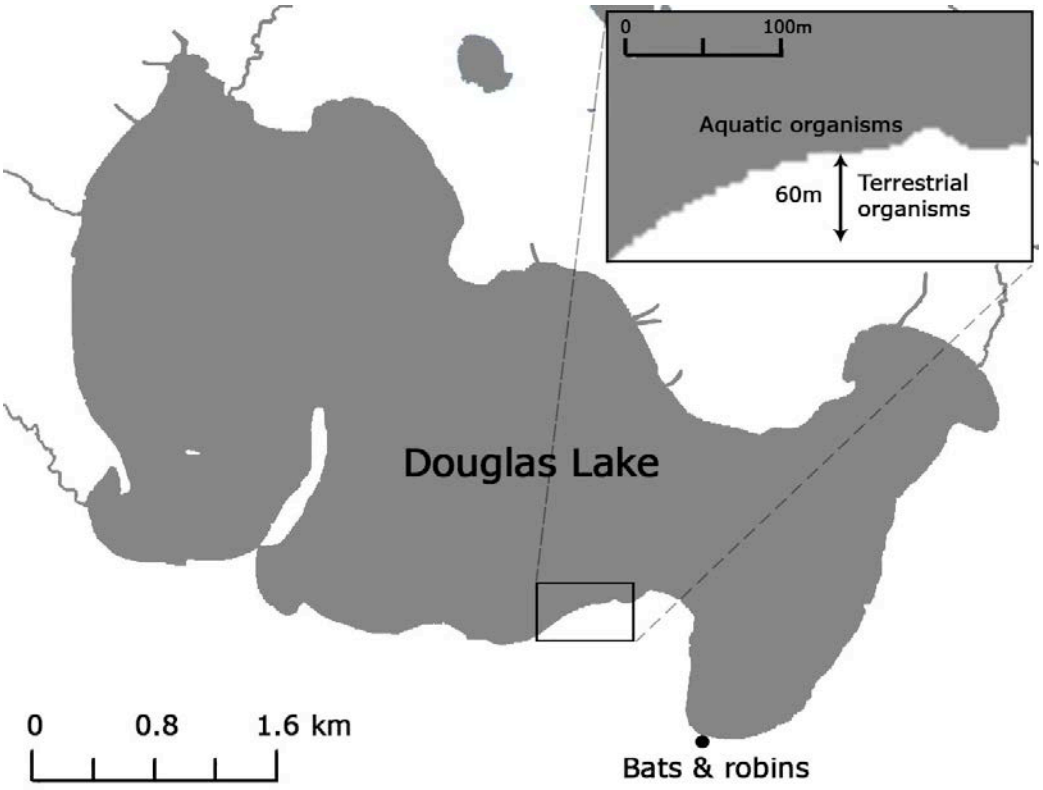

Figure 5.1 Sampling locations at the University of Michigan Biological Station, Michigan, USA. Map modified from www.agcensus.usda.gov.

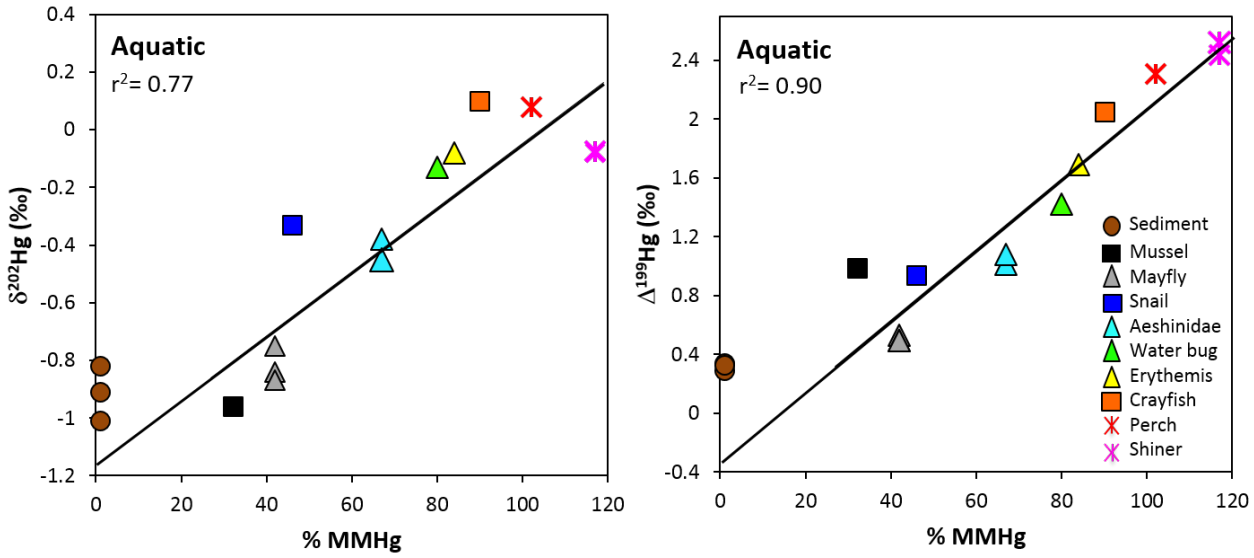

Figure 5.2 Plot of % MMHg versus δ^{202}Hg (a) and Δ^{199}Hg values (b) of aquatic organisms. The solid lines represent the linear regression based on % MMHg versus Hg isotope values of aquatic organisms. Sediment values are not included in the linear regression (see text for explanation).

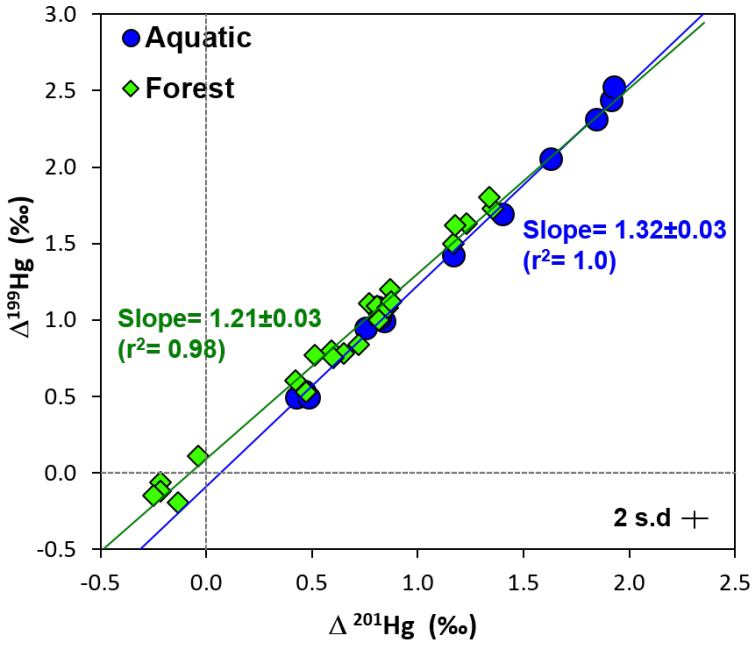

Figure 5.3 Plot of Δ^{201}Hg and Δ^{199}Hg values of aquatic and forest organisms. The lines represent the slope of Δ^{199}Hg/Δ^{201}Hg, which has been used to distinguish the photochemical reduction and degradation of IHg (~1.0) and MMHg (~1.3). Analytical uncertainty is indicated by the error bar (2 s.d).

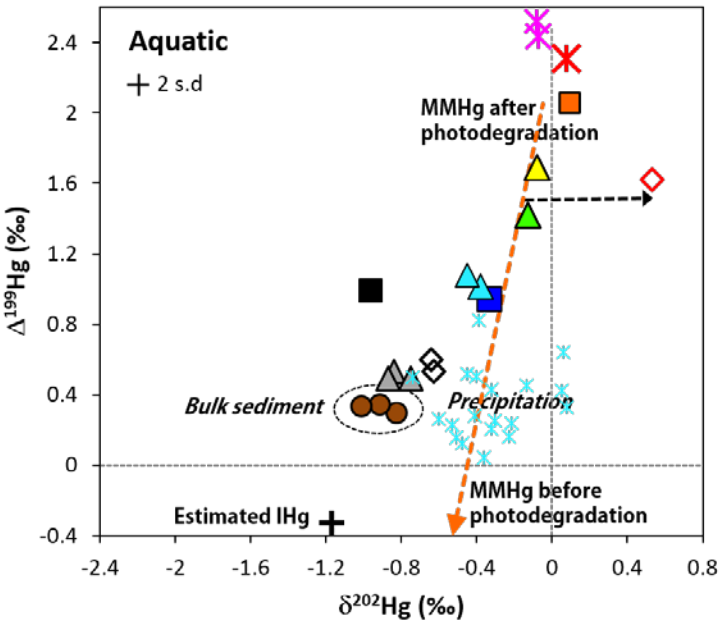

Figure 5.4 Plot of δ^{202}Hg and Δ^{199}Hg values of precipitation, sediment and aquatic organisms. The δ^{202}Hg and Δ^{199}Hg values estimated for IHg and MMHg both before and after photochemical degradation are also shown. The orange arrow represents the experimentally derived photochemical degradation slope for MMHg. The black arrow represents the internal demethylation of MMHg sampled in bat hair. Symbols are the same as Figure 2 except for open diamonds, which represent bat excrement (black) and bat hair (red). Analytical uncertainty is indicated by the error bar (2 s.d).

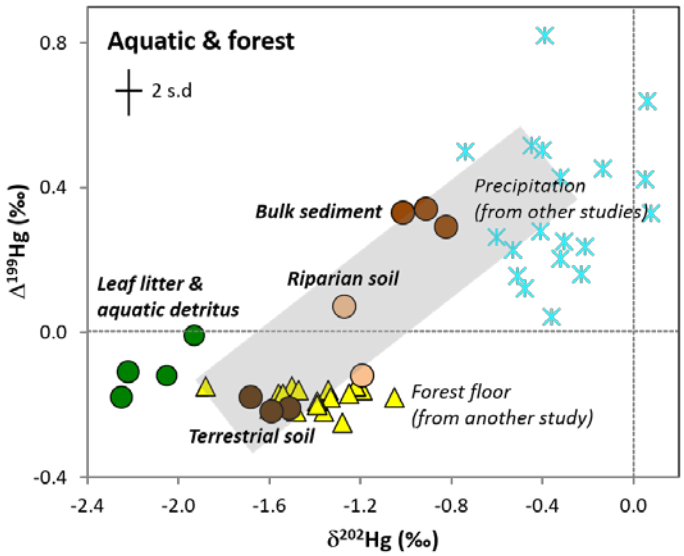

Figure 5.5 Plot of δ^{202}Hg and Δ^{199}Hg values of basal resources from adjacent forest and aquatic ecosystems, and precipitation. Precipitation values are from Demers et al., (2013), and Gratz et al., (2010) and represent precipitation that is not impacted by point source Hg. Forest floor values are from Demers et al., (2013), collected from northeastern Wisconsin forests. Analytical uncertainty is indicated by the error bar (2 s.d).

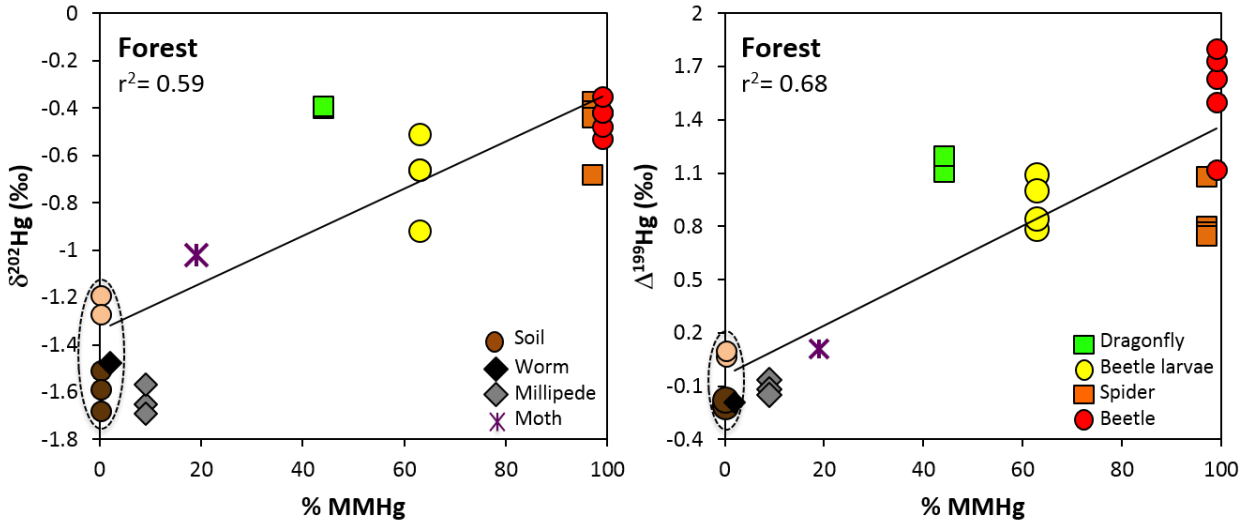

Figure 5.6 Plot of % MMHg versus δ^{202}Hg (a) and Δ^{199}Hg values (b) of forest organisms. The solid lines represent the linear regression based on % MMHg versus Hg isotope values of forest organisms. Values for soil are not included in the linear regression (see text for explanation).

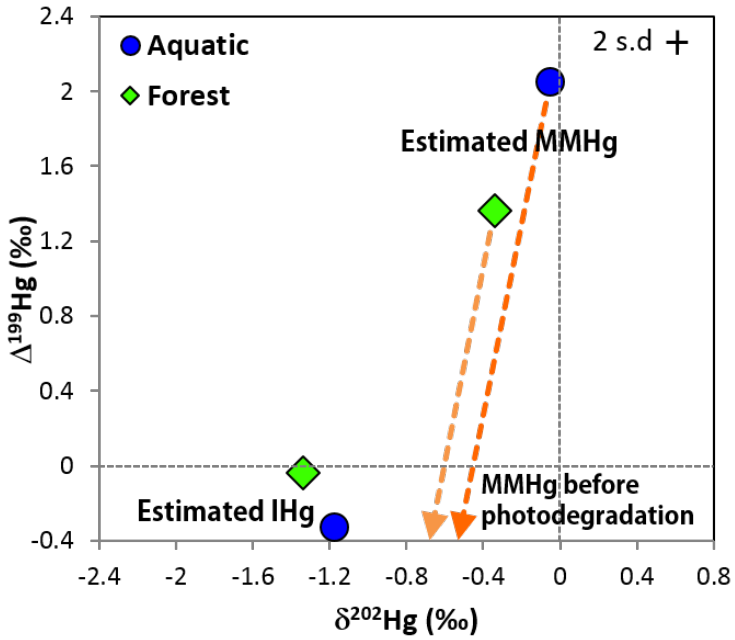

Figure 5.7 Plot of ^{202}Hg and Δ^{199}Hg values estimated for IHg and MMHg from aquatic and forest ecosystems. The orange arrows represent the experimentally derived photochemical degradation slope for MMHg. Analytical uncertainty is indicated by the error bar (2 s.d).

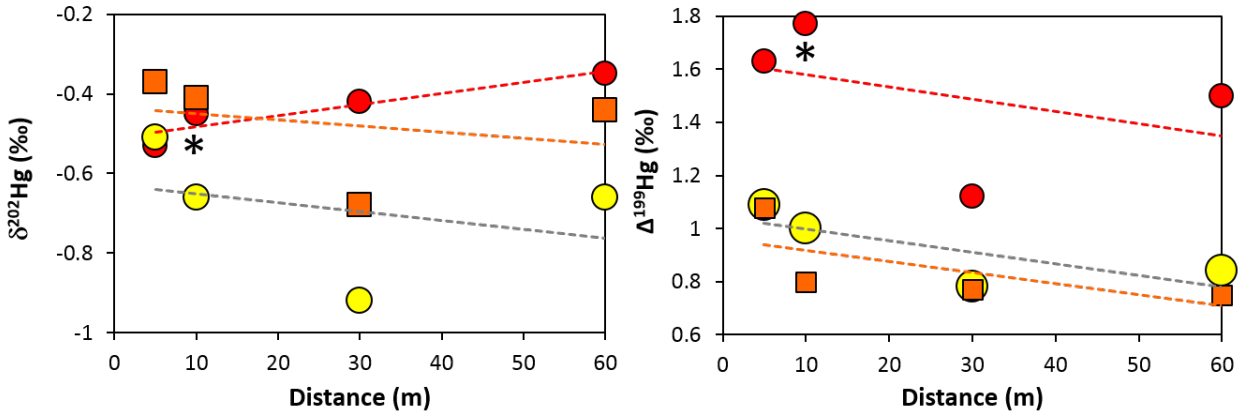

Figure 5.8 Plot of forest gradient (meters) versus δ^{202}Hg (a) and Δ^{199}Hg values of beetles, beetle larvae, and spiders. The lines depict the trend of δ^{202}Hg and Δ^{199}Hg values of beetles (red), beetle larvae (grey), and spiders (orange) with respect to distance from the Douglas Lake shoreline. Asterisks represent the mean values. Symbols are the same as Figure 6.

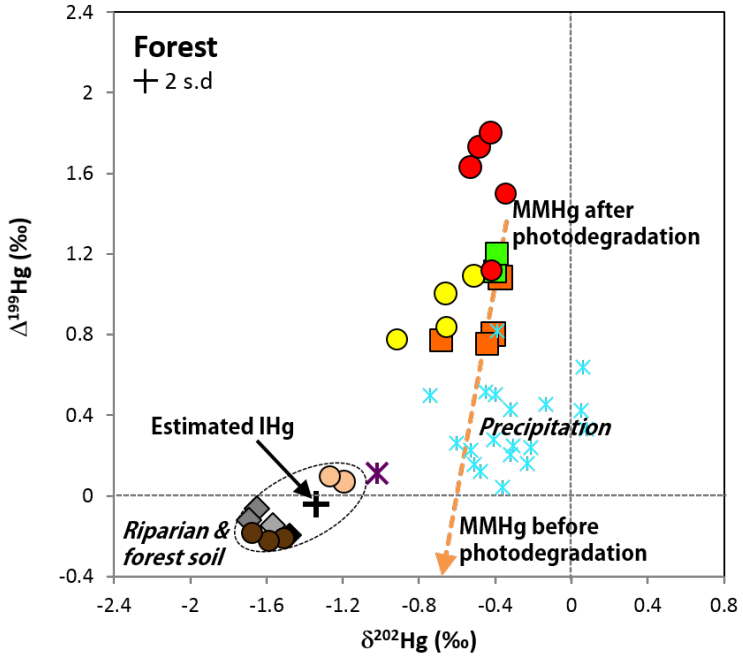

Figure 5.9 Plot of δ^{202}Hg and Δ^{199}Hg values of precipitation, soil, and forest organisms. The δ^{202}Hg and Δ^{199}Hg values estimated for IHg and MMHg both before and after photochemical degradation are also shown. The orange arrow represents the experimentally derived photochemical degradation slope for MMHg. Symbols are the same as Figure 6. Analytical uncertainty is indicated by the error bar (2 s.d)

Table 5.1 Water quality parameters for Douglas Lake. The data shown were obtained from the Douglas Lake Buoy during the aquatic sampling period of May-June, 2013.

Average daytime solar radiation (W/m^2)	Surface water temperature (°C)	Turbidity (mg/L)	DOC (mg/L)
435±239	16.7 to 18.9	9.6 to 10.6	9.80 to 11.1

Table 5.2 THg concentrations (ng/g), % MMHg, stable carbon and nitrogen values and Hg isotope ratios of all basal resources and biota. Asterisks represent values derived from other literatures.

Common name (scientific name/family if known)	THg (ng/g)	% MMHg	$\delta^{15}N$ (‰)	$\delta^{13}C$ (‰)	$\delta^{202}Hg$ (‰)	$\Delta^{199}Hg$ (‰)	$\Delta^{201}Hg$ (‰)	$\Delta^{200}Hg$ (‰)
Aquatic								
Sediment	4.22	1			-0.82	0.29	0.48	-0.09
	4.30	1			-0.91	0.34	0.51	0.06
	4.25	1			-1.01	0.33	0.07	-0.07
Aquatic detritus (decaying deciduous foliage)	26.5	3			-2.05	-0.12	-0.03	-0.06
	26.1	3			-1.93	-0.01	-0.09	0.02
Mayfly (Hexagenia limbata)	42.1	42	3.60	-25.8	-0.84	0.53	0.47	0.13
	45.8	42			-0.75	0.49	0.43	0.09
	46.2	42			-0.87	0.49	0.49	0.15
Zebra mussel (Dreissena polymorpha)	57.7	32	4.36	-30.7	-0.96	0.99	0.84	0.11
Aquatic snail (mixed, NA)	58.1	46	3.82	-22.8	-0.33	0.94	0.76	0.12
Dragonfly larvae (Aeshnidae)	31.7	67	5.77	-23.2	-0.38	1.01	0.82	0.16
	31.9	67			-0.45	1.08	0.81	0.16
Giant waterbug (Belostomatidae)	37.5	80	6.10	-24.1	-0.13	1.42	1.17	0.09
Dragonfly larvae (Erythemis simplicicollis)	39.4	84	7.01	-26.6	-0.08	1.69	1.40	0.08
Crayfish (NA)	40.5	90*			0.12	2.05	1.63	0.09
Yellow perch (Perca flavescens)	95.5	102	8.00	-23.4	0.08	2.31	1.85	0.00
Sand shiner (Notropis stramineus)	186	117	7.92	-27.7	-0.07	2.43	1.92	0.10
	186	117			-0.08	2.52	1.93	0.16
Riparian								
Soil	7.80	4			-1.19	0.07	0.05	0.09
	8.13	4			-1.27	0.10	-0.06	0.08
Earth worm (NA)	169	2	1.43	-25.9	-1.48	-0.19	-0.13	0.00
Millipede (Spirobolida)	480	9	-0.46	-24.0	-1.65	-0.06	-0.21	0.08
	487	9			-1.69	-0.12	-0.22	0.06
Dragonfly (Aeshinidae)	81.9	44	6.32	-23.3	-0.40	1.11	0.77	0.09
	80.5	44			-0.39	1.20	0.87	0.24
Beetle larvae (Necrophila americana)	84.1	63	7.42	-27.1	-0.51	1.09	0.81	0.10
	127	63			-0.66	1.00	0.82	0.00
Spider (mixed Lycosidae, Thomisidae, Tetragnathidae)	170	97	8.38	-25.6	-0.37	1.08	0.86	0.11

	174	97			-0.41	0.80	0.59	0.19
Beetle (mixed Carabidae, Silphidae)	221	99	5.97	-25.7	-0.53	1.63	1.23	0.12
	180	99			-0.48	1.73	1.36	0.11
	184	99			-0.42	1.80	1.34	0.18
Forest								
Soil	26.1	0.3			-1.51	-0.21	-0.25	0.06
	27.3	0.3			-1.59	-0.22	-0.28	0.06
	26.6	0.3			-1.68	-0.18	-0.22	0.03
Leaf litter	39.0	0.3			-2.22	-0.11	-0.08	0.04
	37.9	0.3			-2.25	-0.18	-0.14	0.06
Millipede (Spirobolida)	412	9	-0.32	-27.8	-1.57	-0.15	-0.25	0.04
Bat excrement (Myotis lucifugus)	117	18	6.03	-29.0	-0.63	0.60	0.42	0.11
	117	18			-0.64	0.53	0.47	0.14
Moth (mixed, NA)	18.3	19	4.07	-28.7	-1.02	0.11	-0.04	-0.02
Beetle larvae (Necrophila americana)	107	63	6.29	-29.5	-0.92	0.78	0.65	0.07
	96.8	63			-0.66	0.84	0.72	0.10
Spider (mixed Pholcidae, Lycosidae, Tetragnathidae)	183	97	7.47	-25.4	-0.68	0.77	0.51	0.15
	173	97			-0.44	0.75	0.60	0.06
Beetle (mixed Carabidae, Silphidae)	135	99	6.99	-31.5	-0.42	1.12	0.88	0.12
	214	99			-0.35	1.50	1.17	0.15
Bat hair (Myotis lucifugus)	988	100*			0.53	1.62	1.18	0.06

CHAPTER 6

Conclusion

Mercury has been mined and purified for centuries and used in many commercial products because of its unique and valuable properties (*1*). Hg is continuously released to the environment from various natural and anthropogenic sources, posing significant health risks to wildlife and humans. Since the 1960s, various aspects of Hg sources, biogeochemical processes, and fate have been investigated with the ultimate goal of helping to protect wildlife and humans from Hg exposure. Complex biogeochemical processes governing Hg speciation and transport, however, have made it difficult to clearly link Hg sources to receptors based on Hg concentration alone.

In this dissertation, we paid specific attention to the sources and biogeochemical processes of Hg in aquatic ecosystems, ranging from freshwater lakes, to estuaries, and to marine environments. The ability to precisely measure Hg isotope ratios in diverse environmental samples has enabled us to develop new approaches to tracing environmental sources of Hg (i.e., sediment, precipitation, soil, water), and to establish clear linkages between Hg sources and receptors. The research described in this dissertation demonstrates that the application of Hg isotopes can improve our ability to trace Hg sources in natural environments, and adds new knowledge to the field of aquatic Hg biogeochemistry.

6.1. Summary of key findings

6.1.1. Mercury isotope fractionation

The most critical finding in this dissertation is the absence of Hg isotope fractionation during bioaccumulation and trophic transfer in aquatic food webs. In Chapters 2 and 3, we found that isotope values of fish tissues completely re-equilibrated to the isotopic composition of the diet composed mainly of MMHg. We found that when fish were fed with diets composed of both

IHg and MMHg, the isotope values of fish tissues displayed isotopic compositions reflecting MMHg. Previous studies have observed increasing Hg isotope values with increasing trophic position, and attributed this to the internal metabolic fractionation of Hg (*2*). Our experimental studies have challenged this notion by showing that IHg and MMHg have different isotopic compositions, and the preferential trophic transfer of MMHg is responsible for the observed increasing Hg isotope values with trophic position. Currently, it is analytically challenging to measure Hg isotope ratios in low Hg concentration samples such as water and air. The fact that the isotopic composition representing an environmental source of MMHg (i.e., sediment, precipitation, soil, water) can be retained in fish tissues presents multiple advantages for tracing MMHg sources in natural environments. In fact, this finding has already led to many subsequent studies that measured Hg isotopic compositions in organisms to distinguish the relative importance of MMHg sources and to understand complex biogeochemical processes governing MMHg in natural aquatic ecosystems (*3-8*).

Enabled by the findings of Chapters 2 and 3 we estimated the isotopic composition of MMHg sources to aquatic organisms with varying % MMHg and trophic positions from five Northeast coast (USA) estuaries (Chapter 4). We found significant positive relationships between % MMHg and Hg isotope values in the estuarine food webs, indicating that MMHg accumulated from the local environment is indeed retained in fish tissues during bioaccumulation and trophic transfer. In contrast, we found anomalously high δ^{202}Hg values in eider (seaducks), which are different from other aquatic organisms measured in this study. We hypothesize that the high δ^{202}Hg values is caused by internal demethylation, causing the remaining MMHg to shift toward higher δ^{202}Hg values compared to the reactant MMHg (*9*). This supports the previous hypothesis, which suggested that internal metabolic fractionation of δ^{202}Hg (but not Δ^{199}Hg) may occur in birds, as well as in mammals such as seals, whales, and human hair (*10-14*).

6.1.2. Mercury sources and biogeochemistry in aquatic ecosystems

In addition to understanding processes that cause Hg isotope fractionation, the research described in this dissertation has provided new information to the sources and biogeochemical cycling of Hg in aquatic ecosystems. In Chapter 4, we found that MMHg associated with sediments and that has undergone small amounts of photochemical degradation, acts as the dominant source to many estuarine organisms. There has been a long-standing debate over the

relative importance of MMHg derived from sediment or from the water column as a source to estuarine organisms. Complex biogeochemical processes affecting Hg bioavailability between sediment and the water column (i.e., diffusion, resuspension, advection, particle settling) made it difficult to trace the dominant MMHg sources in the estuarine food webs based on Hg concentrations alone. The ability to establish a clear linkage between Hg source and receptor has allowed us to resolve this long-standing debate in estuaries. While we found some evidence that MMHg introduced externally and accumulated from the water column may be more important as a source to certain feeding guilds at certain localities (i.e., mussels at Bold Point, RI), the ecological variability of MMHg sources was clearly demonstrated by measuring Hg isotope ratios in organisms representing diverse feeding guilds.

In Chapter 5, we estimated the isotopic compositions of both IHg and MMHg in a freshwater lake and adjacent forest food webs by measuring organisms with even broader % MMHg values, and compared the estimated values to assess Hg transport pathways between two ecosystems. We found that MMHg produced *in situ* and that has undergone photochemical degradation is the dominant source to both the aquatic and forest food webs. In addition to MMHg, we found similar isotope values estimated for IHg between the aquatic and forest food webs. We hypothesize that IHg deposited via watershed runoff acts as an important Hg transport pathway between forest and aquatic ecosystems, and that this is more important than the flux of Hg from emergent insects, which was documented by a study in the northern Californian streams (*5*). We also found multiple IHg pools in the bulk lake sediment—one that was deposited through watershed runoff of terrestrial soil and the other deposited through precipitation. While further work is needed to distinguish the relative importance of IHg sources, our study demonstrates that IHg introduced from various sources may differ in its ability to produce MMHg in aquatic ecosystems.

6.2. Suggestions for future work

This dissertation contributes to the field of Hg stable isotope biogeochemistry and aquatic Hg biogeochemistry in a number of important ways. The work presented here also, however, raises many important new questions that need to be answered by additional research. By answering them, we expect that the use of Hg isotopes will enable more precise linkages between Hg source and receptor and help to validate tools developed in this study.

First, it is important to analytically separate IHg and MMHg for the measurement of isotope values in biotic samples. The current measurement of Hg isotope ratios is based on total Hg because it is analytically difficult to separate and measure IHg and MMHg isotopic compositions without introducing matrix effects (*15*). While the studies presented in this dissertation strongly suggest that IHg and MMHg have contrasting isotopic compositions, it is important to confirm this hypothesis by comparing the estimated versus measured IHg and MMHg isotope values. We believe that this confirmation will lead to further support of our methods and evaluation of uncertainties associated with the estimation of isotopic compositions for IHg and MMHg.

Second, it is important to couple feeding experiments with models that can identify important factors affecting Hg isotope bioaccumulation and turnover in organisms. The rate at which Hg isotopes bioaccumulate and turn over organisms is expected to vary substantially depending on the type of food, Hg concentration of the diet, life history characteristics (i.e., size, age), and physiological conditions (i.e., metabolic activities) of the aquatic organisms. In fact, in Chapter 3, we found that the physiological state of fish and total Hg concentration of the diet may influence the turnover of Hg isotopes in various organs and tissues. By coupling feeding experiments with models that can incorporate biological, ecological and environmental factors, we may be able to more accurately use Hg isotope ratios in fish as a monitoring tool for tracing MMHg sources and biogeochemical processes in natural environments.

Finally, in addition to estimating the isotopic compositions of IHg and MMHg, it is important to distinguish the relative importance of IHg sources and their bioavailability for supplying the dominant MMHg source to aquatic ecosystems. Many environmental reservoirs represent mixtures of IHg pools, reflecting diverse origins (*16*, *17*). While it is possible to identify the primary site for MMHg production, tracing the bioavailable IHg source that is responsible for MMHg production and bioaccumulation remains a challenge. We expect that field studies coupled with experimental studies will help to distinguish importance IHg sources, and establish more precise linkages between Hg sources and receptors.

Reference

(1) Fitzgerald, W.F.; Lamborg, C.H. Geochemistry of mercury in the environment. In *Environmental Geochemistry*, Holland, H.D.; Turekian, K.K., Ed. **2003,** 107–48. Treatise Geochem. 9. Oxford, UK: Elsevier

(2) Das, R.; Salters, V. J. M.; Odom, A. L. A case for in vivo mass-independent fractionation of mercury isotopes in fish. *Geochem. Geophys. Geosyst.* **2009**, *10*, Q11012.

(3) Blum, J.D.; Popp, B.N.; Drazen, J.C.; Choy, C.A.; Johnson, M.W. Methylmercury production below the mixed layer in the North Pacific Ocean. *Nat Geosci.* **2013,** *6,* 879-884.

(4) Sherman, L.S.; Blum, J.D. Mercury stable isotopes in sediment and largemouth bass from Florida lakes, USA. *Sci Tot Environ.* **2013,** *448,* 163-175.

(5) Tsui, M.T.K.; Blum, J.D.; Kwon, S.Y.; Finlay, J.C.; Balogh, S.J.; Nollet, Y.H. Sources and transfers of methylmercury in adjacent river and forest food webs. *Environ Sci Technol*. **2012,** *46,* 10957-10964.

(6) Tsui, M.T.K.; Blum, J.D.; Finlay, J.C.; Balogh, S.J.; Nollet, Y.H.; Palen, W.J.; Power, M.E. Variation in terrestrial and aquatic sources of methylmercury in stream predators as revealed by stable mercury isotopes. *Environ Sci Technol.* **2014,** *48,* 10128-10135.

(7) Kwon, S.Y.; Blum, J.D.; Chen, C.Y.; Meattey, D.E.; Mason, R.P. Mercury isotope study of sources and exposure pathways of methylmercury in estuarine food webs in the Northeastern U.S. *Environ Sci Technol.* **2014,** *48,* 10089-10097.

(8) Kwon, S. Y.; Blum, J. D.; Nadelhoffer, K. J.; Dvonch, J. T.; Tsui, M. T. K. Isotopic study of mercury sources and transfer between a freshwater lake and adjacent forest food web. *Sci Tot Environ*, **2015**—in review.

(9) Kritee, K.; Barkay, T.; Blum, J. D.; Mass dependent stable isotope fractionation of mercury during mer mediated microbial degradation of monomethylmercury. *Geochim. Cosmochim. Acta*, **2009,** *73,* 1285-1296.

(10) Day, R.D.; Roseneau, D.G.; Berail, S.; Hobson, K.A.; Donard, O.F.X.; Vander Pol, S.S. et al. Mercury stable isotopes in seabird eggs reflect a gradient from terrestrial geogenic to oceanic mercury reservoirs. *Environ Sci Technol*. **2012,** *46,* 5327 5335.

(11) Laffont, L.; Sonke, J.E.; Maurice, L.; Monrroy, S.L.; Chincheros, J.; Amouroux, D. et al. Hg speciation and stable isotope signature in human hair as a tracer for dietary and occupational exposure to mercury. *Environ Sci Technol*, **2011,** *45,* 9910-9916.

(12) Li, M.; Sherman, L.S.; Blum, J.D.; Granjean, P.; Mikkelsen, B.; Sunderland, E.C. et al. Assesing sources of human methylmercury exposure using stable mercury isotopes. *Environ Sci Technol.* **2014,** *48,* 8800-8806.

(13) Perrot, V.; Pastukhov, M.V.; Epov, V.N.; Husted, S.; Donard, O.F.X.; Amouroux, D. Higher mass-independent isotope fractionation of methylmercury in the pelagic food web of Lake Baikal (Russia). *Environ Sci Technol.* **2012,** *46,* 5902-5911.

(14) Sherman, L.S.; Blum, J.D.; Franzblau, A.; Basu, N. New insight into biomarker of human mercury exposure using naturally occurring mercury stable isotopes. *Environ Sci Technol*. **2013,** *47,* 3403-3409.

(15) Masbou, J.; Point, D.; Sonke, J.E. Application of a selective extraction method for methylmercury compound specific stable isotope analysis (MeHg-CSIA) in biological materials. *J Anal At Spectrom.* **2013,** *28,* 1620-1628.

(16) Lindberg, S.; Bullock, R.; Ebinghaus, R.; Engstrom, D.; Feng, X.; Fitzgerald, W.; Pirrone, N.; Prestbo, E.; Seigneur, C. A synthesis of progress and uncertainties in attributing the sources of mercury in deposition. *Ambio* **2007,** *36* (1), 19-32.

(17) Schluter, K. Review: evaporation of mercury from soils. An integration and synthesis of current knowledge. *Environ. Geol.* **2000,** *39*(3–4), 249–271.